CIGARETTE SMOKE IMPACT ON RESPIRATORY DISEASE IMMUNOPATHOLOGY

Investigating the impact of cigarette smoke on the immunopathogenesis of chronic respiratory disease

Steven Paul Cass, BSc (Hons)

A Thesis

Submitted to the School of Graduate Studies

In Partial Fulfilment of the Requirements

For the Degree Doctor of Philosophy

DOCTOR OF PHILOSOPHY (2021)

McMaster University, Hamilton Ontario

Faculty of Health Sciences, Medical Sciences Graduate Program

TITLE: Investigating the impact of cigarette smoke on the immunopathogenesis of chronic respiratory disease

AUTHOR: Steven Paul Cass, BSc (Hons)

SUPERVISOR: Dr Martin Stämpfli

NUMBER OF PAGES: xviii, 204

LAY ABSTRACT

Currently there are 1.3 billion people who use tobacco across the world. The most common method to consume tobacco is by smoking cigarettes. Cigarette smoking is well-known to cause disease; however, smoking rates are still increasing with more daily cigarette smokers in 2012 than there were in 1980. In this thesis, we explore the impact of cigarette smoke upon the immune system. We first assessed whether cigarette smoking impacts the levels of antibodies, proteins that are produced by the immune system to protect against foreign bodies, in healthy individuals, cigarette smokers without disease and patients with chronic obstructive pulmonary disease (**COPD**). We found that current smokers had decreased antibodies in the airways, thus predisposing cigarette smokers to increased damage. In our second study, we measured the presence of airway and blood autoantibodies. These are antibodies that target self and have the potential to inflict damage. We discovered that patients with COPD had minor changes in autoantibodies and these changes were weakly associated with emphysema. In our third study, we evaluated the impact of cigarette smoke on lung macrophages, cells that eat and destroy foreign bodies, in a mouse model of cigarette smoke exposure. Cigarette smoke increased the number of bone marrow-derived macrophages and this change in macrophage populations was associated with a reduced wound healing ability. Overall, these studies offer insight into how cigarette smoke impairs the function of the immune system and contributes to lung disease.

ABSTRACT

Cigarette smoke is an insidious insult that is associated with a spectrum of respiratory diseases that range from cancer to obstructive diseases such as chronic obstructive pulmonary disease (**COPD**), to restrictive diseases such as idiopathic pulmonary fibrosis (**IPF**). In this thesis, we explore how cigarette smoke impacts immune components that contribute to respiratory disease.

To begin, we assessed the impact of cigarette smoke on airway antibody and autoantibody levels. We assessed sputum, a non-invasive method to sample the lower airways, to directly assess the presence of antibodies and autoantibodies in COPD. Total immunoglobulin M (**IgM**), IgG and IgA were detectable in the sputum of subjects. Notably, in patients with mild to moderate COPD, current smoking status was associated with decreased IgM and IgG. Next, using a comprehensive autoantigen array, we measured matched sputum and serum autoantibodies in 224 individuals. Serum autoantibodies were more abundant than sputum autoantibodies and correlated strongly between two independent COPD cohorts. Overall, the autoantibody profile of a patient with COPD was the same as a control subject. A proportion of autoantibody specificities were differentially expressed in patients with COPD with anti-tissue autoantibodies weakly associated with measures of emphysema. Taken together, these data suggested chronic cigarette smoke exposure was associated with limited differential expression of autoantibodies, but these changes were not a reliable method to identify COPD status.

In our third study, we assessed the impact of cigarette smoke exposure on the composition and function of pulmonary macrophage subpopulations.

Macrophages perform a central role in respiratory host defence and are implicated in the pathobiology of several respiratory diseases. Using a mouse model of cigarette smoke exposure, we reported cigarette smoke-induced expansion of $CD11b^{+}$ macrophage subpopulations including monocyte-derived alveolar macrophages and interstitial macrophages. The altered pulmonary macrophage composition following cigarette smoke exposure contributed to attenuated fibrogenesis in a model of bleomycin-induced lung injury. This study offered insight to pulmonary macrophage composition and function following cigarette smoke exposure.

This thesis summarises the original contributions and work completed during the course of this Ph.D., aimed at understanding the impact of cigarette smoke exposure on immune components central to respiratory disease. In conclusion, these findings shed light on the presence of (auto)antibodies in patients with COPD and the composition of macrophage subpopulations following cigarette smoke exposure.

ACKNOWLEDGEMENTS

This body of work is an amalgamation of all the support and guidance that I have received since starting at McMaster. Coming to Canada to join Dr Martin Stampfli's group is arguably one of the best decisions that I have ever made. I have been fortunate to have a supervisor that involved me in all aspects of science and gave us the freedom to experiment in the lab. Thanks to all his advice, encouragement, and time, I have developed numerous new skills and became much more confident in my own abilities. Thank you for all your time, I appreciate it immensely.

I also want to extend my thanks to the members of my supervisory committee who have provided so much guidance during this degree. Dr Param Nair has supported this project from the start providing invaluable clinical expertise. Moreover, the time Dr Nair took to allow me to shadow him and providing the constant reminder to think of the bigger picture. Furthermore, I also want to thank Dr Matt Miller for his enthusiasm during all our meetings and always championing new ideas and approaches. This led to an ever-improving experimental design. Dr Miller was also influential during my comprehensive exam and provided a welcomed sounding board and reminders to focus on developing a clear message. Completing my supervisory committee is Dr Chris Stevenson without who I would not be here at McMaster. Dr Stevenson has supported me ever since our first meeting at Imperial College's café. Your advice has been invaluable and I greatly appreciate the effort you have put in to allow me to continue my career development. Thank you all for your advice, it has been life changing.

This degree is nothing without the people that I have shared it with. The members of MIRC have been so supportive and there are so many to acknowledge. Drs Allison Felker and Puja Bagri not only provided a sounding board for experiments and helped edit documents, but shared the gigs, dinners and manic playoff series that made graduate school so much fun. Your support has been huge and I'm so thankful that I can call you friends. The collaborative atmosphere of MIRC allowed me to develop scientifically as well as personally. I would like to thank specifically, Dr Rocky Lai, Dr Ehab Ayaub, Dr Dessi Loukov, Dr Joni Hammil, Dr Sam Afkhami, Talveer Mandur and Jann Ang who made this centre the supportive place it is. I also want to thank all members of MIRC's football team, and particularly Arya Afsahi, for providing the outlet we all need to destress after a hard week in the lab. MIRC is a fantastic place to study and I am aware how fortunate I have been to work alongside all of its members.

Over the years I have had a number of different housemates and it is always interesting who you end up with. With Pip Matharu and Dillion Schnurr I lucked out. It's such a shame we weren't able to move out on our own terms but I guess that's life. Living on Ewen felt like home. From Dillon inviting me up to Huntsville, to having a beach weekend with Pip on Lake Huron, it was just a pleasure to live with you both.

The Stampfli lab has been very good to me. We always ended up with the best of people. Thank you, Dr Pam Shen, Dr Gilles Vanderstocken, and Ashley Beaulieu for the all your encouragement and advice. Matt Fantauzzi, may have joined last but helped so much over the final stretch. Plus, we got to

share a lot of music which was perfect for the long lab days. Big thank you to Peipei Wang, Bomi Park, Racheal Heo and Bruce Ly who were always ready to help out. Moreover, our honouree member Olivia Mekheal. Your fibrosis expertise made large parts of these studies. We came along way since that crazy month with Dr Yuqiong Yang in China, including all the hectic lab days and bungee jumping in Yuexiu Park. Finally, of course, Joanna Kasinska, the lab would be nothing without you. You kept everything, and everyone, running even when our boss decided to live in China and Switzerland for a few years. Always so friendly and happy to talk, we couldn't have done any of this without you.

I may have been across an ocean but my parents were always by my side. Only the government halting travel stopped you sharing the Canadian life for two weeks. Your stays were always the highlight of the year, and through those trips we got to see some stunning places across Canada. A dark Edinburgh morning with a suitcase and a bag doesn't feel all that long ago. It's been a whirlwind 6 years, but soon I'll be back to walk along Beadnell beach with you, Katie and the dogs. Your support is always felt and I can't wait to share this with you.

I met so many wonderful people here but two are deserving of particular mention. Danya Thayaparan and Josh McGrath were there through the entire process, going through each milestone together. This Ph.D. was made by your friendship and I struggle to think what it would have been without both of you; luckily, I don't have too. Both of you are so talented and it's been a case of holding onto your coattails and getting dragged along. Along with Martin you

are the reason why I have developed so much personally and scientifically. From sweaty punk gigs, saxophone raves, movie marathons, jumping out of a plane, and watching Josh sink in a Vietnamese river, you have been there for all of it. I'm so glad that I got to share this with both of you.

LIST OF FIGURES

Chapter II

Chapter III

Chapter IV

Appendix

LIST OF TABLES

ABBREVIATIONS

AECOPD	Acute exacerbations in chronic obstructive pulmonary disease
ADEPT	Airways disease endotyping for personalized therapeutics
AM	Alveolar macrophage
ANA	Anti-nuclear antibodies
AT	Anti-tissue antibodies
AhR	Aryl hydrocarbon receptor
BAFF	B-cell activating factor
BMI	Body mass index
BrdU	Bromodeoxyuridine
BAL	Bronchoalveolar lavage
BALF	Bronchoalveolar lavage fluid
CCL2	C-C motif chemokine ligand 2
CXCL	Chemokine ligand
COPD	Chronic obstructive pulmonary disease
CS	Cigarette smoke
CSE	Cigarette smoke extract
CAT	The COPD Assessment Test
cDC	Conventional/classical dendritic cell
CT	Computerised tomography
CCP	Anti-cyclic citrullinated peptide
DAMP	Damage-associated molecular pattern
DNA	Deoxyribonucleic acid
DL_{CO}	Diffusing capacity for carbon monoxide
DTE	Dithioerythritol
DTT	Dithiothreitol
E	Embryonic day
ELISA	Enzyme-linked immunosorbent assay
FEV_1	Forced expiratory volume in 1 second
GOLD	Global initiative for obstructive lung disease
GIRH	Guangzhou Institute of Respiratory Health
ICS	Inhaled corticosteroid
IPF	Idiopathic pulmonary fibrosis
Ig	Immunoglobulin
IFN	Interferon
IL	Interleukin
ILD	Interstitial lung disease
IM	Interstitial macrophage
MHC	Major histocompatibility complex
MMP9	Matrix metalloproteinase-9
Mo-AM	Monocyte-derived alveolar macrophage

nAb	Natural antibody
NET	Neutrophil extracellular trap
NETosis	Neutrophil extracellular trap release
NADP	Nicotinamide adenine dinucleotide phosphate
PAMP	Pathogen-associated molecular pattern
PBS	Phosphate-buffered saline
pDC	Plasmacytoid dendritic cell
pIgR	Polymeric immunoglobulin receptor
PMN	Polymorphonuclear neutrophil
PD-1	Programmed death receptor 1
PD-L1	Programmed death receptor ligand 1
RA	Room air
ROS	Reactive oxygen species
Res-AM	Resident alveolar macrophage
RNA	Ribonucleic acid
T_h	T helper cell
T_{fh}	T follicular helper cell
T_m	T memory cell
T_{reg}	T regulatory cell
TGF-β	Transforming growth factor beta
TNF	Tumour necrosis factor

DECLARATION OF ACADEMIC ACHIEVMENT

Comprehensive exam May 2019 (Pass)

Graduate Courses

MS771 – Research Methodologies in Health Sciences Autumn 2016 (A)

MS716 – Advanced Immunology II Winter 2017 (A+)

MS799 – Independent Study: R Programming Summer 2020 (A+)

Research Exchange Apr – May 2018

Guangzhou Institute of Health - Firestone Institute of Respiratory Health student exchange. "Assessment of autoantibody levels in a Chinese chronic obstructive pulmonary disease cohort"

Research (First Author Publications)

Manuscript 1: *Published in the ERJ*: "Current smoking status is associated with reduced sputum immunoglobulin M and G expression in chronic obstructive pulmonary disease." Cass SP *et al.* Eur Respir J. 2021 Feb 4;57(2):1902338.

Manuscript 2: *Published in AJP-Lung*: "Differential expression of sputum and serum autoantibodies in patients with chronic obstructive pulmonary disease." Cass SP *et al.* Am J Physiol Lung Cell Mol Physiol. 2021 Jun 1;320(6): L1169-L1182.

Manuscript 3: *In review at Allergy.* "Detecting immunoglobulins in processed sputa" Cass SP* & McGrath JJC* *et al.*

Manuscript 4: *In review at Frontiers in Immunology.* "Increased monocyte-derived $CD11b^{+}$ macrophage subpopulations following cigarette smoke exposure are associated with impaired bleomycin-induced tissue remodelling" Cass SP* & Mekhael O* *et al.*

CONTENTS

CHAPTER 1: INTRODUCTION AND OBJECTIVES

1.1. Health impact of cigarette smoke

As of 2020, the World Health Organization reported that 1.3 billion people worldwide are tobacco users[1]. The most common tobacco consumption method is cigarette smoking[1]. Despite the well-known adverse health impact[2,3] and greater likelihood of individuals to self-report poorer health[4,5], an increase of 246 million daily cigarette smokers were recorded between 1980 and 2012[6]. In Canada alone, over 5.5 million individuals continued to smoke cigarettes[7]. Alarmingly, tobacco use is linked with the deaths of more than 8 million people worldwide per year[1] with cigarette smokers losing up to 12 years of life on average[8,9]. Specifically, cigarette smoking related deaths have been associated with diseases including cancer, cardiovascular disease, and respiratory diseases such as chronic obstructive pulmonary disease (**COPD**) and interstitial lung disease (**ILD**)[3,10].

1.2. The impact of cigarette smoke on the immune system

Cigarette smoke is composed of over 7,300 components including known carcinogens, reactive oxygen species (**ROS**), N-nitrosamines, polycyclic aromatic hydrocarbons, aldehydes, amines and heavy metals[11]. Many of these components contribute to inflammation. For example, ROS such as superoxide anion ($O2^{\bullet -}$), hydrogen peroxide (H_2O_2) and the reactive hydroxyl radical ($HO^{\bullet}$)[12] cause oxidative damage to cellular membrane lipids, proteins, and deoxyribonucleic acid (**DNA**)[13]. Subsequently, this damage promotes processes

such as lipid peroxidation[14], mucus secreation[15], and DNA adducts/double strand breaks leading to inflammation[16]. In addition to directly contributing to excessive inflammation, cigarette smoke components can interact with immune components to modulate inflammation. For instance, nicotine, the addictive agent in cigarette smoke, has been shown to reduce innate immune cell function and impair adaptive immune cell proliferation[13,17]. Likewise, hydrocarbons, which comprise a large proportion of molecules in cigarette smoke, are known to directly suppress adaptive immune cell acitvation[18]. Cigarette smoke components directly influence immunity through direct damage and interactions with immune cells.

The diverse array of cigarette smoke components can also affect the immune system indirectly. Hydrocarbon binding to the aryl hydrocarbon receptor (**AhR**), leads to innate immune suppression promoting endotoxin tolerance and decreased cell death[19–21]. Of note, in AhR knockout models cigarette smoke exposure results in an exaggerated immune response with prominent neutrophilia[22]. Cigarette smoke does not only suppress immune system components but can promote inflammation, often through the same cellular pathways. For example, hydrocarbon binding to AhR also promotes adaptive immune cell survival and differentiation[23,24]. Cigarette smoke components are sufficient to exert both pro and anti-inflammatory affects upon the immune system.

Cigarette smoke is composed of a diverse range of components that each have a different capacity to modulate immune function. Adding to this complexity, cigarette smoke components affect the structural, innate and

adaptive cells that form the immune system differently. The impact cigarette smoke has on different immune cells leading to the development of cigarette smoke-associated respiratory disease is not fully understood.

1.2.1. Epithelial cells

As the first line of defence, epithelial cells form a barrier protecting the respiratory tract from external agents. Barrier integrity is essential for overall lung health and the maintenance of tissue homeostasis. Studies have shown that the respiratory barrier is compromised by cigarette smoke exposure. A break down in tight junction integrity, impaired ciliary function, cell hyperplasia and squamous metaplasia induced by cigarette smoke exposure all contribute to a dysregulated barrier[25–27]. In addition to dysregulation of the physical barrier, cigarette smoke also impairs functional responses in infected epithelial cells[28–30]. Together, these impairments predispose the epithelium to increased bacterial colonisation and viral infection in cigarette smokers[29,31]. Epithelial cell immune function is not entirely suppressed when exposed to cigarette smoke. Epithelial cells in response to cigarette smoke exposure release exacerbated levels of proinflammatory mediators such as chemokine ligand (**CXCL**)8[32], CXCL1 and CXCL5[33]. The release of these chemokines contributes to the recruitment of immune cells to the local environment and exacerbated inflammatory response caused by cigarette smoke exposure. Overall, cigarette smoke causes epithelial barrier dysregulation and alters immune function skewing tissue homeostasis.

1.2.2. Macrophages

Macrophages perform a critical role in innate sensing and response to infectious agents as well as tissue repair. Two pulmonary macrophages populations reside in the lung, interstitial macrophages (**IM**), located within the lung interstitium, and alveolar macrophages (**AM**), which reside within the alveolar space[34]. AM account for approximately 80% of the lung-resident macrophages and IM constitute the remaining 20%[35,36].

1.2.2.1. Pulmonary macrophage subpopulations

Pulmonary macrophage subpopulations develop independently from one another[37]. Resident alveolar macrophage (**Res-AM**) populations arise from two different developmental origins. The first is a primitive Res-AM originating from the yolk sac on embryonic day (**E**)10-12 in mice[36,37]. The longevity of these primitive AM are unclear. The second Res-AM population arises from the foetal liver and enters the lungs by E12-16 and the alveolar space after birth[36,37]. This second developmental wave is believed to contribute to the long-lived tissue Res-AM population. These mature Res-AM are predominately self-maintained with limited contribution from circulating monocytes[38]. In addition to Res-AM populations, a postnatal AM subpopulation is recruited from the bone marrow[39]. Monocyte-derived alveolar macrophages (**Mo-AM**) have been shown to share 99.9% of genes with Res-AM[40], but comprise less than 5% of the AM population[36]. Mo-AM transition directly from monocytes and are independent of IM populations[41].

As part of the postnatal developmental wave from bone marrow, monocyte-derived macrophages also populate the lung parenchyma and termed

IM[37]. IM are divided into three subsets based on CD11c and major histocompatibility complex class two (**MHCII**) expression, IM1 ($CD11c^{Neg}MHCII^{Neg}$), IM2 ($CD11c^{Neg}MHCII^{+}$), IM3 ($CD11c^{+}MHCII^{+}$)[42]. Fluorescence microscopy has identified that IM1 populations are located in the pulmonary vasculature while IM3 populations are associated with nerve endings[43,44]. To date, the precise location of IM2 populations within the interstitium is not known. Unlike AM, IM are predominately maintained by bone marrow-derived cells[37,42]. Interestingly, emerging data has identified a small proportion of IM are derived from the yolk sac prenatally and are self-maintained similar to Res-AM populations[44]. These long-lived cells form part of the IM1 and IM2 populations based on cell surface marker expression[44]. Pulmonary macrophages are comprised of a diverse range of cells derived from several development sources and waves.

The different pulmonary macrophage subpopulations have morphological and functional differences[34,45]. IM are smaller and more proinflammatory, but less phagocytic, than larger AM counterparts[45]. *In vivo* phagocytosis assays at steady state demonstrated that the phagocytic capacity of pulmonary macrophages is negatively correlated with the contribution of monocytes, with Res-AM having the greatest phagocytic ability followed by IM1, IM2 and then IM3 sequentially[42]. The classical features of AM function is the ability to phagocytose microbial pathogens, apoptotic debris and surfactant, in addition to wound healing and pathogen recognition processes[46]. In contrast, the function of IM are much less understood. At steady state, IM populations are enriched for inflammatory mediators and monocyte-related genes compared

to AM. Of note, no significant transcriptional difference is observed between each IM subpopulation[42]. While transcriptionally similar, the location of IM subpopulations is associated with functional differences. Vasculature-associated IM1 specifically have been associated with vascular integrity and wound healing while nerve-associated IM3 perform a role in antigen presentation[43,44]. In summary, a diverse range of macrophage subpopulations are present in the lung with defined functional roles in the innate immune response.

1.2.2.2. Skewed macrophage response to cigarette smoke

Macrophage function is intrinsically linked to the surrounding microenvironment. The immune environment transcriptionally regulates macrophages to express cell surface markers and secrete mediators which direct function[47]. These cell surface markers and mediators are split into two, non-mutually exclusive, categories. "M1" macrophages express proinflammatory markers that are associated with anti-microbial and anti-tumour activity, whereas "M2" macrophages are linked to wound healing and anti-inflammatory responses[48,49]. This spectrum of macrophage function is termed macrophage polarisation. To note, macrophages can alter their polarisation status based on a shifting microenvironment enabling the same cell to undertake the diverse functional roles required in response and repair to a given insult.

Cigarette smoke has a diverse relationship with macrophage polarisation. A predominate M1-like profile has been demonstrated in *ex vivo* analysis of Mo-AM from cigarette smokers[50]. In contrast, analysis of bronchoalveolar lavaged (**BAL**) macrophages observed a skewed dual M1/M2-

like profile in cigarette smokers[51]. Thus, the location of pulmonary macrophage sampling impacts the polarisation state in cigarette smokers. The small airways associated with a predominate M1-like profile whereas BAL macrophages predominately expressed a M2-like phenotype[52].

The impact of cigarette smoke on each pulmonary macrophage subpopulation is currently not known. Overall, studies show an expansion of total macrophages in the bronchoalveolar lavage fluid (**BALF**)[53] and lung tissue[54] following cigarette smoke exposure. Notably, bronchial macrophages remain elevated in ex-smokers compared to healthy non-smoking controls[55,56]. Once residing in smoke-exposed airways, macrophages become lipid-laden[53,57] and impaired in their ability to phagocytose bacteria[58] and apoptotic cells[59]. This suppressed phenotype following exposure to cigarette smoke is also associated with a reduced capacity to recognise pathogen-associated molecular patterns (**PAMPs**) and release cytokines[60,61]. Whether this suppressed phenotype is specific to certain macrophage subpopulations is not known.

Cigarette-exposed macrophages exhibit an attenuated profile[61], but notably release increased IL-1α[33,62], plus serine and cysteine proteases[63]. In cigarette smoke exposure animal models, IL-1α has been shown to be necessary for cigarette smoke-induced inflammation[33,62,64]. Moreover in cigarette smoke exposure models, interstitial CX_3CR1^+ mononuclear phagocytes were associated with airspace enlargement[65]. The precise contribution of IM subpopulations to this CX_3CR1 interstitial population following cigarette smoke exposure is yet to be explored. To date, in human samples, macrophages are shown to be localised to sites of alveolar destruction[66] and release increased

proinflammatory mediators[67] but the precise macrophage subpopulations is not known. The specific macrophage subpopulations associated with IL-1α-mediated inflammation and protease-mediated extracellular matrix breakdown is not known.

1.2.3. Dendritic cells

Another mononuclear phagocyte key to the innate immune response is the dendritic cell. Residing in the parenchyma, dendritic cells sample the local environment for foreign bodies facilitating both the activation of proinflammatory pathways and antigen display to adaptive immune cells[68,69]. Similar to macrophages, different dendritic cell populations reside in the lung. Bone marrow-derived, conventional/classical dendritic cells (**cDC**s) are split into two subsets, cDC1 $CD103^+$ (T helper cell type (**T_h**)1 immunity) and cDC2 $CD11b^+$ (T_h2/T_h17 immunity)[70–72]. T_h1 responses are associated with interferon (**IFN**)γ and tumour necrosis factor (**TNF**) production promoting phagocytosis, microbial killing and tolerance induction[73]. T_h2 immunity is associated with interleukin (**IL**)-4, IL-5, and IL-13 production and is important for the generation of immunoglobulin E (**IgE**) responses in helminth infection and allergy[74]. In contrast, T_h17 responses are associated with IL-17 and IL-23 production in microbial defence and in autoimmune disease[75]. In addition to function diversity, cDC subpopulation ontogeny is different. cDC2 cells are recruited to the lung and differentiate from IM1 macrophages[76]. In contrast, cDC1s, also derived from the bone marrow, do not differentiate directly from macrophage populations[76]. To note, cDC1 cells are often directly associated with IM2 macrophages[76]. In addition to cDC's, monocyte-derived dendritic

cells differentiate from $Ly6C^+$ or $CD14^{Hi}$ monocytes during inflammation and are phenotypically similar to cDC1 cells[77,78]. These monocyte-derived dendritic cells have reduced capacity to activate T cells compared to their cDC1 counterparts[79]. The last dendritic cell population present in the lungs is the plasmacytoid dendritic cells (**pDC**). These cells are a key sentinel in the lung interstitium and perform a vital role in the anti-viral immune response[76,80].

Cigarette smoke is associated with the changes in the composition and function of dendritic cells in the lung. *In vivo* studies demonstrated cigarette smoke-mediated recruitment of $CD11b^+$ populations, including cDC2 and monocyte-derived dendritic cells, through a IL-1α dependent pathway[81,82]. The precise contribution of monocyte-derived macrophages, monocyte-derived dendritic cells or cDC2 to this population is not known. In contrast, total $CD11c^+$ populations (including cDC1, cDC2 and pDCs) are observed to be decreased in the lung[83,84]. Overall, cigarette smoke skews the dendritic cell population in the lungs. In chronic smokers, this differential presence of dendritic cells are also observed. $CD83^+$ cells (a human cDC-like cell) were decreased, while $CD1a^+$ cells (human monocyte-derived macrophage-like cell) were increased in cigarette smokers[85,86]. In addition to compositional changes, cigarette smoke has been shown to impair functional T_h1, T_h2 and T_h17 dendritic cell responses[84,87]. Specifically, decreased total dendritic cells numbers following cigarette smoke exposure were associated with impaired anti-viral immunity[83]. Cigarette smoke skews the composition of dendritic cell populations and is associated with impaired dendritic cell function.

1.2.4. Neutrophils

Neutrophils perform a vital role in the recognition and removal of pathogens following infection. Neutrophilia is observed clinically in cigarette smokers[88] and in cigarette smoke-exposed animal models[81,89]. This neutrophilic airway infiltration is driven by an IL-1α dependent pathway[62]. The release of IL-1α in cigarette smokers leads to the induction of CXCL1 and CXCL5 which are both potent neutrophilic chemokines[33]. Concurrently, epithelial and neutrophil release of CXCL8, a human neutrophil chemoattractant, further exacerbates neutrophil recruitment in cigarette smokers[90,91]. This pulmonary neutrophilia is associated with increased neutrophil elastase which is implicated in matrix degradation and airspace enlargement[92]. This link to matrix degradation is highlighted in historical studies of patients with alpha-1 antitrypsin deficiency. In alpha-1 antitrypsin deficiency, patients suffer from an imbalance in proteases resulting in elevated neutrophil elastase in the lungs and accelerated emphysema development[93].

As part of the neutrophilic antimicrobial response, neutrophils have the ability to undergo a precise cell death pathway which releases intracellular components in a net-like release. This process, termed neutrophil extracellular trap release (**NETosis**), is shown to remove and kill bacteria[94]. This antimicrobial response is observed to be increased following cigarette smoke exposure even in the absence of infection[95]. However, despite increased NETosis in cigarette smokers[96], studies show suppressed neutrophil cytokine release and bacterial killing in the presence of cigarette smoke extract[97]. This impaired killing likely reflects the supressed respiratory burst (reduced

inducible nitric oxide synthase and reduced nicotinamide adenine dinucleotide phosphate (**NADPH**) oxidase component release) in cigarette smokers[98]. Thus, while cigarette smoke exacerbates airway neutrophilia, functional aspects of neutrophil-mediated antimicrobial killing are impaired in cigarette smokers.

1.2.5. T lymphocytes

In addition to compromising innate immune cells, cigarette smoke also has a broad impact upon adaptive immune cells. T lymphocytes are composed of a diverse range of cells that perform vital roles within the adaptive immune system. Derived from the bone marrow, T cells mature into different subsets within the thymus each associated with a specific immune function[99]. These subsets include $CD4^+$ helper (**$CD4^+$ T**) cell, $CD8^+$ cytotoxic (**$CD8^+$ T**) cell, regulatory T (**T_{reg}**) cell, memory T (**T_m**) cell and follicular helper T (**T_{fh}**) cell. $CD4^+$ T cells generate cytokines promoting innate and adaptive cell activation[99]. $CD8^+$ T cells survey MHC class I on antigen presenting cells for foreign peptides to trigger cell-mediated death of infected or malignant cells[99]. These responses are regulated by T_{reg} cells that inhibit uncontrolled activation and restore homeostasis[100]. T_m cells develop from previous antigen activation and form a pool of long-lived immunity[101]. Lastly, T_{fh} cells perform a vital role in B cell germinal centre formation and generation of high-affinity antibody responses[102].

Cigarette smoke has immunomodulating effects on T cell subtypes. Cigarette smoke has been shown to upregulate activation markers, inducing T cells to enter a state of T cell anergy[81,103,104]. Anergy is not induced via increased T_{reg} cells, which are suppressed by cigarette smoke exposure[105–107], but through increased expression of cell checkpoint inhibitors on the cell surface of T cell

and cognate antigen presenting cells[108]. This loss of regulatory control results in skewed $CD4^+/CD8^+$ T cell balance in some chronic cigarette smokers, favouring elevated $CD8^+$ T cell numbers[108,109]. Notably, there is greater T cell receptor diversity in $CD8^+$ T cell populations in cigarette smokers providing a greater expanse of potential activating signals[110]. Increased $CD8^+$ T cell numbers in cigarette smokers is associated with elevated perforin and granzyme B release and worsened pulmonary function[54,109]. Despite increased $CD8^+$ T cell numbers and their association with decreased lung function, cigarette smoke promotes T cell exhaustion and impaired killing[103,111,112]. This extends to impaired T cell mediated clearance of malignant cancer cells in cigarette smokers[113,114]. Ultimately, cigarette smoke increases $CD8^+$ T cell numbers which display exhaustion markers and decreased functional capacity.

1.2.6. B lymphocytes

A major component of the humoral immune response is the generation of antibodies, also known as immunoglobulins (**Ig**), by B cells. Two major B cell subtypes, B-1 and B-2 cells, exist. These cells are derived from different developmental origins and have unique cell surface markers and functional properties. B-2 cells (follicular B cell) develop postnatally in the bone marrow, which upon encountering antigen in peripheral sites enter secondary lymphoid follicles and interact with T_{fh} cells to become antibody-producing effector B cells[115]. Long-lived antibody-producing plasma cells and the generation of memory B cells provide lifelong humoral protection[116]. In contrast to these T cell dependent B-2 cells, B-1 cells (T cell-independent innate B cell), are produced in developmental waves beginning in the foetus which upon birth

provide a pool of self-renewing, long-lived antibody secreting cells[117]. While not present in large quantities within the circulation, B-1 cells form a large proportion of B cells in the peritoneal and pleural cavities[117,118]. B-1 cells do not typically undergo affinity maturation or somatic mutation like B-2 cells but rather spontaneously produce low affinity, cross-reactive natural antibodies (**nAb**)[119,120]. While IgM is the most dominant nAb class, IgG nAb are also observed to be released by B-1 cells[121,122]. The spontaneous release of germline nAb, due to a constitutively active B cell receptor, enables nAb to act as part of the innate immune defence against microbial agents[123–126] and contribute to tissue homeostasis[127,128].

1.2.6.1. Antibody-mediated function

The diversity in B cell function is attributed to the different antibodies produced. During development, B cells must undergo successful V(D)J gene rearrangements in order to express germline-encoded Ig[115]. This naïve B cell must then survive clonal deletion and negative selection of self-reactive antibodies, to mature into a naïve transitional B cells[115]. As transitional B cells become exposed to antigen, often in the presence of $CD4^+$ T cells, antibodies undergo affinity maturation and Ig class switching, thus resulting in mature antibody-secreting plasma cells[115]. High affinity antibodies produced by plasma cells bind specific epitopes which dependent on the heavy chain constant region facilitate different effector functions. There are five different heavy chain constant regions, IgM, IgD, IgG, IgA and IgE. IgM and IgD are expressed on the surface of naïve B cells. Upon activation B cells downregulate IgD and solely produce IgM; as such, IgM is closely associated with the primary

adaptive immune response[129]. Subsequently, through class switch recombination activated B cells may begin to produce antibodies of other isotypes. For instance, IgG which is the predominant serum Ig class has four subtypes and is known for its conformational flexibility and functional versatility[129]. IgA is principally produced in areas underlying mucosal surfaces and is secreted into luminal spaces to afford protection through neutralisation[129]. Lastly, IgE, is predominately found proximal to the epitheium[129].

Ig classes perform distinct but complementary functions in adaptive immune processes. IgA and IgG are effective at neutralising pathogens, thereby preventing infection and associated infectious disease[130]. IgG antibodies are also capable of opsonising targets facilitating opsonophagocytosis by macrophages, or destruction via natural killer cell-mediated antibody-dependent cellular cytotoxicity[131]. Additionally, IgM and IgG activate the classical complement pathway, resulting in the recruitment of inflammatory cells, as well as the formation of membrane-attack complexes[132]. The least abundant Ig classes are IgD and IgE. IgD is found on naïve B cells is proposed to have functions related to basophil activation[133], while IgE offers protection against helminths and parasite infection[129]. Antibodies perform a vital role in the humoral immunity through the functional diversity produced by different heavy chain constant regions.

1.2.6.2. The impact of cigarette smoke on B cell function

Cigarette smoke has a two-fold impact on B cells. First, in current smokers, the number of class switched and memory B cells is increased[134]. This is in part due to increased B cell recruitment and survival factors such as CXCL13 and B-cell

activating factor (**BAFF**) in cigarette smokers[135,136]. Second, although B cell activation is not impaired by cigarette smoke exposure[103], IgG serum antibodies are decreased in cigarette smokers[137–139]. Specifically, cigarette smoke decreases serum IgG2 while serum IgG1, -G3 and -G4 isotypes are unaffected by smoking status[140]. In addition, the induction of IgG, and IgM, responses in the saliva of cigarette smokers is shown to be impaired in cigarette smokers[141]. Together, deficiencies in IgG2 and impaired IgG and IgM responses suggest cigarette smokers have a reduced capacity for antibody-mediated effector functions.

1.3. Cigarette smoke-associated disease

Given the insidious nature of cigarette smoke, associated respiratory diseases are often progressive and irreversible. For example, COPD and idiopathic pulmonary fibrosis (**IPF**), which are linked to former and current smoking status[3,142], both gradually lead to physical disability and to date have no cure. Central to these diseases is the impact of cigarette smoke on immune components. Consequently, in addition to a continued emphasis on reducing cigarette smoking prevalence, efforts focusing on understanding the immune mechanisms that lead to cigarette smoke-associated respiratory disease are desperately warranted.

1.3.1. Chronic obstructive pulmonary disease (COPD)

COPD is a common respiratory disease that in Ontario accounts for 21% of primary care patients aged 40 or older who have a smoking history[143]. Worldwide, COPD affects 251 million people[144] and is estimated to be the

seventh leading cause of years of life lost[145]. Characterised by the variable presence of respiratory conditions, COPD encompasses patients with chronic bronchitis (persistent mucus hypersecretion), obstructive bronchiolitis (inflammation leading to narrowing of the small airways) and emphysema (lung parenchyma destruction leading to airspace enlargement and reduced elasticity of the lung)[146]. While these respiratory conditions coexist and are non-mutually exclusive, individuals generally fall into one of two common clusters. Cluster one individuals have low forced expiratory volume in 1 second (**FEV_1**), low body mass index (**BMI**), dyspnoea and extensive computerised tomography (**CT**) confirmed emphysema. This cluster represents an emphysema-dominant patient with severe lung function decline. In cluster two, individuals present with moderately impaired FEV_1, high BMI and thickened airway walls, with little CT confirmed emphysema[147]. This cluster represents subjects with chronic bronchitis-dominant disease and mild lung function decline.

COPD disease aetiology includes noxious particles and/or gases from occupational hazards and air pollution; however, the single most significant risk factor is current or former cigarette smoking[3]. These stimuli in susceptible individuals accelerate the natural lung function decline associated with age[148]. This rapid deterioration in lung function plus dyspnoea and chronic cough, with or without sputum production, are all diagnostic features of COPD[149]. The loss of lung function is stratified into Global Initiative for Obstructive Lung Disease (**GOLD**) stages I to IV. GOLD I patients are individuals with mild lung function decline (> 80% FEV_1), GOLD II - moderate decline (50 - 79% FEV_1), GOLD III - severe decline (30 - 50% FEV_1) and GOLD IV - very severe lung

obstruction (< 30% FEV_1)[149]. In addition to susceptible current and ex-smoker's, < 5% of COPD cases are associated with a genetic risk factor alpha-1 antitrypsin deficiency[150]. This genetic deficiency leads to an imbalance in serine proteinases resulting in an emphysema-dominant COPD[151]. Increasingly, evidence suggests that impaired lung development either during gestation, birth or childhood reduces attainable lung function and also increases the risk of developing COPD[152–154]. As COPD progresses lung function chronically declines which, to date, cannot be halted or cured. Understanding the mechanisms that contribute to the accelerated decline in lung function and identifying patients early in disease is important to initiate intervention strategies promptly to maintain lung function.

1.3.1.1. COPD pathogenesis

COPD pathogenesis is not fully understood; however, 85 – 90% of COPD diagnoses are attributed to current or former smoking[3]. To date, it is understood that chronic cigarette smoke acts upon epithelial cells and macrophages to drive disease development[155]. Chronic epithelial and macrophage activation in COPD results in the establishment of a proinflammatory environment through the release of central mediators such as IL-8, C-C motif chemokine ligand 2 (**CCL2**) and ROS[155]. This inflammatory milieu proceeds cellular infiltration into the lung, predominately composed of polymorphonuclear neutrophils (**PMN**s) and monocytes which are correlated with increasing airflow obstruction[54]. The chronic inflammatory immune environment further contributes to accumulation of bronchial $CD8^+$ T cells[156,157] and airway associated B cells[54] with worsening disease severity. Together, tissue resident

and recruited cells contribute to the persistent release of proteinases which contribute to airway wall destruction and growth factors which contribute to mucus hypersecretion. Together these processes result in lung function decline observed in patients with COPD[155].

Interestingly, cigarette smoke cessation slows the rate of lung function decline[158,159], but does not halt chronic inflammation and disease progression[54–56,160]. Studies have identified that distinct myeloid and lymphoid immune cells were not diminished despite smoking cessation in the lungs of patients with COPD[56,160]. Notably, B cells increased in the lungs of patients with COPD regardless of current smoking status[54,160]. Specifically, total circulating B cells and the percentage of small airways containing B cell-rich lymphoid follicles increased with disease severity[54,161]. The presence of lymphoid follicles in the lung parenchyma and bronchial walls is associated with predominant emphysema in COPD[162]. Moreover, microarray analysis reports transcripts associated with B cell recruitment, Ig and activation were increased in emphysema dominant COPD[163]. An increasing focus has been placed on understanding the role of B cells in COPD pathogenesis.

1.3.1.2. Contribution of antibodies to COPD progression

Cigarette smoke has contrasting immunomodulatory effects which are marked by a number of immunosuppressive functions[164]. In this regard, cigarette smoke contributes to decreased levels[137–140] and impaired induction of antibodies[141]. For instance, in individuals undergoing lung transplantation, subjects with COPD had lower serum IgG levels compared to patients with other diseases[165]. Increasingly IgA deficiency in proposed to contribute to abnormal airway

morphology and disease progression in COPD[166–168]. Areas deficient in bronchial IgA show increased submucosal thickening and airway remodelling, enhanced T cell presence and increased bacterial infection[167–169]. Polymeric immunoglobulin receptor (**pIgR**), which facilitates the transcytosis of IgA across the epithelium[170], is decreased in IgA deficient areas[167]. pIgR genetic knockout mice recapture spontaneous susceptibility to bacterial infection and airspace enlargement[171] which suggests an impaired ability to transport IgA to the apical surface performs an important role in COPD pathogenesis. Consequently, impaired antibody responses in patients with COPD reduce the capacity for antibody-mediated effector functions and contribute to disease pathology.

In COPD, a link between acute exacerbations in chronic obstructive pulmonary disease (**AECOPD**) and antibody deficiencies has been observed[172,173]. Exacerbations are defined by acute and sustained worsening of the patient's condition beyond normal day-to-day variations that warrant additional treatment[174]. Over the course of a single year, patients with COPD can have multiple AECOPD events, each of which can contribute to decline in lung function, increased symptoms and progressively longer recovery times following each event[175–177]. The frequency of exacerbations is used to further classify patients by GOLD stage to assist with individual treatment strategies. GOLD A subjects are patients who have a low symptom score as assessed by the COPD Assessment Test (**CAT**) and fewer than one hospitalisation visit per year. GOLD B includes patients with a CAT score ≥ 10 plus fewer than one hospitalisation visit. GOLD C and D are patients who experienced > 2 moderate

to severe events or ≥ 1 hospitalisations with a CAT score < 10 and ≥ 10 respectively[149]. Given the frequency and associated health consequences of AECOPD, intervention strategies aimed to limit or stop exacerbation occurrence are needed.

A subset of patients who frequently suffer from COPD exacerbations were observed to have underlying primary antibody deficiency syndromes including, common immunodeficiency and specific antibody deficiency in two retrospective cohorts[172,173]. When patients diagnosed with an antibody deficiency syndrome were treated with Ig replacement therapy (intravenous and subcutaneous Ig) hospitalisations were reduced[172,173]. These findings suggest that antibodies perform a role protecting individuals against AECOPD, and that antibody deficiencies may represent an important predisposing factor for AECOPD occurrence.

1.3.1.3. B cell-mediated autoimmunity in COPD

Although the negative impact of cigarette smoke on the lungs is well known, perhaps less publicised is the risk cigarette smoke poses to the development of autoimmune disease such as rheumatoid arthritis and systemic lupus erythematosus[178]. Chronic inflammation, even in the absence of insult, and autoimmune flares/exacerbation events characterise aspects of both autoimmune disease and COPD. Given that cigarette smoking is a major risk factor for the development of COPD as well as autoimmune conditions, and the commonality in certain disease aspects, it has been hypothesised that COPD has an autoimmune component[179]. To this end, increased B cells[54] and lymphoid follicles[161] in COPD, even following cigarette smoking cessation, support a

break in an individual's immune tolerance leading to B cell-mediated autoimmunity. Thus, an autoimmune component may contribute to the chronic inflammation observed in patients with COPD.

Indeed, between a quarter to two-thirds of patients with COPD have increased serum autoantibody titres[180–182]. Notably, the percentage of patients with COPD who have increased serum autoantibody levels varies vastly between studies. This wide range may be a consequence of different assay protocols and the autoantigen specificities selected. For example, studies have focused on the use of indirect immunofluorescence and enzyme-linked immunosorbent assays (**ELISA**) to evaluate autoantibodies in COPD. Indirect immunofluorescence studies rely on the detection of deposited autoantibodies on either genetically engineered cell lines or whole lung tissue[180–183]. Consequently, there is inherit variability between studies and the precise autoantigens targeted and autoantibodies detected. In contrast, ELISAs assess specific specificities and consequently are biased based on specificities selected. To remedy this, there have been calls for consensus on tested autoantibodies. Broader human proteome microarray platforms have been used to offer insight into specific autoantibody specificities most changed[184–187]. These studies highlight the diverse composition of autoantigens expressed in COPD. However, these broader assessments have been limited by the use of single cohort studies. Notably, no specific autoantibodies, such as anti-elastin autoantibodies, have been fully replicated between independent COPD cohorts[188–190]. Studies to validate the presence of autoantibodies in COPD are needed.

COPD autoantibodies have been grouped into two major classes, anti-nuclear antibodies (**ANA**) and anti-tissue antibodies (**AT**)[181]. ANA are intracellular and nuclear antigens (including DNA and ribonucleic acid (**RNA**)) and are often presented under homeostatic conditions to mediate clearance of apoptotic cells[127,191,192]. To note, patients with COPD have increased epithelial cell apoptosis, suggesting a wealth of autoepitopes for ANA generation[193,194]. Conversely, AT are antigens found within the extracellular matrix, on the cell surface or soluble in the bloodstream[181]. Elevated serum AT correlated more strongly with declines in lung function and gas exchange than serum ANA in COPD[181]. Extracellular matrix breakdown and chronic exposure to inflammatory mediators in COPD presents opportunity for a break in tolerance and AT generation in patients. This increased risk for autoantibody generation in COPD is supported by elevated serum autoantibodies particularly in emphysema-dominant patients with COPD[186]. To note, emphysema-dominant COPD is associated with a B cell transcriptional signature[163]. Given that AT autoantibodies are linked to break down in the extracellular matrix, as occurs in emphysema, it is proposed that AT autoantibodies are derived from, and contribute to, the parenchyma destruction and subsequent airspace enlargement in patients with emphysema-dominant COPD.

1.3.1.4. Autoantibody function in disease and homeostasis

Autoantibody function can be broadly separated into type II and type III hypersensitivity reactions in autoimmune disease. Type II hypersensitivity reactions occur in response to antibody deposition on extracellular antigens[195]. Bound autoantibodies mediate classical complement pathway deposition[196],

antibody-dependent cellular phagocytosis by macrophages[197] or natural killer cell-mediated antibody-dependent cellular cytotoxicity[131], ultimately leading to excessive inflammation and tissue destruction. Examples of type II hypersensitivity autoimmune disease are immune haemolytic anaemia and myasthenia Gravis[198]. On the other hand, type III hypersensitivity reactions are caused by the deposition of soluble immune complexes in the small vessels[195]. Once deposited, immune complexes activate complement and inflammatory responses leading to the destruction of the surrounding tissue[199]. Autoimmune diseases such as rheumatoid arthritis and systemic lupus erythematosus are a consequence of type III hypersensitivities[199]. In COPD, complement is observed to be deposited in the small airways[180]. Given that cigarette smoking is associated with type III hypersensitivity reactions such as rheumatoid arthritis and systemic lupus erythematosus, it is proposed that immune complexes deposit in the small airways and promote airspace enlargement in COPD.

Important to consider is the protective role autoantibodies perform in homeostasis alongside any proposed hypersensitivity reactions[192,200,201]. Healthy individuals have circulating autoantibodies which do not confer adverse autoimmune pathology[202,203]. Typically, tissue homeostatic autoantibodies are associated with B-1 cells. In addition to neutralising a microbe's infectious ability, the cross-reactive nature of nAb enables B-1 cells to target autoantigens. Studies suggest these autoreactive nAb mediate opsonisation and efferocytotic clearance of apoptotic cells via recognition of self-antigen in healthy individuals[121,204,205]. Therefore, not all autoantibodies are pathogenic and the presence of an autoantibody reservoir in healthy individuals is part of a normal

immune response. These homeostatic autoantibodies are important contributors to tissue maintenance as well as providing an innate microbial defence.

1.3.2. Interstitial lung disease (ILD)

Consisting of over 200 parenchymal lung diseases, ILD is an overarching term for respiratory diseases which result in impaired gas exchange and lung scarring[206]. ILDs are defined by the specific radiological patterns resulting from aberrant cellular proliferation, inflammation and fibrosis in the lungs[207]. Genetic predisposition plus environmental, occupational and/or medical exposures are considered to trigger ILD development[206,208]. Moreover, exposure to tobacco smoke and other smoke related products is associated with the development of ILDs[208]. For instance, smoking-related respiratory ILDs include respiratory bronchiolitis, desquamative interstitial pneumonia, pulmonary Langerhans cell histiocytosis, smoking-related interstitial fibrosis, combined pulmonary fibrosis and emphysema, and IPF[206,208]. Notably, IPF is the most common ILD and in Canada affects an estimated 30 000 individuals[209].

1.3.2.1. Idiopathic pulmonary fibrosis (IPF) pathogenesis

A restrictive pulmonary disease of unknown aetiology, IPF is linked to a poor prognosis, limited response to current therapies, and high mortality rate in patients[207,208]. In particular current and ex-cigarette smokers have a 60% higher risk of developing IPF than non-smoking individuals[142]. The pathogenesis of IPF is currently not known; however, the current paradigm is that individuals with a genetic susceptibility for impaired barrier integrity, telomere shortening and/or cell senescence in epithelial cells are at increased risk of unresolved

alveolar epithelium damage following persistent microinjury[210]. Disrupted and abnormal epithelium consequently releases profibrogenic mediators such as transforming growth factor beta (**TGF-β**) into the pulmonary environment[210]. Subsequent recruitment of Mo-AM to the lungs is necessary for pulmonary fibrosis development[39,41,211]. Transcriptionally, abnormal epithelial cells and profibrotic AM are observed in IPF patients[212]. The release of TGF-β, IL-9 and IL-10 by macrophages and epithelial cells has been observed to drive pulmonary fibrosis[213,214]. The result of this inflammatory milieu is aberrant extracellular matrix deposition caused by the chronic differentiation of fibroblasts to activated myofibroblasts[215,216]. Furthermore, CCL18 released from macrophages and fibroblasts increases collagen production initiating a positive feedback loop which induces more CCL18 expression[217]. The excess extracellular matrix deposition contributes to the increasing matrix stiffness and mechanical stress that defines the restrictive nature of IPF and the associated progressive lung function decline. Matrix deposition instigates the peripheral and lower lobe bilateral reticulation and honeycombing scarring, in the absence of infection or cancer, which is used to diagnose IPF[207].

1.3.2.2. IPF and current smoking status

Despite current and former smoking being associated with a 60% higher risk of developing IPF[142], the impact of cigarette smoking on IPF prognosis is complex. Reports demonstrated that IPF patients who continue to smoke following diagnosis had a lower mortality rate[218,219]. Moreover, at clinical presentation IPF patients who were currently smoking had better pulmonary function[142,220]. However, when mortality rate was adjusted for age and disease severity in

separate cohorts, the observed prognostic benefit in current smoking patients was abolished[142,220]. Interestingly, in a Japanese IPF cohort demonstrated IPF patients who had never smoked had more frequent acute exacerbations than currently smoking patients when adjusted for disease severity and age[219]. The increased pulmonary function and less frequent exacerbation events in current smokers is currently considered in relation to a "healthy smoker effect" whereby patients with more advanced disease are more likely to have stopped smoking for health reasons[220]. To this end, it has been demonstrated that the longer an individual has stopped smoking the lower the risk of developing IPF[221]. The role of current smoking status and the influence of cigarette smoke on the development of IPF is still not fully understood.

1.3.2.3. Pulmonary macrophages in pulmonary fibrosis pathologies

Pulmonary macrophages have been implicated in lung fibrosis pathogenesis; however, increasing evidence demonstrates that specific macrophage subpopulations are more critical to progression than others. Clinical studies show an association of increased $CD71^{Neg}$ AM (human Mo-AM-like cell) with worsened pathology in IPF patients[222]. In elegant inducible knockout and transgenic models, a key role for Mo-AM has been demonstrated in bleomycin and asbestos models of lung fibrosis[39,41,211]. To note, these recruited profibrotic Mo-AM persisted in the lungs for at least ten months post bleomycin challenge[39]. In contrast, the loss of IM1 cells was associated with increased fibrosis following bleomycin administration[43]. The effect of cigarette smoke on the composition and function of these macrophage subpopulations in pulmonary fibrosis is not known.

Accumulating evidence suggests a role for circulating profibrotic monocytes and M2-polarised macrophages, also known as alternatively activated macrophages, in the development of fibrotic lung disease[217,223–225]. Notably, M2-polarised macrophages were observed to accumulate in the lungs of IPF patients[217] and when depleted in mouse models of pulmonary fibrosis aberrant fibrogenesis was attenuated[225]. While profibrotic macrophages primarily express M2-like markers in pulmonary fibrosis models, a M1-like expression profile is still evident, demonstrating that macrophage polarisation is a spectrum[39]. The influence of cigarette smoke on the immune environment in the context of macrophage polarisation in IPF is not known.

1.4. SUMMARY

Cigarette smoke is a complex insult which has both proinflammatory and immunosuppressive roles. The mechanisms by which cigarette smoke impacts the immune system resulting in respiratory disease is not fully understood. This thesis focuses on the impact of cigarette smoke on the pulmonary immune response. In **chapter II**, we determined the feasibility of using sputum to assess antibodies and then investigate the impact of COPD and smoking status on sputum antibody levels. **Chapter III** expands on **chapter II** and evaluated the presence of autoantibodies in the sputum and serum of patients with COPD, healthy controls and asymptomatic smokers. The intent of these studies was to identify a biomarker for COPD diagnosis. In **chapter IV**, we investigated the impact of cigarette smoke on the composition and function of pulmonary macrophage subpopulations using a mouse model of concurrent cigarette smoke

exposure and bleomycin-induced lung injury. This study sought to identify the specific macrophage subpopulations that contribute to cigarette smoke-associated respiratory disease development.

1.5. CENTRAL PARADIGM

Cigarette smoke is a complex insult that distorts immune homeostasis contributing to irreversible respiratory disease. While medications exist that alleviate symptoms; to date, there is no cure for diseases such as COPD and IPF. Consequently, identifying subjects early in the course of disease is essential to direct early intervention strategies and maintain lung function. Reliable and easy to assess biomarkers are needed to identify those at risk of respiratory disease and susceptible to accelerated disease progression. We proposed antibodies and autoantibodies offered an accessible immune component which to identify the development of cigarette smoke-associated respiratory disease. In addition to research aimed at identifying those with disease, we also investigated cellular immune mechanisms which contribute to the pathobiology of cigarette smoke-associated respiratory disease. Central to the pathogenesis of several respiratory diseases is the accumulation of pulmonary macrophages. To date, the pulmonary macrophage subpopulations altered in cigarette smoke exposure is not known. We postulated that cigarette smoke would be associated with a shift in pulmonary macrophage subpopulations, expanding monocyte-derived populations. We proposed this expansion of monocyte-derived populations would contribute to exacerbated tissue remodelling following acute lung injury. To address these concepts, we proposed the following specific hypothesises.

1.5.1. Study I. Evaluating the impact of smoking status on total sputum and serum antibodies in patients with COPD

To date, little is known regarding antibodies in the sputum of patients with COPD. Therefore, in this study, we characterised immunoglobulin isotypes in the sputum of healthy individuals, cigarette smokers with normal lung function, and patients with COPD. *We hypothesised that immunoglobulins would be detectable in the sputum of healthy individuals and patients with COPD. We further hypothesised that patients with COPD would have decreased sputum immunoglobulin levels as compared to healthy control subjects.*

Objective 1. Investigate the presence of immunoglobulins in the sputum.

Objective 2. Evaluate the impact of COPD, and smoking status, on total sputum antibodies.

1.5.2. Study II. Investigating the expression of sputum and serum autoantibodies in patients with COPD

This second study focused on evaluating the presence of autoantibodies in the sputum. Given that COPD is a respiratory disease, we proposed that profiling the sputum would better reflect immune processes occurring at the site of injury. The premise of this study was that assessing sputum autoantibodies, as compared to serum autoantibodies, in COPD would offer direct insight into pulmonary autoimmune processes and serve as a diagnostic marker of COPD status. *We hypothesised that the diversity of autoantibodies would be increased in the sputum as compared to the serum of patients with COPD. We further hypothesised that patients with COPD, in particular patients with emphysema-*

dominant COPD, wound have increased sputum and serum autoantibody levels compared to control subjects.

Objective 1. Measure sputum and serum autoantibody presence in patients with COPD.

Objective 2. Assess autoantibody specificities differentially expressed in patients with COPD compared to healthy and asymptomatic controls.

Objective 3. Evaluate autoantibody expression in patients with COPD with predominant emphysema.

1.5.3. Study III. Assessing the composition and function of macrophage subpopulations in a mouse model of concurrent cigarette smoke and bleomycin-induced lung injury

In this study, we investigated the effect of cigarette smoke on composition and function of macrophage subpopulations. Macrophages perform a key role in respiratory disease development. We used a well characterised mouse model of cigarette smoke-induced inflammation and bleomycin-induced lung injury to address the impact of cigarette smoke exposure on macrophage subpopulations composition and function. *We hypothesised that cigarette smoke exposure would expand monocyte-derived AM and IM subpopulations. We hypothesised further that cigarette smoke-expanded monocyte-derived populations would exacerbate tissue remodelling in a mouse model of bleomycin-induced lung injury.*

Objective 1. Investigate the composition of macrophage subpopulations following cigarette smoke exposure.

Objective 2. Assess the origin of macrophage subpopulations altered in cigarette smoke exposure.

Objective 3. Investigate the functional differences of macrophage subpopulations using a mouse model of bleomycin-induced lung injury.

CHAPTER II: IMMUNOGLOBULIN LEVELS IN SPUTUM

Evaluating the impact of smoking status on total sputum and serum antibodies in patients with COPD

2.1. Study Outline

Antibodies perform key roles in the immune defence and maintaining tissue homeostasis throughout the respiratory tract. For instance, IgA in the upper respiratory tract and IgG in the lower respiratory tract have been shown to provide a robust defence against viral infections[226]. These antibody classes are decreased in the serum of cigarette smokers and patients with COPD[165,227,228]; however, the presence of antibodies in the respiratory tract is much less understood.

The respiratory environment can be assessed through biopsy, resection, lavage or sputum collection. As compared to other methods the collection of sputum is non-invasive and can be undertaken at hospitals and clinics worldwide. Sputum is mucous material from the lower airways that can be spontaneously expectorated in a focused cough attempt. Furthermore, sputum can be induced following three seven-minute sessions of nebulised hypertonic saline (using increasing saline concentrations of 3%, 4%, and 5% respectively) each followed by a focused cough attempt. Given a sufficient mucous plug weight, ≥50 mg, samples are further processed using dithiothreitol (**DTT**)[229] or phosphate-buffered saline (**PBS**)[230] agitation for mucous dispersion and release of immune mediators and cells. Sputum analysis has been used in studies related

to asthma and infectious disease[231–234]; however, the use of sputum as a matrix for antibody assessment is much less understood.

In this study, we assessed the presence of total antibodies in cigarette smokers and patients with COPD in two independent COPD cohorts. The first cohort was recruited from the Guangzhou Institute of Respiratory Health (**GIRH**), Guangdong China. The second was a multicentre cohort spanning clinics in North America and Europe run by Janssen Pharmaceutical; Companies of Johnson & Johnson (Airways Disease Endotyping for Personalized Therapeutics; **ADEPT**). All participants consented and study design was approved by the Ethics Committee of the First Affiliated Hospital of Guangzhou Medical University (#201722), or Janssen Pharmaceutical and subsequently Hamilton Integrated Research Ethics Board (#2031). These cohorts enabled us to sample Chinese, Black and Caucasian individuals to comprehensively assess antibodies in patients with COPD. We assessed 251 sputum supernatants for the presence of total IgM, IgG and IgA in individuals with and without respiratory disease by ELISA. We further stratify the impact of smoking and COPD status on antibody levels. This study offers insight into the use of sputum as a matrix with which to assess Ig classes in patients with COPD and expands our clinical knowledge of lower airway antibody levels.

2.2. Current smoking status is associated with reduced sputum immunoglobulin M and G expression in chronic obstructive pulmonary disease

Steven P. Cass, Yuqiong Yang, Jing Xiao, Joshua JC. McGrath, Matthew F. Fantauzzi, Danya Thayaparan, Fengyan Wang, Zhenyu Liang, Fei Long, Christopher S. Stevenson, Rongchang Chen and Martin R. Stampfli.

Citation: Cass SP *et al.* Eur Respir J. 2021 Feb 4;57(2):1902338. doi:10.1183/13993003.02338-2019.

Dr Martin Stampfli and I conceived and designed the experiments. Drs Yang and Xiao plus Josh McGrath, Matt Fantauzzi, Danya Thayaparan and I performed the experiments. Dr Stampfli and I analysed and interpreted the data. Drs Yang, Wang, Liang, Stevenson and Chen provided clinical samples. Drs Stampfli, Chen, Long and Liang provided materials. Dr. Stampfli and I wrote and edited the manuscript.

To the Editor:

The relationship between smoking status and total immunoglobulin (Ig) levels in patients with chronic obstructive pulmonary disease (COPD) is not fully understood. Decreased Ig levels have been observed in patients with COPD (1–4), a disease largely attributed to current or former smoking, and cigarette

smokers (5,6). These studies focused predominately on serum (systemic) or salivary (upper respiratory tract) Igs. Levels of Igs in induced sputum, a more direct measure of airway Igs, are less well studied. Given the vital role Igs perform in microbial defence and tissue homeostasis, we assessed airway Igs in induced sputum of smokers and patients with COPD.

To begin, we obtained 99 de-identified, banked, frozen induced sputum supernatant and matched serum samples from the Airways Disease Endotyping for Personalised Therapeutics (ADEPT) study (six sites, European and North American locations; Clinical Trial #NCT01274507; Janssen Pharmaceutical). All subjects provided written informed consent to participate (Hamilton Integrated Research Ethics Board Project #2031). Control subjects had no clinically significant medical condition, airflow limitation, or a history of any chronic pulmonary disease (n=45; 44.4% male; mean predicted $\%FEV_1$: 106.5% ± 11.0%). Control subjects classified as non- or ex-smoker (NES) had quit smoking for greater than one year prior to sample collection and had ≤ 10 smoking pack-year history. Current smoking status was self-reported and confirmed by urinary cotinine. Patients with COPD were diagnosed by a physician and identified as having an $FEV_1/FVC < 0.7$, FEV_1 bronchodilator reversibility < 12%, and postbronchodilator FEV1 value < 80%. Subjects were enrolled during stable disease, defined by a period of no exacerbations within three months prior to sample collection. COPD stage was classified by severity of lung function, ≥ 50% (n=45; 64.4% male; mean predicted $\%FEV_1$: 57.7% ± 11.6%) and < 50% predicted FEV_1 (n=9; 66.7% male; mean predicted $\%FEV_1$: 45.1% ± 5.5%).

Total IgM, IgG, and IgA in induced sputum supernatant and serum was assessed by ELISA as per manufacturer's instructions (BMS2091/ BMS2096/ BMS2098; ThermoFisher Scientific, ON, Canada). Blood draw and sputum induction (7) (as per Pizzichini *et al.* with a plug weight of ≥ 50mg and squamous cell content ≤ 20%) were performed during the same visit. All sputum samples were processed using dithiothreitol (DTT) for optimal mediator release from mucus plugs. We observed no change in total sputum IgM, IgG, and IgA based on COPD severity, sex, body mass index, nor age (data not shown). Bacterial colonisation has been associated with altered Ig levels but was not assessed in this study (8). ADEPT control subjects included current (46.7%), ex- (4.4%) and never smokers (48.9%). All patients with COPD had a smoking history of at least 10 pack years; 51.1% of mild to moderate COPD (≥ 50% predicted FEV_1) and 55.6% of severe COPD (< 50% predicted FEV_1) subjects were current smokers. Notably, current smoking status was associated with decreased total sputum IgM. Moreover, sputum IgG showed a trend towards decline in current smokers (p value = 0.07) (**Figure 1A**). In a previous study, decreased induced saliva IgM and IgG were observed in cigarette smokers (9), suggesting that cigarette smoke suppresses Igs throughout the respiratory tract. Moreover, serum total Ig levels were not changed based on any available clinical parameters, including current smoking status (data not shown). Given the decreased sputum Ig trends in current smokers, we next performed a power calculation to determine sufficient sample size for a sputum Ig and smoking status study. We calculated that 56 subjects per group would be required to accurately assess IgG trends based on an alpha of 0.05 and beta of 0.2. To this

end, a second independent cohort was recruited from the Guangzhou Institute of Respiratory Health, China (GIRH).

A total of 152 induced sputum supernatant samples were collected from subjects recruited by the GIRH (Clinical Trial #NCT03240315; First Affiliated Hospital of Guangzhou Medical University). Of those patients, 54 were current smokers and 98 non/ex-smokers. This study followed inclusion criteria from the Evaluation of COPD Longitudinally to Identify Predictive Surrogate Endpoints (ECLIPSE) study. While these inclusion criteria were less stringent than the ADEPT study, subject characteristics between the cohorts were comparable, with the exception of sex since the GIRH cohort was entirely male, which is a reflection of the high male smoking prevalence in China. Subject stratification into lung function groups was identical to that of the ADEPT study, with COPD patients being defined as having an $FEV_1/FVC < 0.7$ and subsequent predicted FEV_1 value either $\geq 50\%$, (mild to moderate) or $< 50\%$ (severe). Included in this cohort were 39 control subjects (mean predicted $\%FEV_1$: 99.1% ± 9.2%), 52 patients with mild to moderate COPD (mean predicted $\%FEV_1$: 75.3% ± 15.7%), and 61 patients with severe COPD (mean predicted $\%FEV_1$: 36.0% ± 8.9%). Induced sputum supernatant was collected as per Bafadhel *et al.* and processed using phosphate buffered saline (PBS) (10). Total IgM, IgG, and IgA were measured by ELISA in the GIRH cohort as for the ADEPT study. Mirroring observations in the ADEPT cohort, current smoking status, but not COPD severity or other clinical parameters, was associated with decreased induced sputum IgG and IgM in the GIRH cohort (**Figure 1A**). While current smoking status was not associated with decreased IgA (**Figure 1A**), total

sputum IgA was decreased in severe COPD as compared to subjects with milder disease and controls with normal lung function (**Figure 1B**), mirroring previous observation in COPD (1,2).

Of note, the range of total sputum IgM and IgA were variable between the cohorts. Procedural differences in sputum processing, likely contribute to observed differences in total Ig recovery between cohorts; ADEPT samples were processed using DTT while GIRH samples were processed in PBS. To address DTT interference in this ELISA system we processed Ig standard with or without 0.1% DTT for 15mins, at which timepoint the sample was diluted to 0.025% DTT with PBS, and added to the ELISA plate mimicking Pizzichini *et al.* (11). We observed DTT interference in Ig standard binding signal for IgM (54.7% reduction; PBS: 130.1 ng/mL ± 17.7, DTT: 59.0 ng/mL ± 5.0, p value = <0.0001) and IgA (7.7% reduction; PBS: 8.0 ng/mL ± 0.3, DTT: 7.3 ng/mL ± 0.5, p value = 0.02). IgG standard binding signal was increased 15.5% (PBS: 115.2 ng/mL ± 10.6, DTT: 133.1 ng/mL ± 10.2, p value = 0.01) with the inclusion of a DTT processing step. The DTT processing step in the ADEPT cohort contributes to the reduce recoverable total IgM compared to the GIRH cohort. Notably, the increased IgA yield in the ADEPT cohort is likely attributable to improved IgA release from the mucus plug (12). Given, similar cigarette smoking trends were conserved between cohorts, we propose the GIRH cohort validated the ADEPT cohort current smoking status observation. Overall, despite the difference in sample processing, current smoking status was associated with reduced sputum IgM and IgG in both cohorts.

Next, we assessed the relationship between current smoking status and COPD severity with regard to sputum Ig levels. In subjects with normal lung function, current smoking status was not associated with any change in sputum IgM, IgG, nor IgA (**Figure 1C**). GIRH control subjects included current (38.5%), ex- (38.5%) and never smokers (23.1%). In contrast, current smoking status was associated with decreased sputum IgM and IgG in mild to moderate COPD (38.5% current smokers). Of note, subjects with the most severe disease did not have decreased IgM nor IgG based on current smoking status (31.1% current smokers). While the mechanisms are currently not understood, it is possible that less abundant T cell help in patients with early disease that smoke contribute to lower IgM and IgG levels (13). We did not observe changes in total sputum IgA in either mild to moderate or severe disease based on current smoking status. It is plausible that the development of lymphoid follicles and follicle-associated IgA may compensate for mechanisms leading to decreased sputum IgA (14). Alternatively, increased expression of transforming growth factor beta in patients with COPD (15) may lead to preferential IgA class switching (16). Further research is warranted to investigate how cigarette smoke reduces sputum IgM and IgG levels. Overall, current smoking status was associated with reduced sputum IgM and IgG in subjects with mild to moderate COPD, but not in subjects with normal lung function or subjects with severe disease.

Inhaled corticosteroids (ICS) form a major part of the treatment strategy for COPD patients. ICS have previously been observed to be immunosuppressive and, consequently, may reduce Ig levels in patients. We

sought to understand the impact of ICS upon induced sputum Ig levels. In the GIRH COPD cohort, 42.3% of mild to moderate and 78.7% of severe COPD subjects were receiving ICS treatment at the time of sample collection. However, ICS usage was not associated with decreased total Ig isotype in either COPD severity (**Figure 1D**). This highlights the impact of current smoking status on reduced levels of sputum IgM and IgG in patients with COPD.

In closing, we investigated total induced sputum supernatant IgM, IgG, and IgA in two independent cohorts. Current smoking status in subjects with mild to moderate COPD was associated with reduced total induced sputum IgM and IgG. This reduction was not associated with current ICS usage. Our findings highlight the need for studies investigating mechanisms of cigarette smoke-mediated Ig immunosuppression, specifically during early disease progression. Of note, in two independent retrospective studies, COPD-related hospitalisations were reduced in a subset of COPD frequent exacerbators observed to have primary antibody deficiency syndromes following treatment with Ig replacement therapy (intravenous (IV) and subcutaneous Ig) (3,4). While the impact of IVIg therapy on respiratory Ig is not known, targeted treatment of respiratory Ig may improve COPD-related hospitalisations in subjects with low Igs. Notably, we observed no difference in total serum Ig measured, emphasising the need for sampling induced sputum supernatant or bronchoalveolar lavage for assessment of immune processes in COPD. Ultimately, this study highlights the need for further investigation into the impact of current cigarette smoking upon respiratory tract Igs in COPD patients.

REFERENCES

1. Pilette, C. *et al.* Reduced epithelial expression of secretory component in small airways correlates with airflow obstruction in chronic obstructive pulmonary disease. Am. J. Respir. Crit. Care Med. 163, 185–194 (2001).

2. Polosukhin, V. V. *et al.* Bronchial secretory immunoglobulin a deficiency correlates with airway inflammation and progression of chronic obstructive pulmonary disease. Am. J. Respir. Crit. Care Med. 184, 317–327 (2011).

3. Cowan, J. *et al.* A retrospective longitudinal within-subject risk interval analysis of immunoglobulin treatment for recurrent acute exacerbation of chronic obstructive pulmonary disease. PLoS One 10, 1–12 (2015).

4. McCullagh, B. N. *et al.* Antibody deficiency in patients with frequent exacerbations of Chronic Obstructive Pulmonary Disease (COPD). PLoS One 12, 1–13 (2017).

5. McMillan, S. A., Douglas, J. P., Archbold, G. P., McCrum, E. E. & Evans, A. E. Effect of low to moderate levels of smoking and alcohol consumption on serum immunoglobulin concentrations. J. Clin. Pathol. 50, 819–22 (1997).

6. Gonzalez-Quintela, A. *et al.* Serum levels of immunoglobulins (IgG, IgA, IgM) in a general adult population and their relationship with alcohol consumption, smoking and common metabolic abnormalities. Clin. Exp. Immunol. 151, 42–50 (2008).

7. Pizzichini, E., Pizzichini, M. M. M., Efthimiadis, A., Hargreave, F. E. & Dolovich, J. Measurement of inflammatory indices in induced sputum: Effects of selection of sputum to minimize salivary contamination. Eur. Respir. J. 9, 1174–1180 (1996).

8. Murphy, T. F., Brauer, A. L., Grant, B. J. B. B. & Sethi, S. Moraxella catarrhalis in chronic obstructive pulmonary disease: Burden of disease and immune response. Am. J. Respir. Crit. Care Med. 172, 195–199 (2005).

9. Norhagen Engström, G. & Engström, P. E. Effects of tobacco smoking on salivary immunoglobulin levels in immunodeficiency. Eur. J. Oral Sci. 106, 986–91 (1998).

10. Bafadhel, M. *et al.* Profiling of sputum inflammatory mediators in asthma and chronic obstructive pulmonary disease. Respiration 83, 36–44 (2012).

11. Pizzichini, E. *et al.* Indices of airway inflammation in induced sputum: Reproducibility and validity of cell and fluid-phase measurements. Am. J. Respir. Crit. Care Med. 154, 308–317 (1996).

12. Louis, R. *et al.* The effect of processing on inflammatory markers in induced sputum. Eur. Respir. J. 13, 660–667 (1999).

13. Cruz, T. *et al.* Multi-level immune response network in mild-moderate Chronic Obstructive Pulmonary Disease (COPD). Respir. Res. 20, 1–9 (2019).

14. Ladjemi, M. Z. *et al.* Increased IgA Expression in Lung Lymphoid Follicles in Severe COPD. Am. J. Respir. Crit. Care Med. 199, 592–602 (2019).

15. Takizawa, H. *et al.* Increased expression of transforming growth factor-β1 in small airway epithelium from tobacco smokers and patients with chronic obstructive pulmonary disease (COPD). Am. J. Respir. Crit. Care Med. 163, 1476–1483 (2001).

16. Dullaers, M. *et al.* A T Cell-Dependent Mechanism for the Induction of Human Mucosal Homing Immunoglobulin A-Secreting Plasmablasts. Immunity 30, 120–129 (2009).

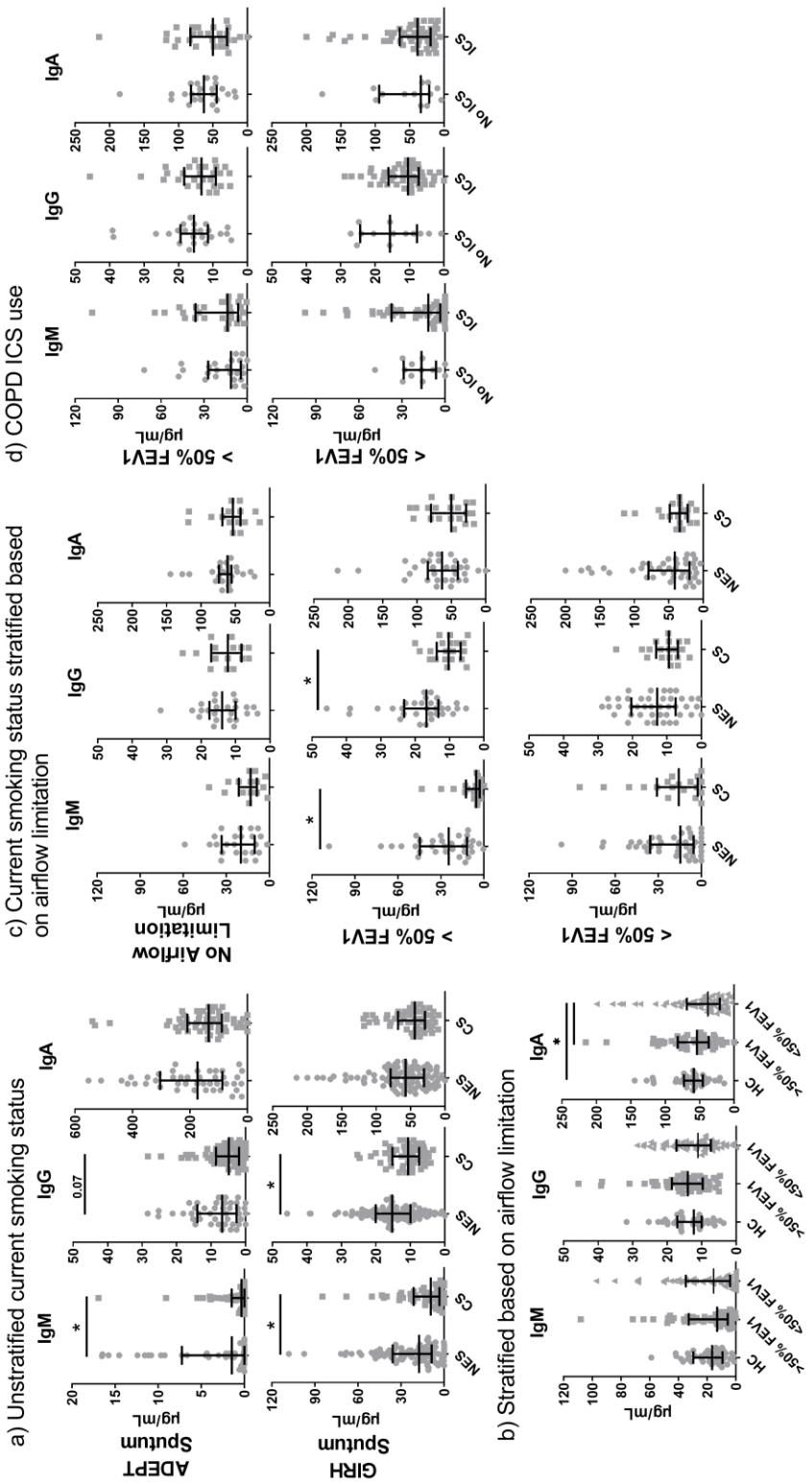
a) Unstratified current smoking status
b) Stratified based on airflow limitation
c) Current smoking status stratified based on airflow limitation
d) COPD ICS use
IgM
IgG
IgA
pg/mL
ADEPT Sputum
GIRH Sputum
No Airflow Limitation
< 50% FEV1
> 50% FEV1
NES
CS
HC
No ICS
ICS
0.07
*

Figure 1. Current smoking status is associated with reduced IgM and IgG levels in the sputum of patients with COPD. a) Total sputum IgM, IgG, and IgA in the Airways Disease Endotyping for Personalized Therapeutics (ADEPT) study and the Guangzhou Institute of Respiratory Health (GIRH) cohorts stratified based on current smoking status. b) Total sputum IgM, IgG, and IgA in the GIRH cohort classified based on airflow limitation. c) Current cigarette smoking status impact on total sputum IgM, IgG, and IgA in the GIRH cohort stratified by airflow limitation. d) Sputum immunoglobulin expression based on COPD severity and inhaled corticosteroid (ICS) use in the GIRH cohort. Data in (a-d) are represented as median and interquartile range. Statistical differences were determined using two-tailed Mann-Whitney test (a, c-d). In (b), statistical differences were determined using Kruskal-Wallis test with Dunn's multiple comparison test. * $p = <0.05$. FEV1 - forced expiratory volume in one second. HC – healthy control/no airflow obstruction. NES - non- and ex-smoker. CS - current smoker.

CHAPTER III: IgG AND IgM AUTOANTIBODIES IN COPD

Investigating the expression of sputum and serum autoantibodies in patients with COPD

3.1. Study Outline

Autoantibodies in COPD are proposed to contribute to disease progression. For instance, increased serum autoantibodies have been associated with emphysema in patients with COPD[181,186]. However, autoantibody studies in COPD are widely variable and suggest that anywhere from a quarter to two-thirds of patients have elevated autoantibody levels[180–182]. For example, anti-elastin autoantibodies are reported to be increased in one cohort, unchanged in another, and decreased in a third cohort[188–190]. A consensus on a specific autoantibody profile in COPD is needed to enable investigators to understand the contribution of autoantibodies to disease pathogenesis.

In this study, we use a broad autoantibody array approach to comprehensively assay the ADEPT and GIRH COPD cohorts for the presence of autoantibodies. Expanding on previous studies which focused on serum autoantibodies, we assessed matched serum and sputum autoantibodies in all participants. We proposed that, as COPD is a respiratory disease, assessing the local (sputum), rather than the systemic (serum) environment, would provide a conserved autoantibody profile for patients with COPD. Therefore, enabling the identification of a conserved set of specificities for further functional analysis and provide a biomarker to identify those subjects susceptible to accelerated

lung function decline. As healthy individuals have circulating autoantibodies[202,203], all analysis must be undertaken in relation to relevant controls and not in isolation as in some previous studies. Consequently, this study included healthy and asymptomatic smokers for direct comparison to patients with COPD. Ultimately, the presence of dysregulated autoantibodies in patients with COPD compared to control subjects would be indicative of a break in immune tolerance and a contributor to disease progression.

3.2. Differential expression of sputum and serum autoantibodies in patients with chronic obstructive pulmonary disease

Steven P. Cass, Anna Dvorkin-Gheva, Yuqiong Yang, Joshua JC. McGrath, Danya Thayaparan, Jing Xiao, Fengyan Wang, Manali Mukherjee, Fei Long, Tao Peng, Parameswaran Nair, Zhenyu Liang, Christopher S. Stevenson, Quan-Zhen Li, Rongchang Chen and Martin R. Stampfli.

Reprint: Reproduced with permission of the © APS 2021: American Journal Physiology-Lung, Cellular, and Molecular Physiology. DOI: 10.1152/ajplung.00518.2020; Published 18 June 2021.

Citation: Cass SP *et al.* Am J Physiol Lung Cell Mol Physiol. 2021 Jun 1;320(6):L1169-L1182.

Dr Martin Stampfli and I conceived and designed the experiments. Drs Yang, Xiao, Mukherjee, and Li plus Josh McGrath, Danya Thayaparan, and I performed the experiments. Drs Stampfli, Dvorkin-Gheva and I analysed and interpreted the data. Drs Yang, Wang, Liang, Nair, Stevenson and Chen

provided clinical samples. Drs Stampfli, Chen, Peng, Long, Liang and Li provided materials. Dr Stampfli and I wrote and edited the manuscript.

ABSTRACT

Chronic obstructive pulmonary disease (COPD) is a complex and progressive respiratory disease. Autoimmune processes have been hypothesised to contribute to disease progression; however, the presence of autoantibodies in the serum has been variable. Given that COPD is a lung disease, we sought to investigate whether autoantibodies in sputum supernatant would better define pulmonary autoimmune processes. Matched sputum and serum samples were obtained from the Airways Disease Endotyping for Personalised Therapeutics (ADEPT) study and at the Guangzhou Institute of Respiratory Health (GIRH). Samples were collected from patients with varying severity of COPD, asymptomatic smokers and healthy control subjects. IgG and IgM autoantibodies were detected in sputum and serum of all subjects in both cohorts using a broad-spectrum autoantigen array. No differences were observed in sputum autoantibodies between COPD and asymptomatic smokers in either cohort. In contrast, 16% of detectable sputum IgG autoantibodies were decreased in COPD subjects compared to healthy controls in the ADEPT cohort. Compared to asymptomatic smokers, approximately 13% of detectable serum IgG and 40% of detectable serum IgM autoantibodies were differentially expressed in GIRH COPD subjects. Of the differentially expressed specificities, anti-nuclear autoantibodies were predominately decreased. A weak correlation

between increased serum IgM anti-tissue autoantibodies and a measure of airspace enlargement was observed. The differential expression of specificities varied between the cohorts. In closing, using a comprehensive autoantibody array, we demonstrate that autoantibodies are present in COPD subjects, asymptomatic smokers and healthy controls. Cohorts displayed high levels of heterogeneity, precluding the utilisation of autoantibodies for diagnostic purposes.

INTRODUCTION

Chronic obstructive pulmonary disease (COPD) is a debilitating respiratory disease defined by progressive airflow limitation and lung function decline (12). Estimated to be the seventh-leading cause of years of life lost (11), COPD caused 3 million deaths worldwide in 2015 (39). The predominate risk factor for COPD is cigarette smoke exposure (12); however, smoking cessation is insufficient to halt disease progression (13, 15, 34, 37). Mechanisms that contribute to the progressive lung function decline observed in COPD are poorly understood. Given the morbidity and mortality associated with COPD, a greater understanding of the mechanisms leading to disease progression is warranted.

An autoimmune component has been hypothesised to contribute to the persistent chronic inflammation observed in COPD (1). Both naïve B cells and cells expressing the plasma cell marker CD138+ accumulate, even following smoking cessation, in the lungs of patients with COPD (13, 15). Tertiary lymphoid tissues containing B cell follicles have been reported to develop in patients with severe disease which to date have an unknown function (29). A B

cell gene signature consisting of transcripts associated with B cell recruitment, immunoglobulin transcription and activation was observed and associated with actively proliferating B cells in lymphoid follicles in emphysema dominant COPD (9). Notably, elevated serum autoantibodies are found in anywhere between one quarter to two-thirds of COPD subjects (3, 10, 26) and have been associated with emphysema (26, 27).

The percentage of COPD subjects with differential serum autoantibody levels differs between studies. This is reflected by the variable expression of singular specificities such as anti-elastin (4, 16, 32). To clarify the presence of serum autoantibodies in COPD, broad human proteome microarray assessments have been undertaken but are limited by small single centre cohort studies (17, 21, 27, 36). Given that COPD is a respiratory disease, we hypothesised that autoantibody measurements in sputum (expectorated matter from the lower respiratory tract) would exhibit increased abundance and greater reproducibility than serum. For instance, studies have shown a subset of patients with severe asthma had sputum autoantibodies, absent from the serum, which increased compared to controls (24). Thus, sputum supernatant offers a matrix with which to directly assess the role of B cell-mediated autoimmunity in COPD pathogenesis.

To address whether a B cell-mediated autoimmune component contributes to chronic inflammation in COPD, we retrospectively assessed two independent COPD cohorts. We used a validated 128-plex autoantigen array to comprehensively assess common autoantibodies associated with autoimmune

diseases. Using this approach, banked, matched sputum and serum samples from subjects with normal lung function and COPD patients were evaluated for common autoantibodies.

MATERIAL AND METHODS

Study population

Cohort one consisted of 115 banked, matched frozen sputum supernatant and serum samples from the cross-sectional Airways Disease Endotyping for Personalised Therapeutics (ADEPT) study (six sites, European and North American locations; Clinical Trial #NCT01274507; Janssen Pharmaceutical). Included in this cohort were healthy controls (HC; never-smokers or ex-smokers who had quit for ≥ 1 year prior to the initial visit and had a smoking history of < 10 pack-years), asymptomatic smokers (AS; positive urinary cotinine at collection), and patients with Global Initiative for Chronic Obstructive Lung Disease (GOLD) stage II and III COPD. Research undertaken at McMaster University and University of Texas Southwestern was approved by the Hamilton Integrated Research Ethics Board (#2031).

Cohort two was collected from the Personalized Prediction Strategy for Acute Exacerbation of COPD cohort at the Guangzhou Institute of Respiratory Health (GIRH) (Clinical Trial #NCT03240315; First Affiliated Hospital of Guangzhou Medical University). Banked, matched frozen sputum supernatant and serum were collected from 109 Chinese subjects including self-reported asymptomatic smokers with no history of respiratory disease and GOLD I – IV

COPD. Research undertaken at GIRH was approved by the Ethics Committee of the First Affiliated Hospital of Guangzhou Medical University (#201722).

COPD was physician diagnosed and identified as FEV1/FVC < 0.7 and FEV1 bronchodilator reversibility < 12% in ADEPT and GIRH cohorts. Next, COPD patients were classified by severity of lung function using GOLD guidelines and placed into either GOLD I and II (mild to moderate disease, >50% FEV1) or GOLD III and IV (severe to very severe disease, <50% FEV1) arms. To note, post bronchodilator FEV1 readings were not available for 17 asymptomatic smokers, 1 GOLD I/II and 3 GOLD III/IV subjects in the GIRH cohort; subjects were classified by physician. Moreover, body mass index readings for the Chinese asymptomatic smokers were limited to only 9 subjects. All samples were collected during stable disease as defined by no requirement for antibiotics and/or systemic steroids or an increase in COPD controller medications (except short acting bronchodilators), in the 3 months (ADEPT) or 4 weeks (GIRH) prior to sample collection.

Sample collection and processing

Serum was collected using standard serum separation tubes, and frozen within 30 min in ADEPT and GIRH cohorts. Spontaneously expectorated or hypertonic saline-induced sputum was collected during the same visit and processed using one of two methods; 0.1% dithiothreitol (DTT; 4:1 v/v) (28) or phosphate buffered saline (PBS; 8:1 v/v) (2). Sputum processing in the ADEPT cohort followed the procedure outlined by Pizzichini et al. (28) with the following alterations. A plug weight of at least 50 mg was required for enrolment. Only

samples with squamous cell content ≤ 20%, based on each site's evaluation, were included in the analyses. GIRH cohort sputum processing followed the protocol outlined by Bafadhel et al. (2) with no exceptions.

128-plex autoantigen microarray

IgG/M autoantibodies from sputum and serum were profiled using a 128-plex autoantigen array at the University of Texas Southwestern Medical Center (ADEPT) and Genecopoeia, Guangzhou (GIRH). Briefly, serum and sputum samples were centrifuged at 15000 rpm for 15 minutes to remove any sediment. 3 µL of serum was pre-treated with DNAse-I to remove free DNA and then diluted 1:50 in PBS and 0.1% Tween 20 (PBST) buffer for autoantibody profiling. 30 µl of sputum supernatant was diluted 1:1 in PBST for antibody profiling. The autoantigen array bearing 124 autoantigens and 4 control proteins were printed in duplicates onto nitrocellulose film slides (Grace Bio-Labs). The diluted serum or sputum samples were incubated with the autoantigen arrays. Stringent washing conditions were used to ensure optimum binding specificity. Bound autoantibodies were measured with cy3-conjugated anti-human IgG (1:2000, Jackson ImmunoResearch Laboratories) and cy5-conjugated anti-human IgM (1:2000, Jackson ImmunoResearch Laboratories), using a Genepix 4200A scanner (Molecular Device) with laser wavelength of 532 nm and 635 nm. The resulting images were analysed using Genepix Pro 7.0 software (Molecular Devices).

The median of the signal intensity for each spot was calculated and subtracted from the local background around the spot, and data obtained from

duplicate spots were averaged. The background subtracted signal intensity of each antigen was normalised to the average intensity of the human IgG or IgM, which were spotted on the array as internal controls. Finally, the normalised fluorescence intensity for each antigen was calculated by subtracting a PBS control which was included on each chip as negative control. Signal-to-noise ratio (SNR) was used as a quantitative measurement of the true signal above background noise. SNR values equal to or greater than 3 were considered significantly higher than background, and therefore true signals.

Autoantigen enzyme-linked immunosorbent assay (ELISA)

ELISAs for the detection of histone H1, small nuclear ribonucleoprotein (SmD3) and 1,2-diacyl-sn-glycero3-phospho-L-serine (DGPS) were developed at McMaster University. Recombinant protein and lipids matched the products used on the autoantigen array. Recombinant histone H1 and SmD3 (Abcam; #ab198676, #ab11320 respectively) were coated on NUNC MaxiSorp ELISA plates (ThermoFisher Scientific) overnight in PBS at 4°C. 1,2-diacyl-sn-glycero3-phospho-L-serine (DGPS) (#P664 P7769-100mg, Sigma-Millipore) was coated overnight at room temperature in 1:9 choloroform:methanol inside a desiccator. ELISA plates were blocked in 5% milk for 1 hour and subsequently washed three times in PBS-Tween 20. To avoid lipid stripping by Tween 20, DGPS plates were washed in PBS only. Sputum supernatant was diluted 1:3 and serum 1:40 in 1% milk. All ELISAs used the same anti-human IgG detection antibody conjugated to alkaline phosphatase (#ab97222, Abcam) and developed with p-nitrophenyl phosphate (#N9389-50TAB, Sigma-Millipore). The optical

density (OD) of all the samples was normalised to remove background noise between wells. All wells were then divided by the negative control signal. All samples are shown as fold increase over background.

GIRH multiplex autoantibody bead array

Multiplex magnetic beads (Bio-Rad laboratories) were coupled with 10 common autoantibodies (27) and incubated with 1:10 and 1:180 of sputum supernatant and serum respectively. Following 1-hour coincubation of the sample with magnetic beads at 37˚C, beads were washed and then incubated at 37˚C for 1 hour with biotin-conjugated anti-human IgG (Thermo Fisher Scientific). The median fluorescence intensity of streptavidin-R-phycoerythrin (Bio-Rad laboratories) labelled microspheres were measured using a Bio-Plex 200 (Bio-Rad laboratories). Bio-Plex Manager™ 6.0 software (Bio-Rad laboratories) was used to generate result files.

Statistical analysis

Data are presented as median values and interquartile range unless otherwise stated. Hierarchical clustering and principal component analysis (PCA) used Log2 transformed (log2(x+1)) signal to noise ratio (SNR), R (www.r-project.org). If the raw signal intensity equalled 0, the SNR was changed to 0, otherwise SNR equalled the original value. Differential expression analysis assessed raw signal intensity values per autoantibody specificity using limma package in R (33). Correlations between variables were tested using Spearman correlation, GraphPad Prism 9.0 (La Jolla, CA USA).

RESULTS

Study participants

Matched sputum and serum samples were assessed retrospectively in subjects with normal lung function and stable COPD from independent ADEPT and GIRH cohorts. The characteristics of these two cohorts are shown in **Table 1**. The GIRH cohort includes patients with milder and more severe airflow obstruction than the ADEPT cohort. Subjects in the GIRH cohort were older, included fewer current smokers, and had lower body mass index. No healthy controls were assessed in the GIRH cohort. While the GIRH cohort was comprised of entirely Chinese males, the ADEPT cohort included both sexes (overall 54.8% male) and was predominately Caucasian, with a minority of samples from Black participants.

Autoantibodies are more abundant in the serum than in the sputum

Prior to stratifying subjects based on disease severity, we analysed the overall expression of autoantibodies in the sputum and serum to gain an unbiased overview. IgG and IgM isotypes were selected to allow for comparison to previous COPD cohorts. Shown in **Figure 1A** are the number of subjects each individual IgG or IgM autoantibody specificity was detected in. The two cohorts followed the same trends. IgG serum specificities were the most highly expressed. Sputum IgG and IgM specificity expression were comparable but less abundant than serum specificities. To note, the median expression of each IgM and IgG autoantibody specificity correlated strongly between serum and sputum (**Figure 1B**). While all autoantibodies expressed in sputum were found

in the serum, not all serum autoantibodies were observed in the sputum. Of these serum-only autoantibodies, 50% (13 of 26) of IgG and 12% (2 of 17) of IgM specificities were shared between cohorts. Next, we directly compared autoantibody specificity expression between the ADEPT and GIRH cohorts. Sputum autoantibodies had weak but significant correlation for IgG and IgM specificities between cohorts. Serum autoantibodies displayed a significant moderate correlation for both isotypes (**Figure 1C**). Unbiased assessment revealed sputum autoantibodies were present in both cohorts, but serum autoantibodies were expressed to a higher degree and to a greater consistency.

Serum IgG autoantibodies define two distinct subject populations not related to disease parameters

We used unsupervised clustering analysis to assess whether sputum and serum autoantibodies could define subject populations. To avoid bias by outliers, any autoantibody specificity expressed in fewer than 20% of all samples was removed. Triaged specificities were not biased toward any subject arm in either cohort. We found no significant hierarchal clustering of subjects based on disease status or specificity (**Figure 2A**; **Figure S1A-C**). Next, we performed PCA to assess whether subjects clustered based on each subject's total autoantibody expression. Each dot represents a composite of a subject's overall autoantibody expression, with each plot restricted to one isotype/sample. Healthy controls were excluded from initial ADEPT PCA to facilitate the comparison with the GIRH study, which lacked healthy controls. We observed distinct clusters in serum IgG and IgM in both cohorts (**Figure 2B**). With the

inclusion of healthy controls subjects in the ADEPT cohort, only the IgG serum cluster was maintained (**Figure S1D**).

Next, we assessed whether any available clinical parameters were associated with the IgG serum autoantibody clusters in both cohorts. While increased airflow obstruction and low body mass index have been associated with increased serum autoantibodies (3), these parameters did not define the clustering in our dataset (**Figure 2C**). Moreover, no clinical parameter, sample collection site (ADEPT), or array chip defined the clustering (**Figure S1E**). Multiple autoantibody specificities drove the IgG serum cluster separation in both ADEPT and GIRH cohorts (**Table S1**). In particular, anti-fibronectin and anti-laminin autoantibodies were observed to be expressed more highly in subjects present in the smaller cluster in both cohorts. Notably, these specificities were not the most differentially expressed in either cluster. In the ADEPT cohort, anti-myelin-associated glycoprotein (MAG) was the major differentiating specificity between clusters. Anti-MAG antibodies were not part of the GIRH array, precluding conformation between the cohorts. In the GIRH cohort, differences in IgG reference/background controls and anti-factor I were the main influence on cluster separation. IgG serum autoantibodies defined two distinct subject clusters in both cohorts but were not associated with any available clinical or technical parameter.

Total median serum but not sputum autoantibodies are altered with worsening airflow obstruction

Subsequently, we stratified subjects based on lung function to analyse whether total autoantibody levels are changed based on disease severity. The median expression of IgG/M sputum autoantibodies were not changed between subjects based on disease status in either cohort. Moreover, serum autoantibodies were not altered between COPD subjects and controls in the ADEPT cohort (**Figure 3**). In contrast, in the GIRH cohort, GOLD I subjects had elevated IgG serum autoantibodies compared to asymptomatic smokers. Moreover, GOLD III subjects had increased IgM serum autoantibodies compared to GOLD II and asymptomatic smokers. In summary, median sputum autoantibody levels were not differentially expressed in COPD in either cohort; however, IgG and IgM serum autoantibodies were increased in GOLD I and GOLD III subjects respectively compared to controls in the GIRH cohort.

COPD-related autoantibody specificities have limited differential expression in patients with COPD

In addition to assessing overall changes in median autoantibody expression, we addressed whether autoantibody specificities previously identified to be altered in COPD were differentially expressed in our cohorts. Among the autoantibody specificities included in the autoantigen array, six IgG specificities have been previously observed to be differentially expressed in COPD cohorts: anti-elastin, -collagen I, -collagen V, -cardiolipin, -La-SSb, and -U1-snRNP-Bl/Bl (16, 26, 27). Of these focused specificities, only serum anti-elastin was increased in COPD subjects although this observation was restricted to the GIRH cohort. In contrast, we observed decreased sputum anti-cardiolipin and

serum anti-U1-snRNP-Bl/Bl in ADEPT and GIRH COPD subjects respectively (**Figure 4**). These data show that COPD status is associated with limited changes in previously identified autoantibody specificities. Differential expression was not conserved between the ADEPT and GIRH cohorts.

COPD status is associated with decreased expression of anti-nuclear antibodies

We next analysed whether any autoantibody group or individual specificity was differentially expressed based on disease severity. Compared to asymptomatic smoking controls, we observed no differential expression of any sputum autoantibody in patients with COPD in either the ADEPT or the GIRH cohort (**Figure 5A-B**). In contrast, in the GIRH cohort, 13.4% of detectable serum IgG and 40.0% of detectable serum IgM autoantibodies were altered compared to asymptomatic smokers (**Figure 5A**). The greatest fold change observed was a 2.6- and 4.4-fold reduction in anti-histone H4 IgG and IgM respectively in subjects with FEV1 < 50% (**Table S2**; **Table S3**). To note, only 11.1% of IgM differentially expressed serum autoantibodies were altered more than 1.5-fold. Of these differentially expressed specificities, we observed a difference between the expression of anti-nuclear antibodies (ANA) and anti-tissue antibodies (AT) (26). Specifically, we observed a net decrease in serum ANA levels in COPD (**Figure 5C**). In contrast, IgM AT specificities predominately increased (**Figure 5D**).

Next, we expanded the ADEPT analysis to include healthy control subjects. Compared to healthy controls, 16.1% of detectable IgG sputum

autoantibody specificities were decreased in COPD subjects (**Figure 5B**). As in the GIRH serum, ANA sputum autoantibody specificities were decreased (**Figure 5E**). In contrast to the GIRH cohort where differential fold-change was less than 4.4-fold in the serum, differential expression observed in the sputum was greater than 4.8-fold in COPD (**Table S4**). Anti-DGPS was the only sputum autoantibody to increase in COPD subjects. Notably, if we quantify unadjusted fold differences between control groups and COPD subjects, as per Packard *et al.* (27), we replicated increased trend of IgG serum autoantibodies in COPD (**Figure S2A-B**). This statistical finding was replicated in the GIRH cohort (**Figure S2C**). Thus, these cohorts replicated increased autoantibody titres from previous studies based on the same statistical approach. When adjusted for ICS, age and sex fewer differentially expressed specificities were observed, with a proportion of specificities observed to decrease.

To validate the expression of specific autoantibodies, we analysed the same samples using alternate assay platforms. First, we measured sputum and serum autoantibodies using an autoantibody bead array developed by the GIRH. Of the 10 autoantigens tested, we observed no change in serum or sputum autoantibodies in COPD compared to controls (**Figure S3A**). Second, we developed ELISA platforms to detect anti-histone H1, -small nuclear ribonucleoprotein D3 polypeptide (SmD3) and -DGPS autoantibodies. In contrast to the autoantigen array, serum and sputum anti-histone H1 and -SmD3 autoantibodies were not altered in either cohort. Notably, we observed increased serum, but decreased sputum anti-DGPS autoantibodies in subjects with <50% FEV1 in the GIRH cohort in contrast to the autoantigen array findings (**Figure**

S3B). Taken together, we only resolve fold change in autoantibodies in COPD subjects were only resolved using a high sensitivity assay.

In two independent cohorts we observed a net reduction of ANA specificities in COPD subjects. 25.0% of the 16 differentially expressed sputum IgG specificities in the ADEPT cohort were observed to be differentially expressed in the GIRH COPD IgG serum (anti-histone H1, -histone H2B, -myelin basic protein, -SmD3). Of 36 IgM serum specificities decreased in the GIRH cohort 8.3% of these specificities corresponded with IgG sputum specificities decreased in the ADEPT cohort (anti-myelin basic protein, -nucleolin, -Scl-70/topoisomerase I). Overall, using an age, sex and ICS adjusted assessment of multiple autoantibody specificities, we observed no differential expression of any sputum autoantibody compared to asymptomatic smokers. In contrast, ~12% of detectable serum autoantibodies were differentially expressed greater than 1.5-fold in COPD subjects compared to asymptomatic smokers in the GIRH cohort. These changes were associated with reduced IgG and IgM ANAs, as well as an increased in IgM ATs in COPD.

ICS, AECOPD and smoking status are not associated with changes in autoantibody expression

Clinical parameters such as inhaled corticosteroids (ICS), a history of acute exacerbations of COPD (AECOPD), and current smoking status are associated with immune suppression and consequently could lead to reduced autoantibody levels (5, 7, 22, 23, 35). The majority of COPD subjects were treated with ICS and/or LAMA (**Figure 6A-B**). In both cohorts, ICS dose was

not correlated with the total median IgG or IgM autoantibody expression (**Figure 6C-D**). Notably, IgM serum anti-U1snRNP-C ($p = 0.04$, $r = -0.304$) and IgG serum anti-tissue transglutaminase (TTG) ($p = 0.04$, $r = -0.230$) weakly correlated with increased ICS dose in the GIRH cohort (**Figure S4**). Current smoking status was not associated with decreased total autoantibodies or any specific differentially expressed specificity in either COPD cohort (**Figure 6E-F**), as previously reported (3). Lastly, a history of acute exacerbations of COPD (AECOPD) leading to hospitalisation was not associated with changes in autoantibodies in the GIRH cohort (**Figure S5**). Exacerbation and hospitalisation rates were not available for the ADEPT cohort. In closing, ICS, AECOPD and current smoking status were not associated with altered autoantibodies in COPD.

Serum IgM autoantibodies specificities weakly correlate with surrogate markers of emphysema

Increased autoantibodies have been associated with subjects that have emphysema-dominant COPD (26, 27, 32). Consequently, the association between airspace enlargement and autoantibody levels was assessed using available surrogate indices from each cohort. In the GIRH cohort, airspace enlargement was defined as percentage of low attenuation areas less than a threshold of -950 Hounsfield units (% LAA-950) on CT scan. In the ADEPT cohort, the diffusing capacity of the lungs for carbon monoxide (DLCO), a measure of gas exchange in the lungs was used. In the ADEPT cohort, no correlation between % predicted DLCO and total autoantibodies, ANAs, ATs,

or any differentially expressed sputum IgG specificities was observed (**Figure S6**). In the GIRH study, we found weak positive correlation between higher % LAA-950 and total median serum IgM autoantibodies ($p = 0.0004$, $r = 0.390$). This was complemented by a weak negative correlation between total median sputum IgG and % LAA-950 ($p = 0.0196$, $r = -0.260$) (**Figure 7A**). Moreover, these changes correlated with decreased sputum ANA (IgG - $p = 0.0040$, $r = -0.318$; IgM - $p = 0.0084$, $r = -0.293$) and increased serum IgM AT ($p = 0.002$, $r = -0.409$) and ANA ($p = 0.0028$, $r = -0.330$) (Figure 7B).

Of the autoantibodies specificities differentially expressed in COPD, a proportion had minor correlation with % LAA-950 in the GIRH cohort. IgM serum anti-core histone ($p = 0.0027$, $r = 0.331$), -entactin EDTA ($p = 0.0003$, $r = 0.392$), -glycated albumin ($p = 0.0109$, $r = 0.283$) weakly positively correlated. In contrast, IgM serum anti-histone H4 ($p = 0.0374$, $r = -0.233$) and anti-myelin basic protein ($p = 0.029$, $r = -0.244$) negatively correlated with % LAA-950 (**Figure 7C**). Furthermore, increased IgG serum anti-elastin ($p = 0.0105$, $r = 0.285$) and decreased anti-histone H4 ($p = 0.0100$, $r = -0.286$), -myelin basic protein ($p = 0.0026$, $r = -0. 332$) and -vimentin ($p = 0.0046$, $r = -0.313$) were observed to weakly correlate with % LAA-950 (**Figure 7D**). Overall, in the GIRH cohort IgM serum autoantibodies and decreased sputum IgG ANAs were weakly associated with increased airspace enlargement.

DISCUSSION

Using an autoantigen array platform, we retrospectively measured matched sputum and serum samples from two independent COPD cohorts for the

presence of common anti-nuclear and anti-tissue autoantibodies. Reflecting previous inconsistent autoantibody levels in COPD (3, 10, 26), we observed no conserved increase in expression of autoantibody specificities between cohorts. Compared to asymptomatic smokers, 13.4% of IgG serum autoantibodies in the GIRH cohort were differentially expressed. While 40.0% of GIRH IgM serum autoantibodies were altered, only 11.1% of these were differentially expressed by more than 1.5-fold. Notably, autoantibodies in COPD were observed to be both increased and decreased compared to controls. Sputum autoantibodies were not differentially expressed in COPD subjects compared to asymptomatic smokers, yet 16.1% of IgG sputum autoantibodies were observed to be downregulated compared to healthy controls. In summary, we observed less than 4.4-fold differential expression of serum autoantibodies and no change in sputum autoantibodies in COPD subjects compared to asymptomatic smokers.

We used a validated human autoantigen array previously used in autoimmune diseases and COPD (18, 27, 40). To date, there is no consensus whether distinct autoantibody profiles exist in COPD. Multiple autoantibodies are proposed to be differentially expressed including specificities which target intra/extracellular matrix proteins, immune molecules and neo-autoantigens (17, 21, 27, 36). To capture this heterogeneity, we used an autoantigen array platform similar to Packard et al. that includes 128 autoantigens (27). This approach assessed comprehensively autoantibodies commonly observed in autoimmune diseases, including anti-elastin, -cardiolipin and -collagen I/V that were previously associated with COPD. The current study focused on IgG/M to validate previous COPD studies; however, evidence suggests a role for

decreased IgA levels contributing to airspace remodelling (31). The role of IgA autoantibodies in COPD pathogenesis is not known and warrants future investigation.

Although systemic comorbidities are often present, COPD is a respiratory disease that predominately occurs as a result of inhaled noxious particle exposure. Consequently, we hypothesised direct analysis of airway autoantibodies would increase both the sensitivity and comparability of autoantibody measurements between cohorts. In contrast, we found that serum autoantibodies were more abundant, more frequently differentially expressed and more strongly correlated between cohorts. To note, while sputum autoantibodies were still significantly correlated, differing sputum processing protocols may have contributed to the weaker correlation between cohorts. ADEPT samples were processed with the mucolytic DTT, while the GIRH samples were processed using PBS. DTT has been shown to increase the yield of recoverable immunoglobulins from the sputum (20). Consequently, total autoantibody recovery in the GIRH cohort may not have been optimal. Interestingly, sputum and serum measurements were strongly correlated and showed that a fraction of autoantibodies were only present in the serum. This may reflect that the systematic compartment is influenced by comorbidities altering the overall autoantibody profile in COPD. Thus, sputum and serum autoantibodies are well conserved and show minimal biased between systemic and local autoantibody reservoirs in COPD.

Increased levels of autoantibodies are reported in one-quarter to two-thirds of patients with COPD (3, 10, 26). To date, there has been no consensus on specific autoantibodies tested in COPD that may contribute to the variable number of patients considered "autoantibody positive". Interestingly, we show that an individual's autoantibody profile was not sufficient to cluster subjects based on disease status. This suggests that cigarette smokers, individuals at higher risk of disease onset, and healthy controls had indistinguishable profiles compared to those of COPD subjects. This may demonstrate why the distinction of autoantibody positive versus negative has been difficult in COPD and why independent cohorts do not fully validate each other. The lower number of subjects with increased autoantibody expression in this study may also be a consequence of rigorous assessment of over 120 different specificities with adjustment for age, sex and ICS usage. We propose that this broad assessment allows greater perspective on autoimmune processes occurring in the lung and prevents the overinterpretation of singular specificities. Moreover, given strong sex differences in autoimmune diseases (38) and the immunosuppressive effects of ICS (35), we resolve any effect of disease pathogenesis on differential autoantibody expression by correcting for clinical parameters. In this regard, we observed no differential expression of autoantibodies based on age, sex or ICS. Overall, our findings suggest that COPD subject autoantibody profile is similar to that of asymptomatic smokers and therefore does not provide substantial diagnostic tool.

Autoantibodies in COPD have been proposed to contribute to disease progression. For instance, increased serum autoantibodies have been associated

with emphysema (26, 27), a pathology associated with high % LAA-950 and low DLCO. We observed weak positive correlation between serum IgM autoantibodies and % LAA-950 in the GIRH cohort. Moreover, serum IgM AT were more strongly positively correlated ($p = 0.0002$, $r = 0.409$) than IgM ANA ($p = 0.0028$, $r = 0.330$) supporting previous observations (26). There was no correlation between any sputum IgG/M autoantibodies and emphysema measurements. Furthermore, there was no association between serum or sputum autoantibody levels and DLCO. Overall, we observed limited association between autoantibodies and emphysema in two cohorts. While these data do not preclude a link between emphysema and autoantibodies further investigation in well stratified patient populations is necessary to validate any association between autoantibodies and airspace enlargement.

Sputum autoantibodies are proposed to offer insight into exacerbation risk in patients with COPD. Four specific COPD endotypes with differences in lung function, symptomatic score and blood cell counts were defined by sputum autoantibody profiles. Of which two clusters were positively or negatively associated with hospitalisation rate (19). In this present study, we assessed the association of autoantibodies with hospitalisation rate following the stratification of subjects based on lung function. There was no association between sputum, or serum, autoantibodies with hospitalisation events in any lung function group. Taken together, these data suggest that while sputum autoantibodies may offer a biomarker to identify at-risk patients in specific COPD endotypes, autoantibodies do not offer a prognostic benefit for broader, GOLD-defined populations. In both cohorts', samples were collected during

stable disease and do not represent autoantibody levels during the course of exacerbation. These data suggest that historical AECOPD hospitalisation is not associated with differences in sputum or serum autoantibodies during stable COPD. The role autoantibodies perform during, and perhaps initiating, AECOPD is not known.

Our analysis, adjusted for age, sex and ICS dose we demonstrated that sputum autoantibodies are decreased compared to healthy controls but did not change relative to asymptomatic smokers. In contrast, serum autoantibody specificities were both increased and decreased in COPD compared to asymptomatic smokers. While differences were observed in the autoantigen array, no difference were observed in alternate assay platforms such as the ELISA and autoantigen multiplex bead array. Notably, these latter platforms have smaller dynamic ranges than the autoantigen array and consequently are likely less sensitive to resolve small differences.

Autoantibody specificities which decreased in COPD consisted mainly of autoantibodies that bind anti-nuclear antigens such as chromatin and spliceosome components. Luminal IgG/M ANA autoantibodies have been demonstrated to perform roles in tissue homeostasis (6, 8, 14, 25, 30). Notably, parameters associated with decreased antibody levels such as current cigarette smoking status (5, 23), ICS use (35) and a subset of COPD subjects with frequent exacerbations (7, 22) did not define the decreases we observed in autoantibody levels. Therefore, it is plausible that the loss of ANA specificities may lead to impaired apoptotic debris removal and subsequent secondary

necrosis, expanding upon the protective nature of autoantibodies in COPD, as proposed by Daffa *et al.* (8).

In summary, using an autoantigen array-based approach in two independent cohorts, we observed limited conserved differential expression of sputum and serum autoantibodies in COPD. Notably, sputum autoantibodies are present in COPD but do not offer a prognostic benefit over serum autoantibody analyses. Our study demonstrates that the overall autoantibody signature in COPD subjects is comparable to asymptomatic smokers and healthy controls, suggesting that COPD is not associated with a distinct autoantibody profile. A proportion of ANA/AT specificities were differentially expressed with increasing COPD severity. These specificities predominately decreased with COPD severity. While we observed differences in serum and sputum autoantibodies and correlations between autoantibody specificities and markers of airspace enlargement, these observations were not conserved between cohorts. Ultimately, our data indicate that broad IgG/M autoantibody expression profiles, whether in the serum or sputum, cannot serve as a robust biomarker for disease identification or progression across COPD cohorts.

REFERENCES

1. Agusti A, MacNee W, Donaldson K, Cosio M. Hypothesis: Does COPD have an Autoimmune Component? Thorax 58: 829, 2003. doi: 10.1136/thorax.58.10.829.

2. Bafadhel M, McCormick M, Saha S, McKenna S, Shelley M, Hargadon B, Mistry V, Reid C, Parker D, Dodson P, Jenkins M, Lloyd A, Rugman P, Newbold P, Brightling CE. Profiling of sputum inflammatory mediators in asthma and chronic obstructive pulmonary disease. Respiration 83: 36–44, 2012. doi: 10.1159/000330667.

3. Bonarius HPJ, Brandsma CA, Kerstjens HAM, Koerts JA, Kerkhof M, Nizankowska-Mogilnicka E, Roozendaal C, Postma DS, Timens W. Antinuclear Autoantibodies are more Prevalent in COPD in Association with Low Body Mass Index but not with Smoking History. Thorax 66: 101–7, 2011. doi: 10.1136/thx.2009.134171.

4. Brandsma CA, Kerstjens HAM, Geerlings M, Kerkhof M, Hylkema MN, Postma DS, Timens W. The search for autoantibodies against elastin, collagen and decorin in COPD. Eur Respir J 37: 1288–1289, 2011. doi: 10.1183/09031936.00083510.

5. Cass SP, Yang Y, Xiao J, McGrath JJC, Fantauzzi MF, Thayaparan D, Wang F, Liang Z, Long F, Stevenson CS, Chen R, Stampfli MR. Current smoking status is associated with reduced sputum immunoglobulin M and G expression in chronic obstructive pulmonary disease. Eur Respir J 57, 2021. doi: 10.1183/13993003.02338-2019.

6. Chen Y, Park Y-B, Patel E, Silverman GJ. IgM Antibodies to Apoptosis-Associated Determinants Recruit C1q and Enhance Dendritic Cell Phagocytosis of Apoptotic Cells. J Immunol 182: 6031–6043, 2009. doi: 10.4049/jimmunol.0804191.

7. Cowan J, Gaudet L, Mulpuru S, Corrales-Medina V, Hawken S, Cameron C, Aaron SD, Cameron DW. A retrospective longitudinal within-subject risk interval analysis of immunoglobulin treatment for recurrent acute exacerbation of chronic obstructive pulmonary disease. PLoS One 10: 1–12, 2015. doi: 10.1371/journal.pone.0142205.

8. Daffa NI, Tighe PJ, Corne JM, Fairclough LC, Todd I. Natural and disease-specific autoantibodies in chronic obstructive pulmonary disease. Clin Exp Immunol 180: 155–163, 2015. doi: 10.1111/cei.12565.

9. Faner R, Cruz T, Casserras T, Lopez-Giraldo A, Noell G, Coca I, Tal-Singer R, Miller B, Rodriguez-Roisin R, Spira A, Kalko SG, Agusti A. Network analysis of lung transcriptomics reveals a distinct b-cell signature in emphysema. Am J Respir Crit Care Med 193: 1242–1253, 2016. doi: 10.1164/rccm.201507-1311OC.

10. Feghali-Bostwick CA, Gadgil AS, Otterbein LE, Pilewski JM, Stoner MW, Csizmadia E, Zhang Y, Sciurba FC, Duncan SR. Autoantibodies in Patients with Chronic Obstructive Pulmonary Disease. Am J Respir Crit Care Med 177: 156–63, 2008. doi: 10.1164/rccm.200701-014OC.

11. Global Burden of Disease (GBD) 2017 Causes of Death Collaborators. Global, regional, and national age-sex-specific mortality for 282 causes of death in 195 countries and territories, 1980–2017: a systematic analysis for the Global Burden of Disease Study 2017. Lancet 392: 1736–1788, 2018. doi: 10.1016/S0140-6736(18)32203-7.

12. GOLD Executive Committee. Global Strategy for the Diagnosis, Management, and Prevention of Chronic Obstructive Lung Disease 2017 Report. 2017.

13. Hogg JC, Chu F, Utokaparch S, Woods R, Elliott WM, Buzatu L, Cherniack RM, Rogers RM, Sciurba FC, Coxson HO, Paré PD. The Nature of Small-Airway Obstruction in Chronic Obstructive Pulmonary Disease. N Engl J Med 350: 2645–2653, 2004. doi: 10.1056/NEJMoa1210384.

14. Kenyon KD, Cole C, Crawford F, Kappler JW, Thurman JM, Bratton DL, Boackle SA, Henson PM. IgG Autoantibodies against Deposited C3 Inhibit Macrophage-Mediated Apoptotic Cell Engulfment in Systemic Autoimmunity. J Immunol 187: 2101–2111, 2011. doi: 10.4049/jimmunol.1003468.

15. Lapperre TS, Postma DS, Gosman MME, Hacken NHT, Hiemstra PS, Timens W, Sterk P, Mauad T. Relation between duration of smoking cessation and bronchial inflammation in COPD. Thorax 61: 115–121, 2006. doi: 10.1136/thx.2005.040519.

16. Lee S-H, Goswami S, Grudo A, Song L-Z, Bandi V, Goodnight-White S, Green L, Hacken-Bitar J, Huh J, Bakaeen F, Coxson HO, Cogswell S, Storness-Bliss C, Corry DB, Kheradmand F. Antielastin autoimmunity in tobacco smoking-induced emphysema. Nat Med 13: 567–569, 2007. doi: 10.1038/nm1583.

17. Leidinger P, Keller A, Heisel S, Ludwig N, Rheinheimer S, Klein V, Andres C, Hamacher J, Huwer H, Stephan B, Stehle I, Lenhof HP, Meese E.

Novel autoantigens immunogenic in COPD patients. Respir Res 10: 1–7, 2009. doi: 10.1186/1465-9921-10-20.

18. Li Q-Z, Karp DR, Quan J, Branch VK, Zhou J, Lian Y, Chong BF, Wakeland EK, Olsen NJ. Risk factors for ANA positivity in healthy persons. Arthritis Res Ther 13: R38, 2011. doi: 10.1186/ar3271.

19. Liang Z, Long F, Wang F, Yang Y, Xiao J, Deng K, Gu W, Zhou L, Xie J, Jian W, Chen X, Jiang M, Zheng J, Peng T, Chen R. Identification of clinically relevant subgroups of COPD based on airway and circulating autoantibody profiles. Mol Med Rep 20: 2882–2892, 2019. doi: 10.3892/mmr.2019.10498.

20. Louis R, Shute J, Goldring K, Perks B, Lau LCK, Radermecker M, Djukanovic R. The effect of processing on inflammatory markers in induced sputum. Eur Respir J 13: 660–667, 1999. doi: 10.1183/09031936.99.13366099.

21. Ma A, Wen L, Yin J, Hu Y, Yue X, Li J, Dong X, Gupta Y, Ludwig RJ, Krauss-Etschmann S, Riemekasten G, Petersen F, Yu X. Serum levels of autoantibodies against extracellular antigens and neutrophil granule proteins increase in patients with COPD compared to non-COPD smokers. Int J COPD 15: 189–200, 2020. doi: 10.2147/COPD.S235903.

22. McCullagh BN, Comellas AP, Ballas ZK, Newell JD, Zimmerman MB, Azar AE. Antibody deficiency in patients with frequent exacerbations of Chronic Obstructive Pulmonary Disease (COPD). PLoS One 12: 1–13, 2017. doi: 10.1371/journal.pone.0172437.

23. McMillan SA, Douglas JP, Archbold GP, McCrum EE, Evans AE. Effect of low to moderate levels of smoking and alcohol consumption on serum immunoglobulin concentrations. J Clin Pathol 50: 819–22, 1997. doi: 10.1136/jcp.50.10.819.

24. Mukherjee M, Bulir DC, Radford K, Kjarsgaard M, Huang CM, Jacobsen EA, Ochkur SI, Catuneanu A, Lamothe-Kipnes H, Mahony J, Lee JJ, Lacy P, Nair PK. Sputum autoantibodies in patients with severe eosinophilic asthma. J Allergy Clin Immunol 141: 1269–1279, 2018. doi: 10.1016/j.jaci.2017.06.033.

25. Nagele EP, Han M, Acharya NK, DeMarshall C, Kosciuk MC, Nagele RG. Natural IgG Autoantibodies Are Abundant and Ubiquitous in Human Sera, and Their Number Is Influenced By Age, Gender, and Disease. PLoS One 8, 2013. doi: 10.1371/journal.pone.0060726.

26. Núñez B, Sauleda J, Antó JM, Julià MR, Orozco M, Monsó E, Noguera A, Gómez FP, Garcia-Aymerich J, Agustí A. Anti-tissue Antibodies are Related

to Lung Function in Chronic Obstructive Pulmonary Disease. Am J Respir Crit Care Med 183: 1025–1031, 2011. doi: 10.1164/rccm.201001-0029OC.

27. Packard TA, Li QZ, Cosgrove GP, Bowler RP, Cambier JC. COPD is associated with production of autoantibodies to a broad spectrum of self-antigens, correlative with disease phenotype. Immunol Res 55: 48–57, 2013. doi: 10.1007/s12026-012-8347-x.

28. Pizzichini E, Pizzichini MMM, Efthimiadis A, Hargreave FE, Dolovich J. Measurement of inflammatory indices in induced sputum: Effects of selection of sputum to minimize salivary contamination. Eur Respir J 9: 1174–1180, 1996. doi: 10.1183/09031936.96.09061174.

29. Polverino F, Cosio BG, Pons J, Laucho-Contreras M, Tejera P, Iglesias A, Rios A, Jahn A, Sauleda J, Divo M, Pinto-Plata V, Sholl L, Rosas IO, Agustí A, Celli BR, Owen CA. B cell-activating factor an orchestrator of lymphoid follicles in severe chronic obstructive pulmonary disease. Am J Respir Crit Care Med 192: 695–705, 2015. doi: 10.1164/rccm.201501-0107OC.

30. Quartier P, Potter PK, Ehrenstein MR, Walport MJ, Botto M. Predominant role of IgM-dependent activation of the classical pathway in the clearance of dying cells by murine bone marrow-derived macrophages in vitro. Eur J Immunol 35: 252–260, 2005. doi: 10.1002/eji.200425497.

31. Richmond BW, Mansouri S, Serezani A, Novitskiy S, Blackburn JB, Du RH, Fuseini H, Gutor S, Han W, Schaff J, Vasiukov G, Xin MK, Newcomb DC, Jin L, Blackwell TS, Polosukhin V. Monocyte-derived dendritic cells link localized secretory IgA deficiency to adaptive immune activation in COPD. Mucosal Immunol 14: 431–442, 2021. doi: 10.1038/s41385-020-00344-9.

32. Rinaldi M, Lehouck A, Heulens N, Lavend'homme R, Carlier V, Saint-Remy J-M, Decramer M, Gayan-Ramirez G, Janssens W. Antielastin B-cell and T-cell immunity in patients with chronic obstructive pulmonary disease. Thorax 67: 694–700, 2012. doi: 10.1136/thoraxjnl-2011-200690.

33. Ritchie ME, Phipson B, Wu D, Hu Y, Law CW, Shi W, Smyth GK. Limma powers differential expression analyses for RNA-sequencing and microarray studies. Nucleic Acids Res 43: e47, 2015. doi: 10.1093/nar/gkv007.

34. Rutgers SR, Postma DS, ten Hacken NHT, Kauffman HF, Van Der Mark TW, Koëter GH, Timens W. Ongoing airway inflammation in patients with COPD who do not currently smoke. Thorax 55: 12–18, 2000.

35. Settipane GA, Pudupakkam RK, McGowan JH. Corticosteroid effect on immunoglobulins. J Allergy Clin Immunol 62: 162–166, 1978. doi: 10.1016/0091-6749(78)90101-X.

36. Shindi R, Almehairi A, Negm OH, Kalsheker N, Gale NS, Shale DJ, Harrison TW, Bolton CE, John M, Todd I, Tighe PJ, Fairclough LC. Autoantibodies of IgM and IgG classes show differences in recognition of multiple autoantigens in chronic obstructive pulmonary disease. Clin Immunol 183: 344–353, 2017. doi: 10.1016/j.clim.2017.09.020.

37. Turato G, Stefano A, Maestrelll P, Mapp CE, Ruggieri MP, Roggeri A, Fabbri LM, Saetia M. Effect of Smoking Cessation on Airway Inflammation in Chronic Bronchitis. Am J Respir Crit Care Med 152: 1262–1267, 1995.

38. Whitacre CC. Sex differences in autoimmune disease. Nat Immunol 2: 777–780, 2001. doi: 10.1038/ni0901-777.

39. World Health Organization (WHO). Chronic obstructive pulmonary disease (COPD) [Online]. World Health Organization: 2017. https://www.who.int/news-room/fact-sheets/detail/chronic-obstructive-pulmonary-disease-(copd) [5 Apr. 2021].

40. Zhu H, Luo H, Yan M, Zuo X, Li Q-Z. Autoantigen Microarray for High-throughput Autoantibody Profiling in Systemic Lupus Erythematosus. Genomics Proteomics Bioinformatics 13: 210–8, 2015. doi: 10.1016/j.gpb.2015.09.001.

	Healthy Control	Asymptomatic Smoker	> 50% FEV_1	< 50% FEV_1
(A) ADEPT				
N	28	30	47	10
Age	49.4 ± 7.1	49.0 ± 7.3†	57.7 ± 5.7†	59.5 ± 4.8†
Sex Male (%)	11 (39.3%)	16 (53.3%)	30 (63.8%)	6 (60.0%)
Current Smoker ($Cotinine^+$)	0	28 (93.3%)	33 (70.2%)	6 (60%)
Race (%)				
White/Caucasian	26 (92.9)	24 (80.0)	44 (93.6)	9 (90.0)
Black/African American	2 (7.1)	6 (20.0)	3 (6.4)	1 (10.0)
Body Mass Index	26.2 ± 3.0	26.5 ± 3.2†	26.3 ± 4.0†	25.1 ± 4.5†
GOLD Stage (% of group)				
GOLD II	-	-	47 (100)	-
GOLD III	-	-		10 (100)
FEV_1, % of predicted*	107.4 ±11.3	102.3 ± 11.2	61.8 ± 8.9†	45.5 ± 5.3†
(B) GIRH				
N	-	25	44	40
Age	-	58.9 ± 9.2†	67.6 ± 8.4†	66.1 ± 7.8†
Sex Male (%)	-	28 (100)	44 (100)	40 (100)
Current Smoker (Reported) (%)	-	16 (64.0)	16 (36.4)	12 (32.4)
No Smoking Status Data	-	0	0	3
Race (%)				
Chinese	-	25 (100)	44 (100)	40 (100)
Body Mass Index*[1]	-	24.2 ± 4.0†	23.0 ± 3.4†	20.7 ± 3.8†
GOLD Stage (% of group)				
GOLD I	-	-	15 (34.1)	-
GOLD II	-	-	29 (65.9)	-
GOLD III	-	-	-	27 (67.5)
GOLD IV	-	-	-	13 (32.5)
FEV_1, % of predicted** [1]	-	98.1 ± 13.0	75.7 ± 14.7†	35.6 ± 17.0†

Table 1. Study patient demographics. Patient demographics of non-Hispanic White and Black subjects recruited as part of the ADEPT study and Chinese subjects recruited by the GIRH. Forced Expiratory Volume in 1 second (FEV1). ± SD * Post Bronchodilator, Post Blood Draw. *[1] Incomplete (see text description). † p = < 0.05 between cohorts.

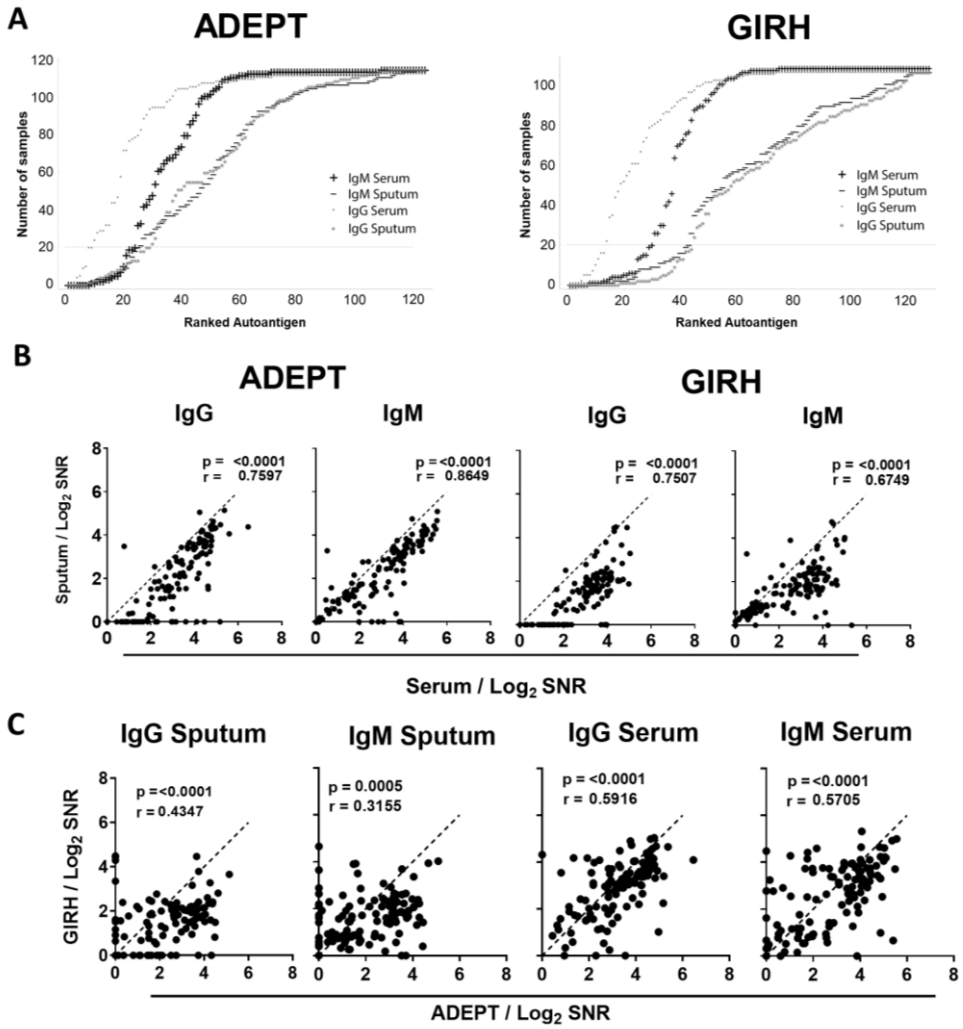

Figure 1. Autoantibody specificities are more abundant in serum compared to sputum. (A) Number of subjects positive for each individual unstratified autoantibody specificity, shown based on antibody isotype and sample type. Each isotype and subsequent sample type curve feature all autoantibody specificities ranked from least-to-most detected independently from one another. (B) Serum versus sputum expression per autoantibody specificity. (C) Autoantibody expression comparison between cohorts. Each point (B-C) represents the median IgG and IgM autoantibody expression per specificity. (ADEPT n = 123, GIRH n = 120).

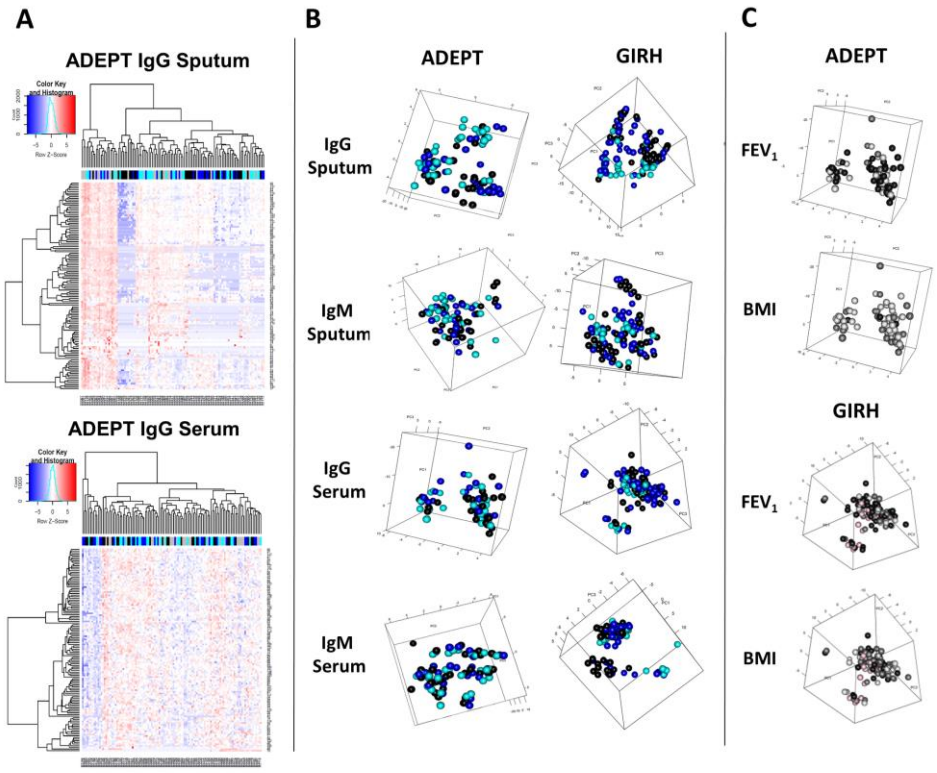

Figure 2. IgG serum autoantibodies form two distinct autoantibody clusters not related to clinical parameters. All data is Log2 transformed signal to noise ratio (SNR) for each autoantibody per subject. Each point represents one subject's autoantibody profile. Healthy control samples from the ADEPT cohort were excluded from this analysis. Values adjusted for age, gender and ICS, limma package R. (A) Heatmaps generated from Log2 transformed SNR for ADEPT IgG sputum and serum. (B) Principal component analysis (PCA) of ADEPT and GIRH IgG and IgM serum and sputum. (C) IgG Serum PCA hyper imposed with clinical parameters. Healthy control – open. Asymptomatic smoker - light blue. > FEV1 50% COPD – dark blue. < FEV1 50% COPD – closed. (ADEPT n = 115, GIRH n = 109). Forced expiratory volume in 1 second (FEV1): <69% - open, 70 - 88% - light grey, 89 -119% - dark grey, >120% - black No post bronchodilator FEV1 determined – Pink. Body mass index (BMI): <19.9% - closed, 20.0 – 24.9% - dark grey, <25.0% – light grey, Not determined – Pink.

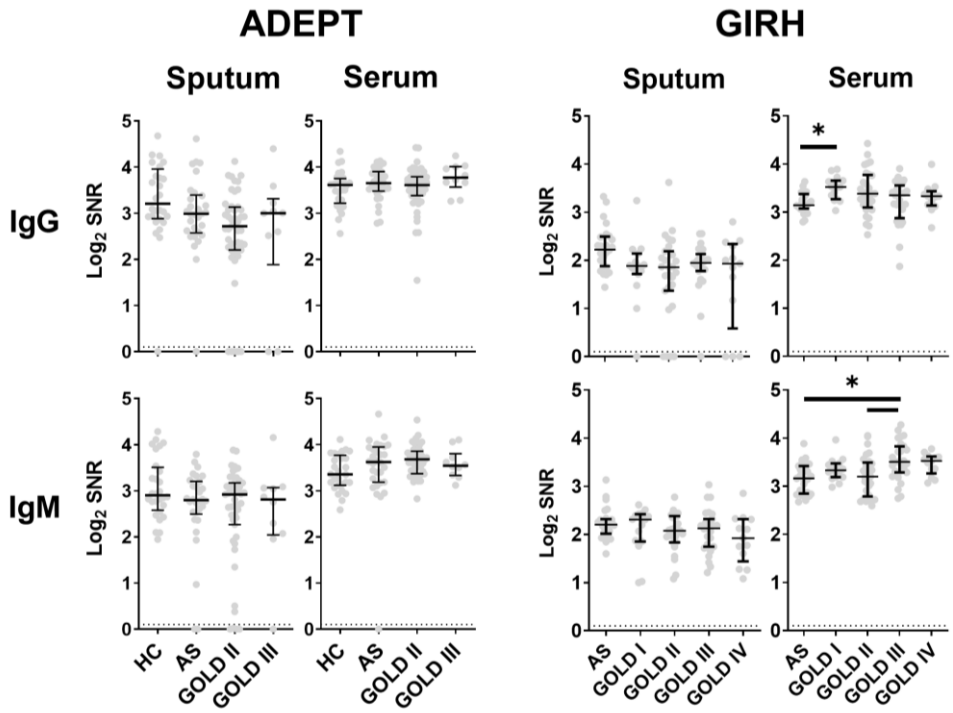

Figure 3. Median autoantibody expression in patients with COPD and control subjects. Each point represents an individual subject's median autoantibody expression as expressed as Log2 transformed SNR. Dotted line represents limit of detection. Plots show median and inter-quartile range. (ADEPT: HC n = 28, AS n = 30, GOLD II n = 47, GOLD III n = 10, GIRH: AS n = 25, GOLD I n = 15, GOLD II n = 29, GOLD III n = 27, GOLD IV n = 13.) SNR – Signal-to-noise ratio. HC – Healthy control. AS – Asymptomatic smokers.

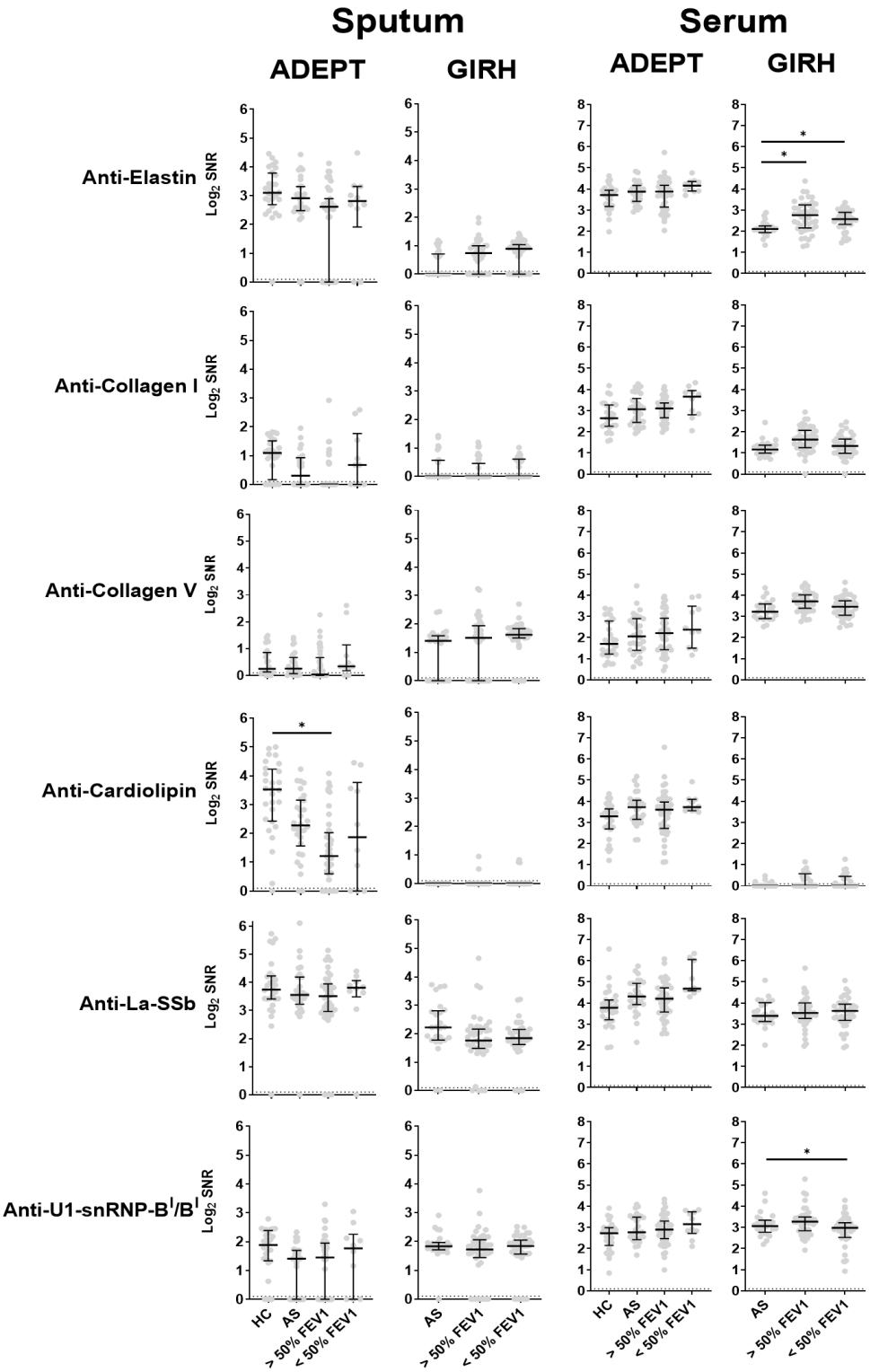
Sputum
Serum
ADEPT
GIRH
ADEPT
GIRH
Anti-Elastin
Anti-Collagen I
Anti-Collagen V
Anti-Cardiolipin
Anti-La-SSb
Anti-U1-snRNP-B^{I}/B^{I}
Log$_2$ SNR
HC
AS
> 50% FEV1
< 50% FEV1
*

Figure 4. Limited differential expression of previously published COPD-related autoantibody specificities. Age, gender and ICS adjusted limma analysis of selected autoantibody specificities assessed via the autoantigen array. Each point represents subject's autoantibody expression as expressed as Log2 transformed SNR. Plots show median and inter-quartile range. Dotted line represents autoantibody expression below level of detection. (ADEPT: HC n = 28, AS n = 30, >50% FEV1 n = 47, <50% FEV1 n = 10, GIRH: AS n = 25, >50% FEV1 n = 44, <50% FEV1 n = 40). SNR – Signal-to-noise ratio. FEV1 - Forced expiratory volume in 1 second. HC – Healthy control. AS – Asymptomatic smokers.

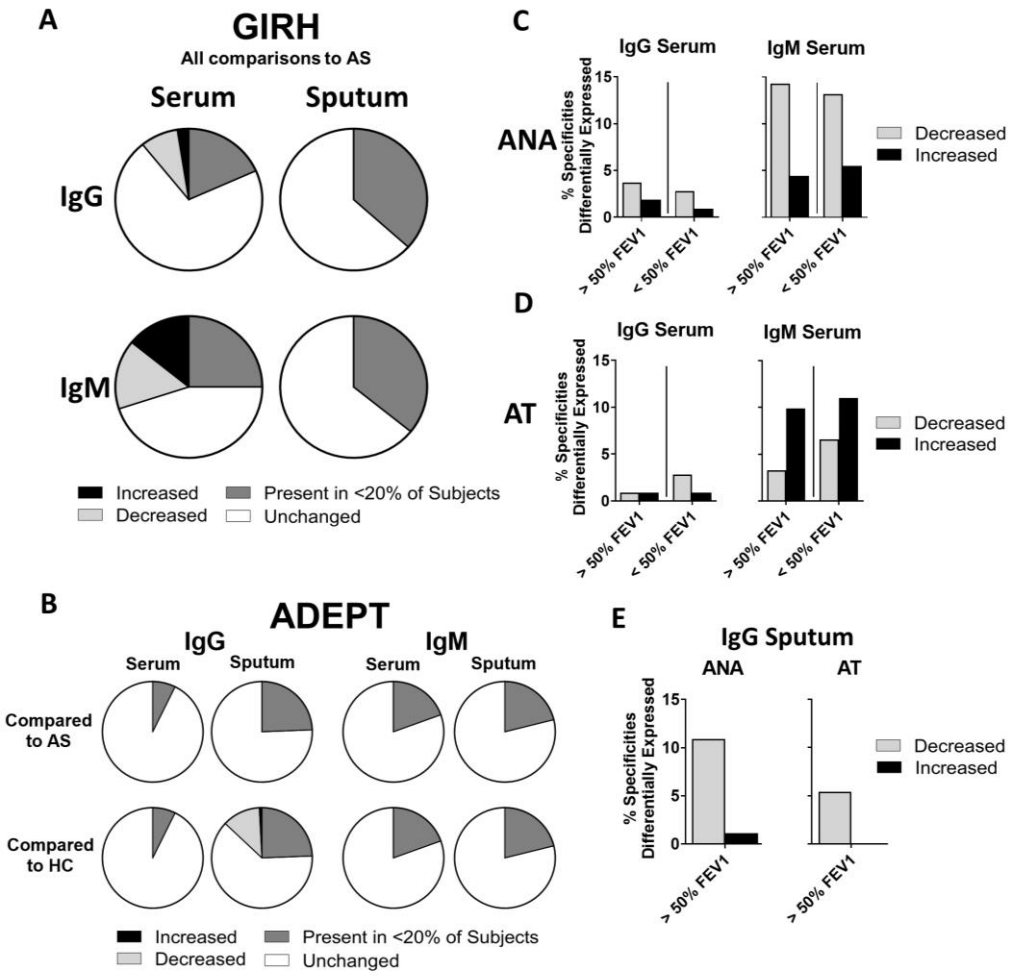

Figure 5. Anti-nuclear autoantibody specificities are predominately differentially expressed in GIRH and ADEPT cohorts. Parts of whole charts show proportional change in autoantibody expression as determined by age, gender and ICS adjusted limma analysis in the GIRH (A) and ADEPT (B) cohorts. No differentially expressed autoantibodies were observed in the ADEPT cohort between patients with COPD and AS. The proportion of (C) anti-nuclear antibody (ANA) and (D) anti-tissue antibodies (AT) altered in GIRH COPD subjects compared to AS. (E) ANA and AT specificities differentially expressed in ADEPT COPD subjects compared to HC. (ADEPT n = 123, GIRH n = 120). ANA - anti-nuclear antibody. AT - anti-tissue antibodies. HC – Healthy control. AS – Asymptomatic smokers.

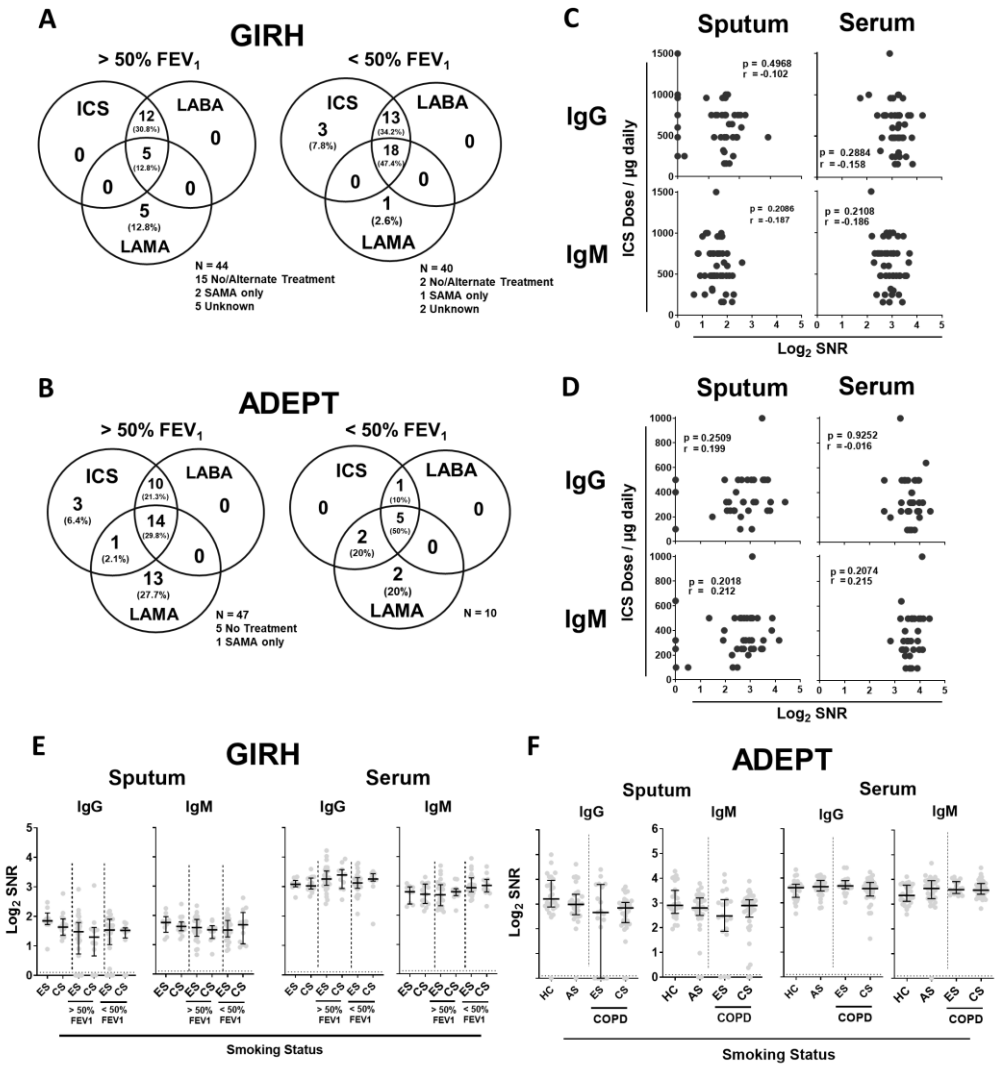

Figure 6. Clinical parameters including inhaled corticosteroid dose and current smoking status are not associated with changes in autoantibodies. Venn diagrams detail the number of individuals receiving common COPD medication at sample collection in (A) GIRH and (B) ADEPT cohorts. Autoantibody levels based on ICS use in patients with COPD in (C) GIRH and (D) ADEPT (ADEPT n = 36, GIRH n = 47). Current smoking status based on self-reported smoking status (E) GIRH and (F) cotinine positive urine on any visit ADEPT (ADEPT: HC n = 28, AS n = 30, COPD ES n = 18, COPD CS n = 39; GIRH: ES n = 9, CS n = 15, >50% FEV1 ES n = 28, >50% FEV1 CS n = 10, <50% FEV1 ES n = 25, <50% FEV1 CS n = 11). Correlation plots show Spearman's rank correlation coefficient (B & D). Plots show median and inter-quartile range. One-way ANOVA Kruskal-Wallis test (E-F). ES – Ex-smoker. CS – Current smoker. ICS - inhaled corticosteroids, LABA - long-acting β2-agonists, LAMA - long-acting muscarinic antagonists, SAMA - short-acting muscarinic antagonist. FEV1 - Forced expiratory volume in 1 second. SNR – Signal-to-noise ratio.

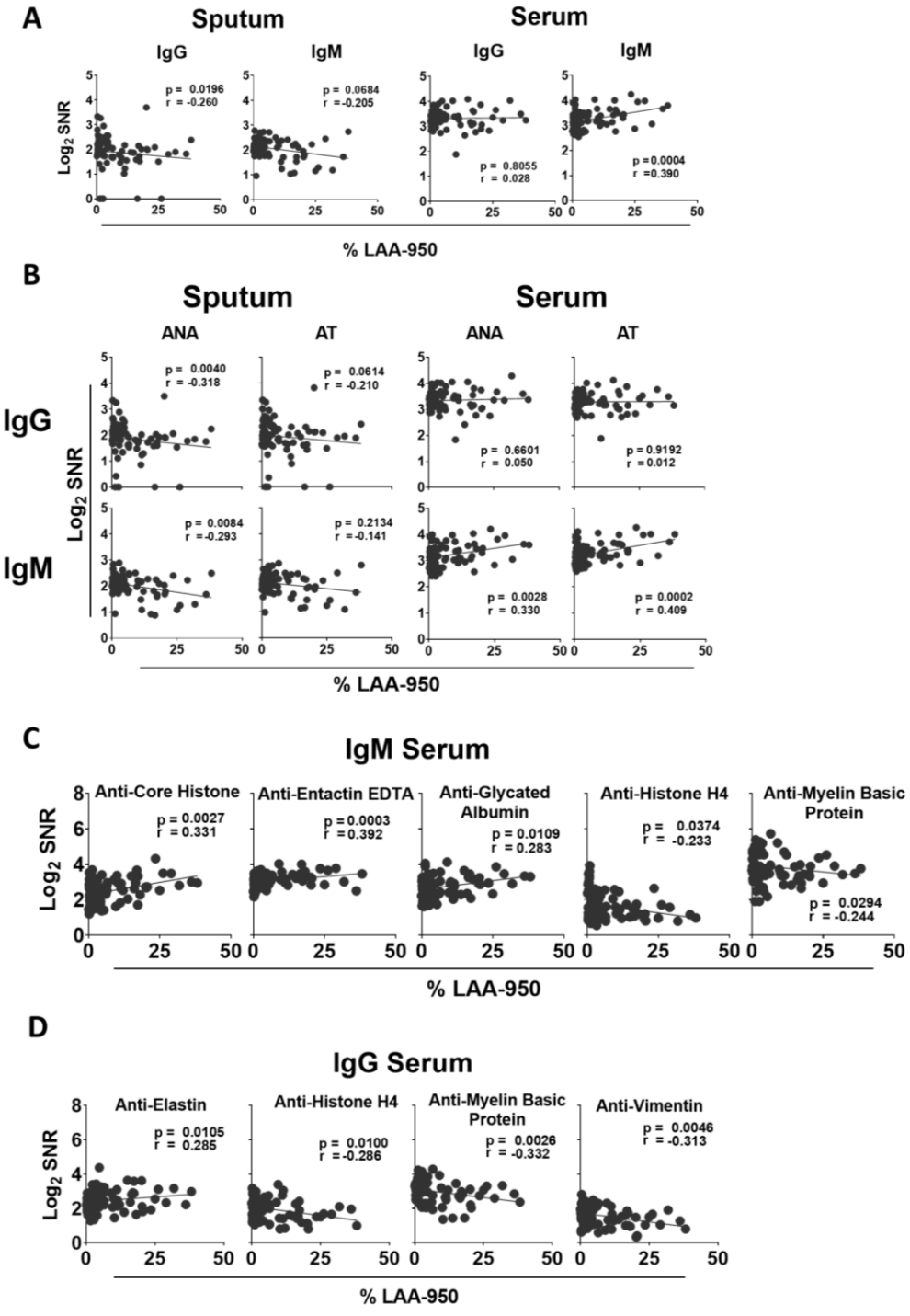
A
Sputum
Serum
IgG
IgM
IgG
IgM
p = 0.0196
r = -0.260
p = 0.0684
r = -0.205
p = 0.8055
r = 0.028
p = 0.0004
r = 0.390
Log2 SNR
% LAA-950
B
Sputum
Serum
ANA
AT
ANA
AT
IgG
IgM
p = 0.0040
r = -0.318
p = 0.0614
r = -0.210
p = 0.6601
r = 0.050
p = 0.9192
r = 0.012
p = 0.0084
r = -0.293
p = 0.2134
r = -0.141
p = 0.0028
r = 0.330
p = 0.0002
r = 0.409
Log2 SNR
% LAA-950
C
IgM Serum
Anti-Core Histone
Anti-Entactin EDTA
Anti-Glycated Albumin
Anti-Histone H4
Anti-Myelin Basic Protein
p = 0.0027
r = 0.331
p = 0.0003
r = 0.392
p = 0.0109
r = 0.283
p = 0.0374
r = -0.233
p = 0.0294
r = -0.244
Log2 SNR
% LAA-950
D
IgG Serum
Anti-Elastin
Anti-Histone H4
Anti-Myelin Basic Protein
Anti-Vimentin
p = 0.0105
r = 0.285
p = 0.0100
r = -0.286
p = 0.0026
r = -0.332
p = 0.0046
r = -0.313
Log2 SNR
% LAA-950

Figure 7. Weak association of IgM serum autoantibodies in the GIRH cohort with airspace enlargement. (A) Correlation of total median autoantibody expression as expressed as Log2 transformed SNR with % LAA-950. (B) Total anti-nuclear antibody (ANA) and total anti-tissue antibody (AT) specificities correlated with % LAA-950. Most differentially expressed (C) IgM serum and (D) IgG serum autoantibodies association with % LAA-950. Spearman's rank correlation coefficient. (GIRH n = 80). SNR – Signal-to-noise Ratio. % LAA-950 – Percentage low attenuation areas less than a threshold of -950 Hounsfield units. SNR – Signal-to-noise ratio.

Autoantibody Specificity	FC	P.Value	adj.P.Value
(A) ADEPT			
Myelin-associated glycoprotein	58.0	3.4E-82	3.9E-80
Fibronectin	2.9	1.1E-03	4.1E-02
Laminin	1.8	5.9E-05	3.4E-03
Proteoglycan	1.4	2.0E-03	4.7E-02
Heperan Sulfate	1.4	2.4E-03	4.7E-02
Nucleolin	-1.4	2.4E-03	4.7E-02
(B) GIRH			
IgG control 1:8	27.3	1.6E-27	9.3E-26
IgG control 1:4	25.3	1.0E-19	3.8E-18
IgG control 1:16	21.9	7.6E-37	8.8E-35
IgG control 1:2	19.1	4.2E-14	9.6E-13
Factor I	10.6	4.3E-15	1.2E-13
Heparan sulfate proteoglycan	2.7	3.0E-05	4.9E-04
Fibronectin	2.4	5.0E-06	9.6E-05
Laminin	2.1	3.5E-04	4.4E-03
Heparan Sulphate	1.9	3.4E-04	4.4E-03
Proteoglycan	1.5	5.2E-03	5.0E-02
Ro/SSA (60 kDa)	1.5	2.6E-03	3.0E-02
Glycoprotein 2 (GP2)	1.5	5.2E-03	5.0E-02

Table S1. IgG serum autoantibody differential expression analysis identifies anti-fibronectin and anti-laminin drive cluster separation in the two-independent cohorts. Limma analysis of autoantibodies specificities that are differentially expressed between principal component analysis (PCA) clusters. Results are Log2 transformed signal-to-noise adjusted for sex, age and inhaled corticosteroids. FC – Fold change. 10.6084/m9.figshare.14068889

Autoantibody Specificity	>50% FEV_1 vs. AS			<50% FEV_1 vs. AS		
	FC	**P.Value**	**adj.P.Val**	**FC**	**P.Value**	**adj.P.Val**
Histone H4	-1.9	1.7E-04	3.9E-03	-2.6	1.3E-06	1.0E-04
Histone H1	-	-	-	-2.4	1.3E-06	1.0E-04
Vimentin	-	-	-	-2.2	1.8E-05	5.8E-04
U1-snRNP B/B'	-	-	-	-2.0	2.1E-04	4.4E-03
Myelin basic protein	-	-	-	-1.7	7.9E-06	3.2E-04
Complement C1q	-1.4	2.7E-06	1.5E-04	-1.4	4.5E-05	1.2E-03
Elastin	1.5	3.0E-04	5.3E-03	1.7	2.5E-05	7.1E-04
Core Histone	1.5	8.4E-06	3.2E-04	1.8	1.5E-08	3.4E-06
SmD3	1.5	1.5E-03	2.5E-02	-	-	-
anti-Ig control 1:8	-1.3	2.8E-03	4.1E-02	-	-	-
Histone H2B	-1.5	2.2E-03	3.4E-02	-	-	-
PCNA	-1.5	3.0E-04	5.3E-03	-	-	-
TTG	-1.4	3.2E-03	4.4E-02	-	-	-

Table S2. GIRH serum IgG autoantibody specificities altered in COPD subjects compared to asymptomatic smokers. Differential autoantibody expression in was determined following age and ICS adjusted limma analysis compared to asymptomatic smokers using raw signal intensity per autoantigen. AS – Asymptomatic smokers. FC – Fold change. TTG - Tissue Transglutaminase. PCNA - Proliferating Cell Nuclear Antigen. 10.6084/m9.figshare.14068898

	>50% FEV_1 vs. AS			<50% FEV_1 vs. AS		
	FC	**P.Value**	**adj.P.Val**	**FC**	**P.Value**	**adj.P.Val**
Histone H4	-2.8	3.1E-07	5.1E-06	-4.4	2.6E-10	2.5E-08
Myelin basic protein	-	-	-	-2.3	7.3E-03	2.8E-02
Nucleolin	-1.5	3.8E-09	1.8E-07	-1.9	5.8E-15	1.1E-12
U1-snRNP C	-1.5	1.7E-05	1.5E-04	-1.8	5.3E-08	1.3E-06
SmD2	-	-	-	-1.6	1.4E-06	2.0E-05
U1-snRNP A	-1.3	1.5E-04	1.1E-03	-1.5	6.0E-07	9.1E-06
Complement C3a	-	-	-	-1.4	8.1E-03	3.0E-02
CENP-B	-1.2	3.7E-03	1.6E-02	-1.3	2.7E-06	3.3E-05
Sm/RNP	-1.2	1.9E-03	9.8E-03	-1.3	1.2E-04	9.2E-04
Complement C1q	-1.3	6.4E-09	1.8E-07	-1.3	2.7E-07	4.8E-06
Scl-70/Topoisomerase I	-1.2	7.5E-03	2.8E-02	-1.3	3.6E-04	2.2E-03
LC1	-1.2	1.6E-05	1.5E-04	-1.2	5.3E-04	3.2E-03
Myosin	-1.1	9.3E-03	3.4E-02	-1.2	2.1E-03	1.1E-02
PL-12	-1.2	3.6E-03	1.6E-02	-1.2	5.1E-03	2.1E-02
La/SSB	-1.2	8.3E-04	4.8E-03	-1.1	7.3E-03	2.8E-02
Alpha Fodrin	-	-	-	-1.1	1.1E-02	3.8E-02
PL-7	-1.1	1.2E-03	6.3E-03	-1.1	6.3E-03	2.5E-02
BPI	-	-	-	1.2	2.0E-04	1.4E-03
Vitronectin	-	-	-	1.2	3.5E-03	1.6E-02
Complement C3	-	-	-	1.2	1.3E-04	9.9E-04
Sm	-	-	-	1.2	2.9E-03	1.3E-02
Muscarinic receptor	1.1	1.3E-03	7.0E-03	1.2	4.9E-06	5.7E-05
Hemocyanin	-	-	-	1.3	2.4E-03	1.2E-02
Fibrinogen IV	1.3	6.6E-06	6.8E-05	1.3	5.9E-06	6.4E-05
MDA5	-	-	-	1.3	1.1E-03	6.3E-03
AQP4	1.1	5.2E-03	2.1E-02	1.3	1.6E-07	3.2E-06
DNA Polymerase beta (POLB)	-	-	-	1.4	2.4E-05	2.1E-04
CRP	-	-	-	1.4	1.2E-05	1.2E-04
Glycated Albumin	1.3	1.1E-04	8.8E-04	1.5	1.2E-07	2.7E-06
PM/Scl 100	1.2	2.8E-04	1.9E-03	1.5	5.2E-09	1.8E-07
Entaktin EDTA	1.2	3.2E-04	2.1E-03	1.5	5.9E-09	1.8E-07
Core Histone	1.7	1.5E-06	2.0E-05	2.0	4.8E-09	1.8E-07
PCNA	-1.2	3.9E-03	1.7E-02	-	-	-
TTG	-1.1	2.5E-03	1.2E-02	-	-	-
Factor B	1.1	1.2E-02	4.2E-02	-	-	-
Insulin	1.2	4.7E-04	2.9E-03	-	-	-

Table S3. GIRH serum IgM autoantibody specificities altered in COPD subjects compared to asymptomatic smokers. Differential autoantibody expression in was determined following age and ICS adjusted limma analysis compared to asymptomatic smokers using raw signal intensity per autoantigen. AS – Asymptomatic smokers. FC – Fold change. SmD - Smith Antigen D. U1-snRNP-A - U1 small nuclear ribonucleoprotein A. CENP-B - Centromere Protein B. LC1 - Liver cytosol 1. PL-12 - Alanyl-tRNA synthetase (AARS). PL-7 - Threonyl-tRNA synthetase (TARS). BPI - Bactericidal permeability-increasing protein. MDA5 - Melanoma Differentiation-Associated Protein 5. AQP4 - Aquaporin 4. CRP - C-reactive protein. PCNA - Proliferating cell nuclear antigen. TTG - Tissue Transglutaminase. 10.6084/m9.figshare.14068901

Autoantibody Specificity	>50% FEV_1 vs HC		
	FC	**p-value**	**adj. p-value**
Myelin basic protein	-16.8	5.5E-07	2.1E-04
Fibronectin	-15.0	6.6E-04	3.3E-02
SmD3	-13.5	2.2E-05	2.8E-03
Complement C8	-12.3	2.1E-03	5.0E-02
Factor I	-11.3	1.8E-03	5.0E-02
SmD1	-10.6	2.2E-05	2.8E-03
Histone H1	-7.9	2.0E-03	5.0E-02
Histone H2B	-7.4	8.0E-04	3.3E-02
SmD	-7.3	7.9E-04	3.3E-02
Cardolipin	-7.2	8.9E-04	3.4E-02
U1-snRNP-68	-7.1	5.0E-04	3.3E-02
Histone-total	-6.9	1.3E-03	4.2E-02
Laminin	-5.8	6.4E-04	3.3E-02
Scl-70	-4.9	1.9E-03	5.0E-02
Nucleolin	-4.8	1.0E-03	3.4E-02
DGPS	8.5	3.7E-05	3.4E-03

Table S4. Sputum IgG autoantibody expression in COPD subjects is decreased compared to healthy controls in the ADEPT cohort. Specific sputum IgG autoantibodies decrease in COPD, with the exception of 1,2-diacyl-sn-glycero3-phospho-L-serine (DGPS). Differential autoantibody expression in was determined following age, gender and ICS adjusted limma analysis compared to asymptomatic smokers using raw signal intensity per autoantigen. HC – Healthy control. FC – Fold change. Sm - Smith Antigen. Scl-70 - Topoisomerase I 70KDa subunit. DGPS - 1,2-diacyl-sn-glycero3-phospho-L-serine. 10.6084/m9.figshare.14068904

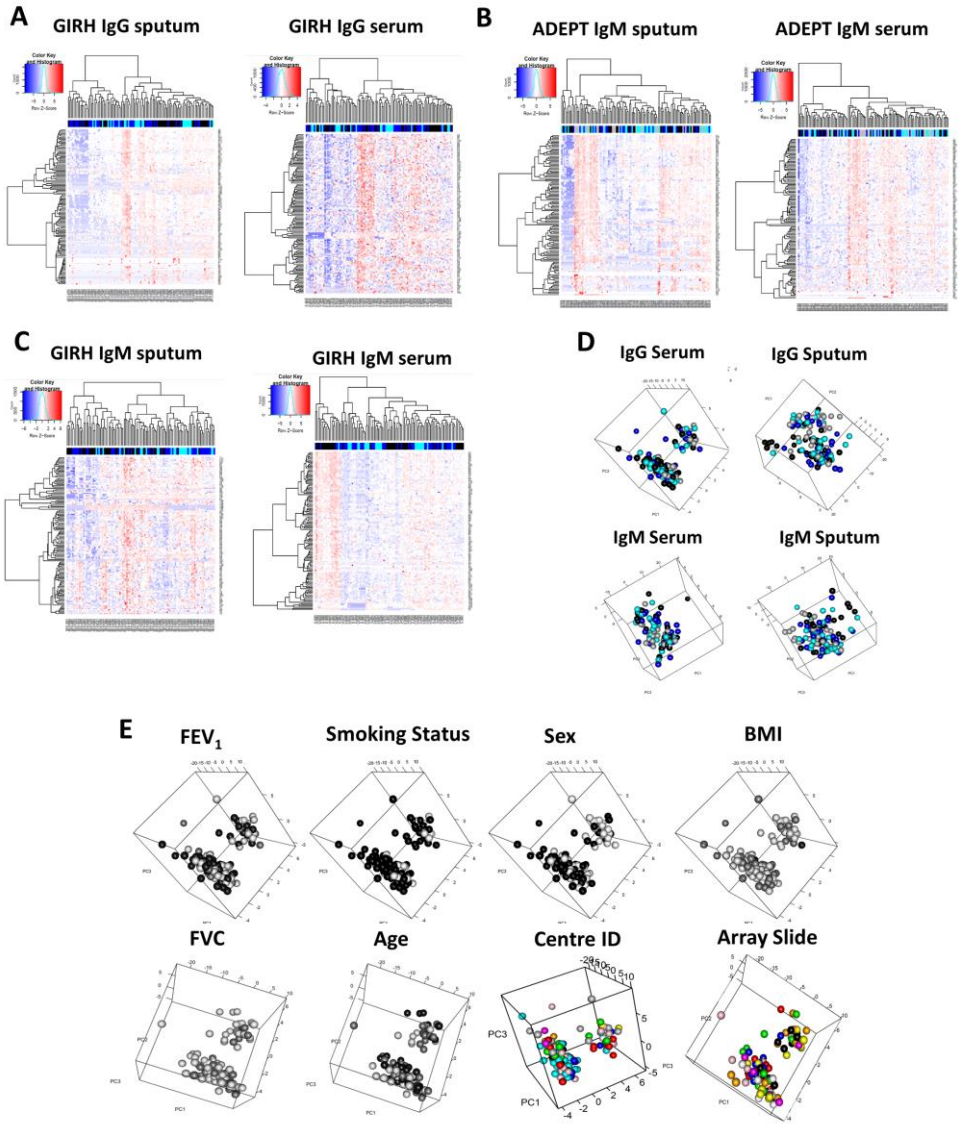
A
GIRH IgG sputum
GIRH IgG serum
B
ADEPT IgM sputum
ADEPT IgM serum
C
GIRH IgM sputum
GIRH IgM serum
D
IgG Serum
IgG Sputum
IgM Serum
IgM Sputum
E
FEV1
Smoking Status
Sex
BMI
FVC
Age
Centre ID
Array Slide

Figure S1. Sputum and serum autoantibodies do not cluster based on disease status or autoantibody specificity. All data is Log2 transformed signal to noise ratio (SNR) for each autoantibody per subject. Values adjusted for age, gender and ICS, limma package R. (A-C) Heatmaps generated from Log2 transformed SNR for each sample condition. Principal component analysis (PCA) of ADEPT (D) IgG and IgM serum and sputum with healthy control samples included. Each point represents one subject's autoantibody profile. (E) ADEPT IgG serum PCA hyper imposed with available parameters. Healthy control – open. Asymptomatic smoker - light blue. >50% FEV1 COPD – dark blue. <50% FEV1 COPD – closed. Forced expiratory volume in 1 second (FEV1): <69% - open, 70 - 88% - light grey, 89 -119% - dark grey, >120% - black. Current smoking status: Current smoker – closed, Non/ex-smoker – open. Gender: Male – closed. Female – open. Body mass index (BMI): <19.9% - closed, 20.0 – 24.9% - dark grey, <25.0% – light grey. (ADEPT n = 123, GIRH n = 120). 10.6084/m9.figshare.14068835

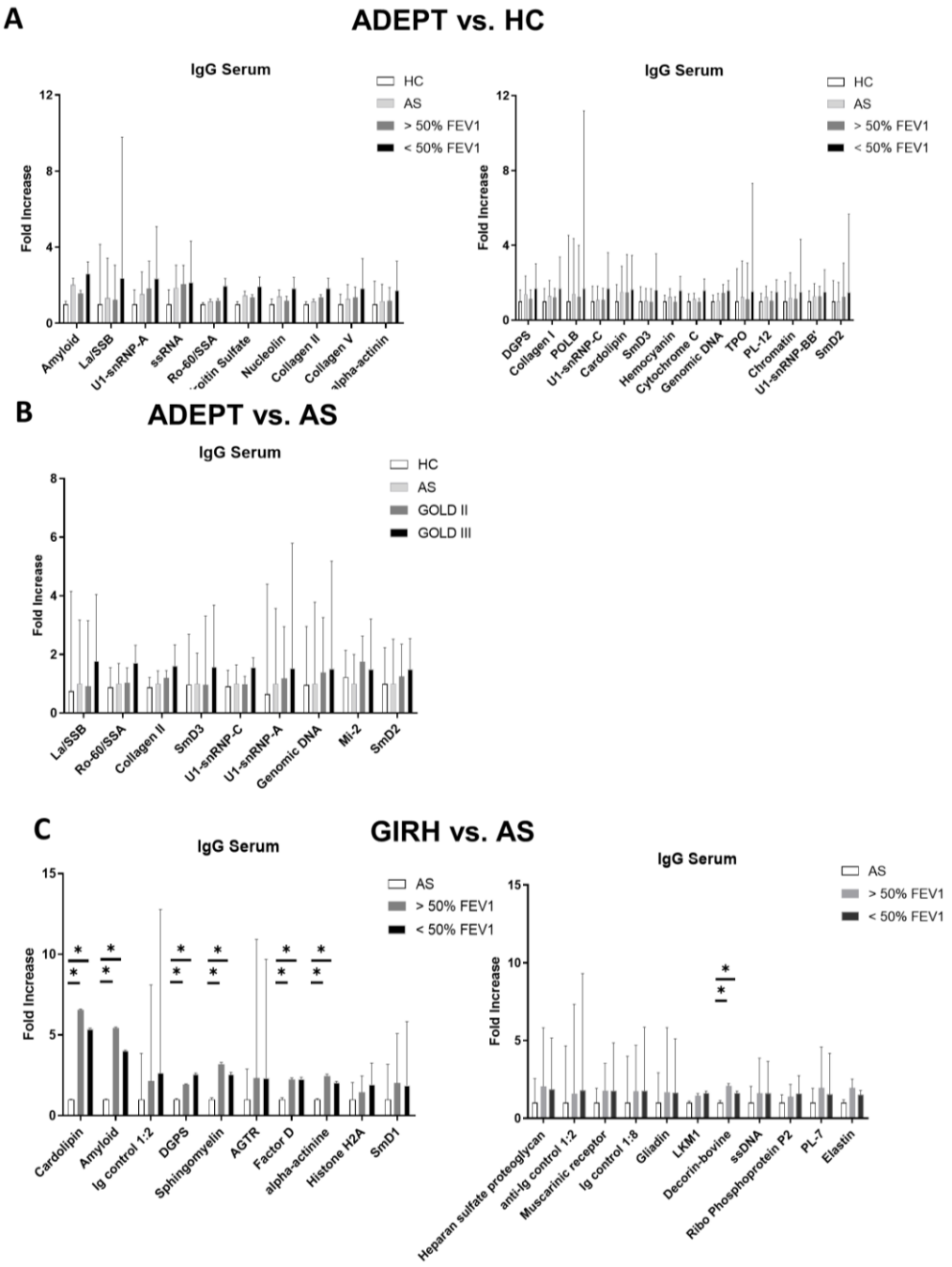
A
ADEPT vs. HC
IgG Serum
HC
AS
> 50% FEV1
< 50% FEV1
Fold Increase
Amyloid
La/SSB
U1-snRNP-A
ssRNA
Ro-60/SSA
Nucleolin
Collagen II
Collagen V
DGPS
Collagen I
POLB
U1-snRNP-C
Cardolipin
SmD3
Hemocyanin
Cytochrome C
Genomic DNA
TPO
PL-12
Chromatin
SmD2
B
ADEPT vs. AS
IgG Serum
HC
AS
GOLD II
GOLD III
Fold Increase
La/SSB
Ro-60/SSA
Collagen II
SmD3
U1-snRNP-C
U1-snRNP-A
Genomic DNA
Mi-2
SmD2
C
GIRH vs. AS
IgG Serum
AS
> 50% FEV1
< 50% FEV1
Fold Increase
Cardolipin
Amyloid
Ig control 1:2
DGPS
Sphingomyelin
AGTR
Factor D
alpha-actinine
Histone H2A
SmD1
Heparan sulfate proteoglycan
anti-Ig control 1:2
Muscarinic receptor
Ig control 1:8
Gliadin
LKM1
Decorin-bovine
ssDNA
Ribo Phosphoprotein P2
PL-7
Elastin

Figure S2. Serum autoantibodies analysed as fold increase over control as per Packard *et al*. (A) ADEPT samples compared to HC. (B) ADEPT samples compared to AS. (C) GIRH samples compared to HC. Only samples with a greater than 1.5-fold increase are shown. Shown are means and standard error of the mean. Multiple T test with two stage step up method of Benjamini, Krieger and Yekutieli. *p = < 0.05. (ADEPT n = 123, GIRH n = 120). HC – Healthy control. AS – Asymptomatic smokers. TPO - Thyroid peroxidase. PL-12 - Alanyl-tRNA synthetase (AARS). DGPS - 1,2-diacyl-sn-glycero3-phospho-L-serine. AGTR - Angiotensin II Receptor Type-1. SmD - Smith Antigen D. LKM1 - Liver kidney microsome type 1. PL-7 - Threonyl-tRNA synthetase (TARS). 10.6084/m9.figshare.14068847

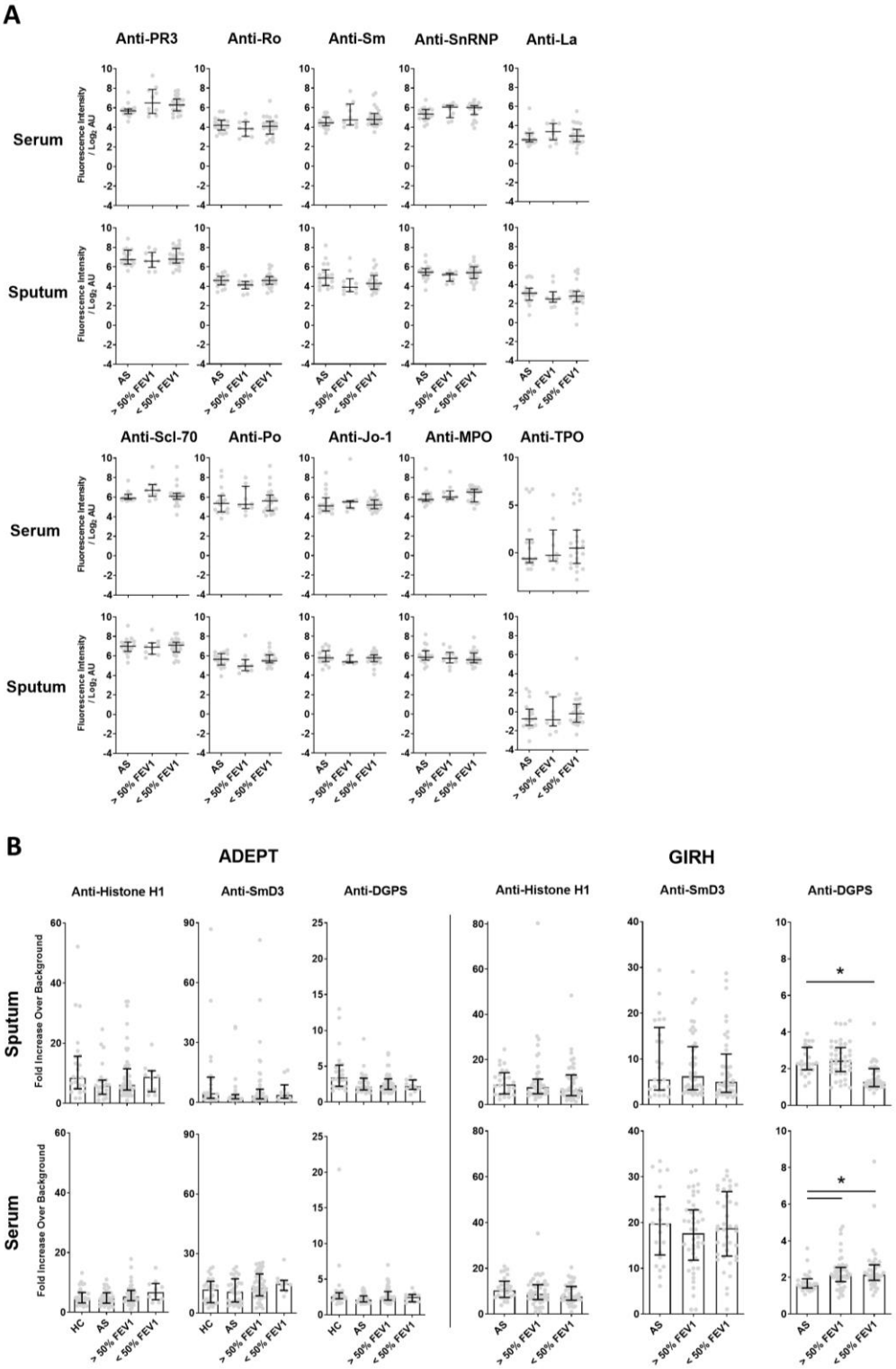
A
Anti-PR3
Anti-Ro
Anti-Sm
Anti-SnRNP
Anti-La
Serum
Sputum
Fluorescence Intensity / Log2 AU
Anti-Scl-70
Anti-Po
Anti-Jo-1
Anti-MPO
Anti-TPO
AS
> 50% FEV1
< 50% FEV1
B
ADEPT
GIRH
Anti-Histone H1
Anti-SmD3
Anti-DGPS
Fold Increase Over Background
HC
*

Figure S3. Common autoantibodies do not increase in induced sputum and serum measured by autoantigen multiplex bead array and ELISA. (A) Common IgG autoantibody specificities assessed via multiplex array in the GIRH cohort. Shown is the Log2 transformed fluorescence intensity. (GIRH: AS n = 17, >50% FEV1 n = 10, <50% FEV1 n = 23). (B) Sputum and serum anti-IgG histone H1, -SmD3 and -DGPS autoantibodies measured by ELISA. Data is shown as fold increase over the background (negative sample control). (ADEPT: HC n = 24, AS n = 24, >50% FEV1 n = 45, <50% FEV1 n = 10; GIRH: AS n = 27, >50% FEV1 n = 46, <50% FEV1 n = 43). All plots show median and inter-quartile range. One-way ANOVA Kruskal-Wallis test. *p = < 0.05. HC – Healthy control. AS – Asymptomatic smokers. FEV1 – Forced expiratory volume in 1 second. MFI - Median fluorescence intensity. PR3 - Proteinase 3. RO - Lupus RO Protein. Sm - Smith Antigen. SnRNP - Small Nuclear Ribonucleoprotein. La - Lupus La Protein. Scl-70 - Topoisomerase I. PO - Myelin protein Po. Jo-1 - Antihistidyl–tRNA Synthetase. MPO - Myeloperoxidase. TPO - Thyroid Peroxidase. DGPS - 1,2-diacyl-sn-glycero3-phospho-L-serine. 10.6084/m9.figshare.14068874

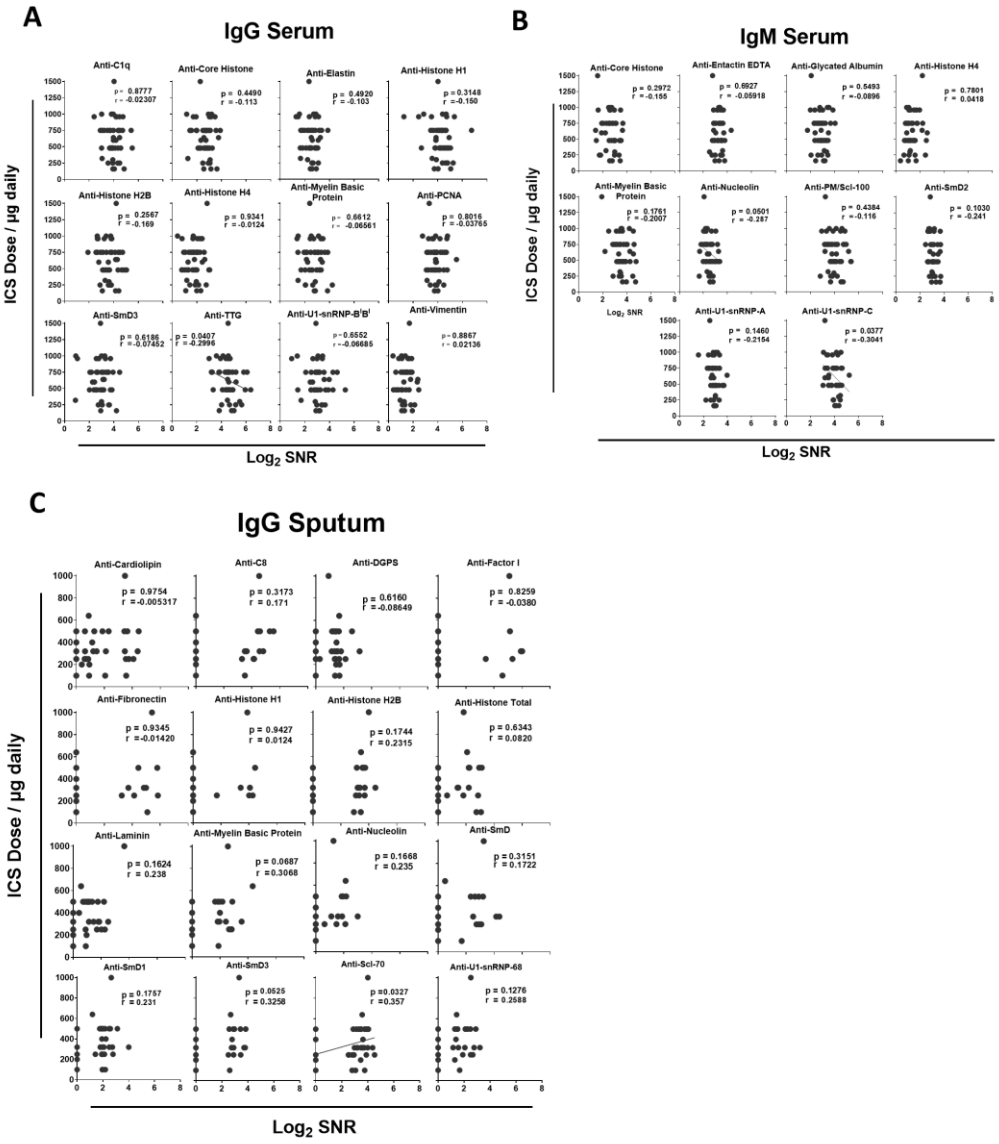

Figure S4. Differentially expressed specificities association with ICS daily use. IgG (A) and IgM (B) serum differentially expressed autoantibodies correlated with ICS use in the GIRH cohort. Differentially expressed IgG sputum (C) in the ADEPT cohort correlated with ICS daily use. Correlation plots show Spearman's rank correlation coefficient. (ADEPT n = 36, GIRH n = 47). ICS - inhaled corticosteroids. SNR – Signal-to-noise ratio. C1q - Complement component 1q. TTG - Tissue Transglutaminase. PCNA - Proliferating Cell Nuclear Antigen. SmD - Smith Antigen D. U1-snRNP-U1 - small nuclear ribonucleoprotein. C8 - Complement component 8. DGPS - 1,2-diacyl-sn-glycero3-phospho-L-serine. 10.6084/m9.figshare.14068880

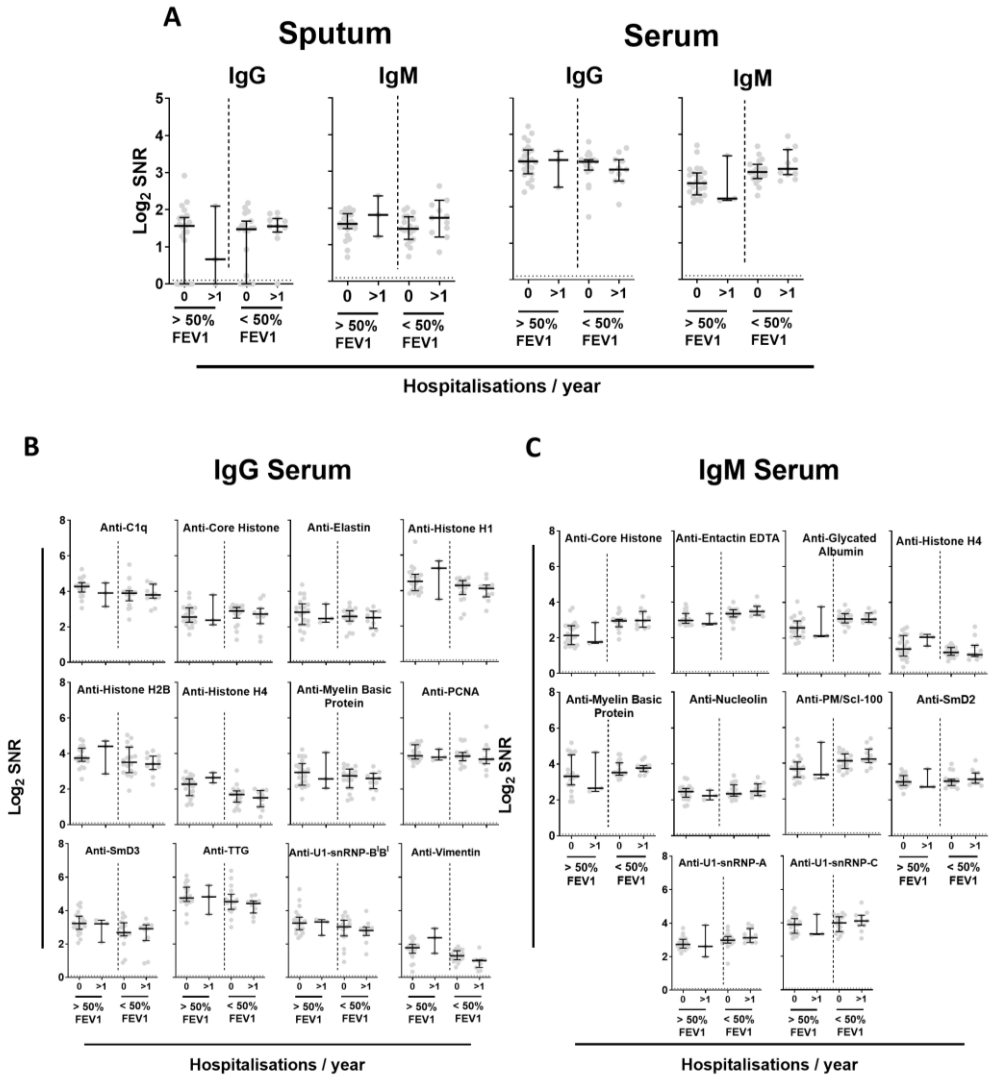

Figure S5. Exacerbation hospitalisation rate association with autoantibodies. Number of historical exacerbations in the previous one year. (A) Median total autoantibody levels. Levels of IgG (B) and IgM (C) serum autoantibodies most differentially expressed in subjects with number of historical exacerbations in one year. Plots show median and inter-quartile range. One-way ANOVA Kruskal-Wallis test. (GIRH: >50% FEV1 0 n = 22, >50% FEV1 >1 n = 3, <50% FEV1 0 n = 18, <50% FEV1 >1 n = 11). SNR – Signal-to-noise ratio. C1q - Complement component 1q. PCNA - Proliferating Cell Nuclear Antigen. SmD - Smith Antigen D. U1-snRNP-U1 - small nuclear ribonucleoprotein. 10.6084/m9.figshare.14068883

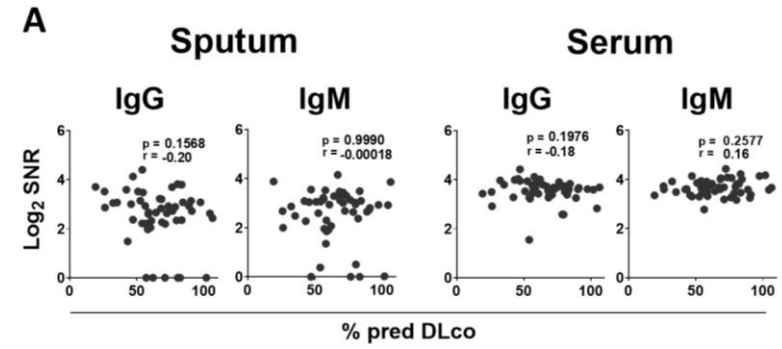
A
Sputum
Serum
IgG
IgM
IgG
IgM
p = 0.1568
r = -0.20
p = 0.9990
r = -0.00018
p = 0.1976
r = -0.18
p = 0.2577
r = 0.16
Log2 SNR
% pred DLco

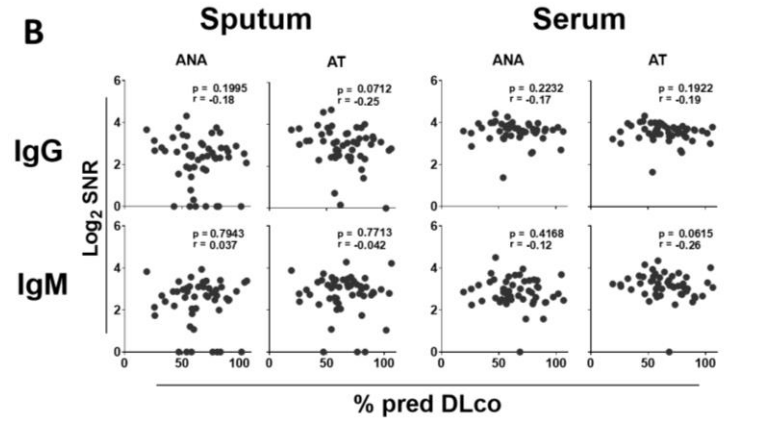
B
Sputum
Serum
ANA
AT
ANA
AT
IgG
IgM
p = 0.1995
r = -0.18
p = 0.0712
r = -0.25
p = 0.2232
r = -0.17
p = 0.1922
r = -0.19
p = 0.7943
r = 0.037
p = 0.7713
r = -0.042
p = 0.4168
r = -0.12
p = 0.0615
r = -0.26
Log2 SNR
% pred DLco

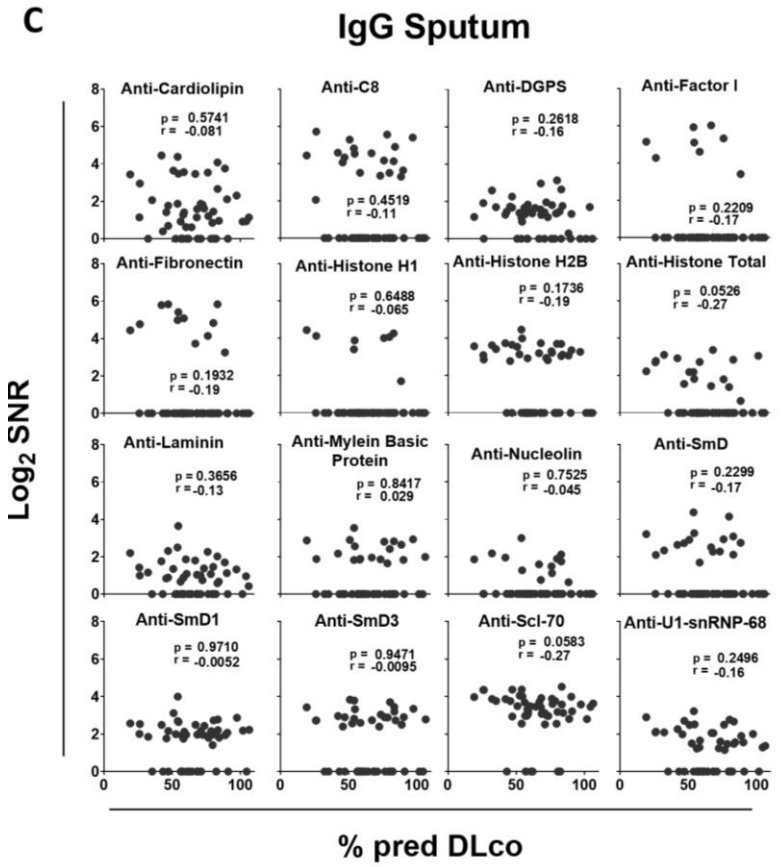
C
IgG Sputum
Anti-Cardiolipin
p = 0.5741
r = -0.081
Anti-C8
p = 0.4519
r = -0.11
Anti-DGPS
p = 0.2618
r = -0.16
Anti-Factor I
p = 0.2209
r = -0.17
Anti-Fibronectin
p = 0.1932
r = -0.19
Anti-Histone H1
p = 0.6488
r = -0.065
Anti-Histone H2B
p = 0.1736
r = -0.19
Anti-Histone Total
p = 0.0526
r = -0.27
Anti-Laminin
p = 0.3656
r = -0.13
Anti-Mylein Basic Protein
p = 0.8417
r = 0.029
Anti-Nucleolin
p = 0.7525
r = -0.045
Anti-SmD
p = 0.2299
r = -0.17
Anti-SmD1
p = 0.9710
r = -0.0052
Anti-SmD3
p = 0.9471
r = -0.0095
Anti-Scl-70
p = 0.0583
r = -0.27
Anti-U1-snRNP-68
p = 0.2496
r = -0.16
Log2 SNR
% pred DLco

Figure S6. Differentially expressed specificities association with carbon monoxide gas transfer in the ADEPT cohort. Predicted DLCO association with total median autoantibody levels in ADEPT cohort (A). Association of DLCO with anti-nuclear (ANA) and anti-tissue (AT) antibody specificities (B). IgG sputum differentially expressed autoantibodies with DLCO (D). Correlation plots show Spearman's rank correlation coefficient. (ADEPT n = 51). SNR – Signal-to-noise Ratio. DLCO - Diffusing capacity of the lungs for carbon monoxide. C8 - Complement component 8. PCNA - Proliferating Cell Nuclear Antigen. SmD - Smith Antigen D. U1-snRNP - U1 small nuclear ribonucleoprotein. 10.6084/m9.figshare.14068886

CHAPTER IV: MACROPHAGE SUBPOPULATION COMPOSITION AND FUNCTION FOLLOWING CIGARETTE SMOKE EXPOSURE

Investigating the composition and function of macrophage subpopulations in concurrent cigarette smoke and bleomycin-induced lung injury

4.1. Study Outline

Macrophages perform a central role in chronic inflammation and tissue destruction in cigarette smoke-associated respiratory diseases such as COPD and IPF[41,142,155]. While cigarette smoke is known to increase lung and BAL macrophages[53,61], the contribution from specific macrophage subpopulations to this total population is not known. Moreover, macrophage subpopulations are reported to have different proinflammatory[45] and phagocytic capacities[42]. The impact of cigarette smoke on these functions is not known.

To determine the impact of cigarette smoke on macrophage subpopulation dynamics, we used a well characterised model of cigarette smoke exposure. This model system exposes mice to whole body cigarette smoke for approximately 50 minutes twice a day for the duration of the exposure protocol (12 cigarettes per exposure, 24 per day). A previous study demonstrated that cigarette smoke exposure is well-tolerated in mice with corticosterone levels within the normal range (50 – 300 ng/mL). Furthermore, carboxyhaemoglobin and cotinine levels, markers of cigarette smoke exposure, were at equivalent levels to that observed in human cigarette smokers[81]. Consequently, this system

provides a suitable model with which to study the impact of cigarette smoke exposure on pulmonary macrophage subpopulation composition.

Macrophages perform a key role in the maintenance and repair of the lung environment[235]. In cigarette smoke-associated respiratory diseases such as COPD and IPF these repair processes become dysregulated and result in aberrant airway remodelling[208,236–238]. Bleomycin-induced lung injury models are used to study mechanisms of tissue remodelling. Bleomycin, a chemotherapeutic agent, is known to induce a robust fibrotic response that mimics aberrant fibroblast proliferation and differentiation, excessive deposition of extracellular matrix proteins, and destruction of the alveolar architecture as seen in IPF[238]. The bleomycin model has defined phases with which to investigate different immune functions. During the first ~7 days bleomycin induces increased oxidative damage[239] resulting in a proinflammatory environment characterised by IL-1, IL-6 and TNF-α[240]. Following this initial inflammation phase, cytokine levels diminish and there is a transition to a fibrotic phase with extracellular deposition[241]. After ~21 days fibrogenesis peaks before a spontaneous resolution and fibrotic reversal phase[242]. We therefore utilised this system to study the impact of cigarette smoke on the inflammatory and fibrogenesis phases of bleomycin-induced injury with a focus on the roles of different macrophage subpopulations at each stage.

This study used concurrent cigarette smoke exposure and bleomycin-induced lung injury to investigate the impact of cigarette smoke on macrophage subpopulation composition and function. Understanding the dominant

subpopulations present following cigarette smoke exposure will direct future treatment strategies aimed at preventing aberrant macrophage expansion in cigarette smoke-associated disease.

4.2. Increased monocyte-derived CD11b^{+} macrophage subpopulations following cigarette smoke exposure are associated with impaired bleomycin-induced tissue remodelling

Steven P. Cass*, Olivia Mekhael*, Danya Thayaparan, Joshua JC. McGrath, Spencer Revill, Matthew F. Fantauzzi, Peiyao Wang, Amir Reihani, Aaron Hayat, Christopher Stevenson, Anna Dvorkin-Gheva, Fernando M. Botelho, Martin R. Stämpfli, and Kjetil Ask

Manuscript status: In review at Frontiers in Immunology

Drs Martin Stampfli and Kjetil Ask, plus Olivia Mekhael and I conceived and designed the experiments. Dr Fernando Bethello plus Josh McGrath, Matt Fantauzzi, Peiyao Wang, Spencer Revill, Amir Reihani, Aaron Hayat, Danya Thayaparan, Olivia Mekhael and I performed the experiments. Dr Anna Dvorkin-Gheva, Olivia Mekhael and I analysed and interpreted the data. Drs Stevenson, Stampfli and Ask provided materials. Olivia Mekhael and I wrote and edited the manuscript.

ABSTRACT

Rationale. The accumulation of macrophages in the airways and the pulmonary interstitium is a hallmark of cigarette smoke-associated inflammation. Notably, pulmonary macrophages are not a homogenous population but consist of several subpopulations. To date, the manner in which cigarette smoke exposure affects the relative composition and functional capacity of macrophage subpopulations has not been elucidated.

Methods. Using a whole-body cigarette smoke exposure system, we investigated the impact of cigarette smoke on macrophage subpopulations in C57BL/6 mice using flow cytometry-based approaches. Moreover, we used bromodeoxyuridine labelling plus *Il1a*$^{-/-}$ and *Il1r1*$^{-/-}$ mice to assess the relative contribution of local proliferation and monocyte recruitment to macrophage accumulation. To assess the functional consequences of altered macrophage subpopulations, we used a model of concurrent bleomycin-induced lung injury and cigarette smoke exposure to examine tissue remodelling processes.

Main Results. Cigarette smoke exposure altered the composition of pulmonary macrophages increasing CD11b^{+} subpopulations including monocyte-derived alveolar macrophages (Mo-AM) as well as interstitial macrophages (IM)1, -2 and -3. The increase in CD11b^{+} subpopulations was observed at multiple cigarette smoke exposure timepoints. Bromodeoxyuridine labelling and studies in *Il1a*$^{-/-}$ mice demonstrated that Mo-AM and IM3 accumulated in the lungs of cigarette smoke-exposed mice. Compositional changes in macrophage subpopulations were associated with impaired induction of fibrogenesis

including decreased α-smooth muscle actin positive cells following intratracheal bleomycin treatment. Mechanistically, *in vivo* and *ex vivo* assays demonstrated predominant macrophage M1 polarisation and reduced matrix metallopeptidase 9 activity in cigarette smoke-exposed mice.

Conclusion. Cigarette smoke exposure modified the composition of pulmonary macrophage by expanding $CD11b^{+}$ subpopulations. These compositional changes were associated with attenuated fibrogenesis, as well as predominant M1 polarisation and decreased fibrotic activity. Overall, these data suggest that cigarette smoke exposure altered the composition of pulmonary macrophage subpopulations contributing to impaired tissue remodelling.

INTRODUCTION

A strong association has been shown between cigarette smoking and respiratory diseases such as, chronic obstructive pulmonary disease (COPD), lung cancer, and interstitial lung disease. Central to the pathogenesis of these cigarette smoke (CS)-associated respiratory diseases is the macrophage (1–3). Increased in the lungs following CS exposure (4,5), macrophages perform a vital role in CS-induced inflammation6. Of note, pulmonary macrophages consist of several subpopulations with independent and diverse functional roles (7–11). The composition and functional consequences of CS exposure on pulmonary macrophage subpopulations is yet to be elucidated.

Pulmonary macrophages can be stratified into two broad populations, alveolar macrophages (AM) and interstitial macrophages (IM). In mice, the first developmental wave occurs in the yolk sac on embryonic day (E)10-12 producing primitive AM (12,13). The longevity of primitive AM is unclear; however, a second developmental wave arises from the foetal liver and enter the lungs by E12-16 (12,13). These pre-AMs enter the lumen postnatally (12,13) and mature into long-lived tissue resident alveolar macrophages (Res-AM). These mature Res-AM are predominately self-maintained with limited contribution from circulating monocytes (14). A third AM subpopulation, monocyte-derived alveolar macrophages (Mo-AM), are recruited from the bone marrow after birth (14). Mo-AM share 99.9% of genes with Res-AM (15) but contribute to less than 5% of the alveolar population under homeostatic conditions (13). In addition to AM populations, IM are present and constitute approximately 20% of the pulmonary macrophage environment at steady state (13,16). The majority of IM are produced postnatally in the bone marrow and populate the lung parenchyma throughout life (12,17). Notably, a proportion of IM are derived from the yolk sac and are self-maintained similar to Res-AM populations (11). IM are further divided into three subpopulations based on CD11c and MHCII expression (IM1 - $CD11c^{Neg}MHCII^{Neg}$, IM2 - $CD11c^{Neg}MHCII^{Hi}$, IM3 - $CD11c^{Hi}MHCII^{Hi}$) (17). In total five pulmonary macrophage populations, Res-AM, Mo-AM plus IM1, -2 and -3 are detectable by flow cytometry-based techniques in mice.

The developmental origin of macrophage subpopulations is associated with differing function. At steady state, the phagocytic capacity is greatest in

AM populations, followed by IM1, IM2 and poorest in IM3 (17). In contrast, IM populations are enriched for inflammatory mediators and monocyte-related genes distinct from AM (17). These observations have been replicated in COPD, wherein IM were found to be more proinflammatory, but less phagocytic, than AM counterparts (7). Macrophages are key in tissue remodelling processes and interstitial CX_3CR1 mononuclear phagocytes, encompassing IM1, -2 and -3 populations (17), have been reported to promote CS-induced emphysema (18). Moreover, in pre-clinical pulmonary fibrosis models, aberrant tissue remodelling has been specifically associated with increased Mo-AM (9,10,19) and reduced IM1 (8). Given that macrophage subpopulations instigate inflammation that can lead to respiratory disease, further investigation of the impact of CS on individual macrophage subpopulations is warranted.

In this study, we investigated the impact of CS exposure on macrophage subpopulation composition and function. Using a whole-body CS exposure system, we assessed CS-induced alterations in macrophage populations, including $CD11b^+$ subpopulations Mo-AM, IM1, -2 and -3, in the lungs. Moreover, we evaluated the impact of concurrent bleomycin treatment and CS exposure to understand macrophage subpopulation polarisation and ability to facilitate tissue remodelling. These data explored the impact of CS exposure on macrophage subpopulation composition, origin and function to offer insight into CS-associated respiratory disease.

MATERIALS AND METHODS

Animals. 6- to 8-week-old female C57BL/6 mice were purchased from Charles River Laboratories (PQ, Canada). Female IL-1α-deficient (*Il1a*$^{-/-}$) mice were obtained from MiceCenter for Experimental Medicine and Systems Biology, University of Tokyo, Japan and bred in-house. Female IL-1R1-deficient (*Il1r1*$^{-/-}$) mice (C57BL/6 background) with respective wild-type controls were obtained from The Jackson Laboratories (Maine, USA). Mice were subjected to a 12-hour light–dark cycle and had ad libitum access to food and water and housed under specific pathogen-free conditions. All experiments were approved by the Animal Research Ethics Board at McMaster University (#19-08-23).

Experimental CS exposure model. Mice were exposed to twelve 3R4F reference cigarettes with filters removed (University of Kentucky, Lexington, USA) or room air (RA), twice daily for five days per week. Mice were exposed for up to 24-weeks using a whole-body CS exposure system SIU-48 (Promech Lab AB, Vintrie Sweden). Upon exposure completion, mice were euthanized by exsanguination and cardiac puncture.

Tissue processing for flow cytometric analysis. Single cell suspensions were produced as follows. Mouse right middle, inferior, and post-caval lobes were enzymatically digested (150U/mL collagenase type I) for 1-hour shaking at 37°C. Bronchoalveolar lavage (BAL) was collected following 2x 500µL phosphate-buffered saline (PBS) washes of the single left lung lobe and BAL samples were then spun at 300 g for 5-minutes to pellet cells. To assess bone marrow, a single femur was removed and cells were flushed out using 5mL

RPMI. Digested lung, flushed bone marrow, and harvested spleens were all crushed through 40µm mesh. Lung cells were treated with ACK lysis buffer (1mL, 1-minute) to lyse red blood cells. Approximately 80µL of blood was drawn using retro-orbital bleeding, lysed using 1x Red Blood Cell lysis buffer (#00-4333-57, eBioscience) and spun at 300 g for 5-minutes. All single cell suspensions were stained for flow cytometric analysis using antibodies shown in **Table S1**. Gating strategies are shown in **Figure S1A-D**. All samples were run on a BD LSRFortessa (BD Biosciences, ON, Canada).

Bromodeoxyuridine delivery. CS- or RA-exposed mice were intraperitoneally injected with bromodeoxyuridine (BrdU) for three consecutive days prior to sacrifice. 200µg on day -3 then subsequently 100µg on day -2 and -1 to assess macrophage turnover. BrdU incorporation into cells was assessed by flow cytometry.

Experimental pulmonary fibrosis model. Tissue remodelling was induced with a single intratracheal instillation of bleomycin (0.05U/mouse in a volume of 50µl sterile saline) by oropharyngeal administration. Control animals received 50µl vehicle alone. Weights of animals were monitored regularly, and tissue harvest was conducted 7 (inflammatory phase) or 21 (fibrotic phase) days following bleomycin intubation. Lung function assessments were conducted using a flexiVent® mechanical respirator according to manufacturer's protocol at day 21 (flexiVent®, SCIREQ, Montreal, PQ, Canada) (20).

Isolation and stimulation of lung CD45$^+$ adhered cells. CD45$^+$ cells from lung single-cell suspensions were positively selected using mouse CD45 microbeads

and LS columns (#130-052-301 and #130-042-401, Miltenyi Biotech) and cultured on a flat 96-well plate for 90-minutes. Non-adherent cells were stringently washed with PBS before remaining adherent cells were treated for 24-hours with recombinant murine transforming growth factor beta 1 (TGF-β1) (30ng/mL; BioLegend, USA), IL-4 (20ng/mL; PeproTech, Canada) and IL-6 (5ng/mL; PeproTech, Canada). Macrophage "M2" polarisation was assessed by arginase activity in cell lysates, as described previously (21). Matrix metallopeptidase 9 (MMP9; #DY6718 R&D Systems, ON, Canada) ELISA, and CyQUANT™ lactose dehydrogenase (LDH; #C20301 ThermoFisher Scientific, ON, Canada) cytotoxicity assay, and soluble collagen assessed using sircol assay (SircolTM Soluble Collagen Assay #CLRS1000, Biocolor, UK) were performed on cell culture supernatant.

Tissue collection for protein and RNA multiplex analysis. Lung (right superior lobe) homogenate was processed using Bullet Blender 24 Gold (Next Advance, Troy NY USA) either in PBS or RLT lysis buffer (Qiagen, Valencia, CA, USA) for protein and RNA analysis respectively. Protein from lung homogenate supernatant was assessed using the Discovery Assay® Mouse Cytokine Array/Chemokine Array 31-Plex (MD31; Eve Technologies Corp, Calgary, AB, Canada). Total RNA from RLT lysed lung homogenate was extracted using the RNeasy mini kit (Qiagen, Valencia, CA, USA, #74104). Following RNA integrity and quantity quality control the nCounter Elements system (NanoString Technologies, Seattle, WA, USA) was employed to quantify the expression levels of 25 mouse genes (**Table S2**).

Lung processing for histopathology. Mouse single left lungs were inflated and fixed in 10% formalin for 24-hours prior to embedment in paraffin wax. A tissue microarray (TMA) was generated containing 5μm lung sections cut and stained on a Bond RX fully automated research Stainer (Leica Biosystems) (21). Immunohistochemistry (IHC) staining on lung serial sections was performed for hematoxylin & eosin (H&E), α-smooth muscle actin (α-SMA), and Masson's trichrome blue (MTri). IHC stained-microscope slides were digitalised using an Olympus VS120-L100-W slide scanner at a 20× magnification and quantified using HALO™ Image Analysis Software (Halo Plus 3.2, Indica Labs).

Statistical analysis. Results expressed as mean ± standard error of the mean. Graphs and statistical tests were performed using GraphPad Prism 9.1 (GraphPad Software, Inc) and R (www.r-project.org). For RNA analysis samples were preprocessed and normalised using nSolver 2.5 software (www.nanostring.com) using three housekeeping genes Actb, Pgk1, and Ywhaz plus negative and positive controls. 25 mouse genes (**Table S2**) were used to perform principal component analysis (PCA), hierarchical clustering and differential expression analysis in R. Two-way ANOVA followed by Tukey's multiple comparisons test was used to determine significance when two concurrent variables were compared. Unpaired t test with Welch's correction was used to assess significance between only two groups. A $p < 0.05$ was considered statistically significant.

RESULTS

CD11b$^+$ macrophage subpopulations increase in the lungs of CS-exposed mice. CS is known to cause the expansion of the total lung macrophages (4,5) but the impact on macrophage subpopulation diversity is not known. Using the nomenclature proposed by Gibbings et al. (17) (**Table 1**), we demonstrated an expansion of all CD11b$^+$ populations including Mo-AM and IM1, -2 and – 3 at all CS timepoints (**Figure 1A**). Res-AM were unchanged at 2 and 12 weeks of CS but decreased at 24-weeks. The alterations in macrophage subpopulation numbers were not driven by changes in total lung cellularity but represent changes to each subpopulation individually (**Figure S2A**). Independent of CS exposure length, each CD11b$^+$ macrophage subpopulation was increased in CS-exposed mice.

The size and location of macrophages has been associated with phagocytic and inflammatory differences (7). In this study, CD11b$^+$ populations, Mo-AM (16.0%), IM1 (8.2%), and IM3 (7.1%), decreased in size at 12 weeks of CS (**Figure S2B**), corresponding to clinical observations of expanded small macrophages in COPD lung sections (7). We further assessed the presence of macrophage subpopulations in the BAL as a measure of macrophage location within the airways. While Res-AM decreased, each CD11b$^+$ subpopulation, including all IM, were increased in the BAL of CS-exposed mice at 8 weeks of CS (**Figure 1B**). Clinically, airway macrophages are reported to be lipid-laden, and thus more granular (22). In our model, Res-AM became 197.9% and CD11b+ subpopulations 121.5-150.1% more granular

than respective RA populations in the BAL (**Figure S2C**). Overall, we observed increased number of small, more granular, $CD11b^+$ macrophages subpopulations following CS exposure.

Increased $CD11b^+$ macrophage turnover in CS-exposed mice. To elucidate mechanisms contributing to increased $CD11b^+$ macrophage populations, we assessed immune mediators associated with macrophage recruitment and survival in the lung homogenate. At 12 weeks of CS exposure myeloid chemoattractants CCL2 and CCL3 increased, as well as IL-1α (**Figure 2A**). IL-1α has previously been associated with CS-mediated myeloid cell recruitment (6,23). Next, we measured immune mediators associated with monocyte differentiation and macrophage survival, M-CSF, GM-CSF and IL-6, all of which increased in the lung tissue of CS-exposed mice (**Figure 2B**). Immune mediators associated with macrophage recruitment and survival were increased in CS-exposed mice.

To understand pulmonary lung dynamics, we assessed macrophage subpopulation turnover using thymidine analogue BrdU. BrdU uptake can be used as a surrogate measure of cell turnover and the balance between local proliferation and cell recruitment. While the total Res-AM trended to decrease following CS exposure the percentage of Res-AM positive for BrdU increased (**Figure 2C**). Of note, the decreasing trend in total Res-AM was associated with increased cell death in CS-exposed mice as measured by flow cytometry Live/Dead positive staining (**Figure 2D**). Taken together, this suggests Res-AM proliferated in response to CS exposure to refill the environmental niche opened

by increased Res-AM cell death. In contrast, $CD11b^+$ populations had proportionally equal or fewer percentage $BrdU^+$ cells, but increased total $BrdU^+$ cells, following CS exposure (**Figure 2E-H**). The fixed percentage of BrdU positive cells indicated a stable rate of BrdU incorporation. Consequently, the increase in total $BrdU^+$ Mo-AM and IM3 likely reflected a predominant recruitment of cells to the lungs. Total lung cell numbers were equivalent in RA and CS mice suggesting that changes were reflective of compositional shifts within the lung. Overall, CS was associated with Res-AM proliferation and a recruitment of Mo-AM and IM3 cells to the lung.

Monocytes and macrophage-lineage bone marrow progenitor cells are transiently decreased at 12 weeks of CS exposure. Given the expansion of $CD11b^+$ populations including Mo-AM and IM3 in the lung, we next assessed the impact of CS on lung, blood, spleen, and bone marrow monocytes. In the lung, we observed that $Ly6C^{Lo}$ monocyte populations, primed for macrophage differentiation, were not altered by CS exposure at 12-weeks. In contrast, classical inflammatory $Ly6C^{Hi}$ monocytes were reduced by CS (**Figure 3A**). There was no change in either monocyte population in the circulation (**Figure 3B**). In the spleen, a known monocyte reservoir (24), CS resulted in decreased total spleen cells (**Figure S3A**) and consequently both monocyte populations (**Figure 3C**). CS exposure decreased both monocyte populations in the bone marrow at 12-weeks (**Figure 3D**). No changes in either monocyte population were observed in any tissue at 2- and 24-weeks CS exposure, with the exception of $Ly6C^{Lo}$ monocytes, which were decreased following 2 weeks of CS exposure in the bone marrow (**Figure S3B-E**).

Next, we assessed macrophage progenitor cells in the bone marrow. The linearity of commitment toward cell terminal differentiation in order is $Lineage^{Neg}Sca1^{+}c\text{-}Kit^{+}$(LSK), monocyte-macrophage dendritic cell progenitor (MDP), common monocyte progenitor (cMoP) and finally monocyte populations (25–27). We observed all LSK progenitor cell populations were decreased in CS-exposed mice at 12 weeks (**Figure 3E**; **Figure S3F**). To note, more committed progenitor MDP and cMoP populations were unchanged by CS exposure (**Figure 3E**). CS exposure was associated with a transient reduction in lung, spleen and bone marrow monocyte and macrophage progenitor populations at 12 weeks of CS exposure.

CS-exposed pulmonary macrophage expansion is IL-1α dependent. The IL-1α axis is critical in the recruitment of myeloid cells to the lung following CS exposure (6,28,29). Consequently, we assessed the impact of IL-1α and IL1-R1 deficiency on macrophage subpopulations composition in CS-exposed mice. Res-AM were significantly attenuated in both *Il1a*$^{-/-}$ and *Il1r1*$^{-/-}$ mice following CS exposure (**Figure 4**; **Figure S4A**). Mo-AM and IM3, which were the predominant subpopulations increased in total $BrdU^{+}$ cells, had attenuated expansion in *Il1a*$^{-/-}$ mice following CS exposure (**Figure 4**). There was no change in Mo-AM or IM3 populations in *Il1r1*$^{-/-}$ mice following CS exposure (**Figure S4A**). Moreover, IL-1α- and IL1-R1-deficiency was not associated with changes in IM1 or IM2 populations (**Figure 4**; **Figure S4A**). Cell number changes were not driven by differences in total cell number (**Figure S4B-C**). Thus, CS was associated with IL-1α dependent expansion of Mo-AM, IM3, and Res-AMs.

CS exposure skews macrophage subpopulation composition during impaired bleomycin-induced tissue remodelling. Monocyte-derived macrophages, which contribute to the expanded $CD11b^+$ macrophages in our model, have been shown to be necessary for fibrogenesis (9,10,19). Using a model of concurrent mild bleomycin-induced lung injury, we assessed the impact of CS on macrophage function at two timepoints, day 7 (pre-tissue remodelling and peak inflammation) and day 21 (peak fibrogenesis) (**Figure 5A**). While bleomycin-treated mice had equivalent weight loss regardless of exposure (**Figure S5A**), 3/5 (60%) and 4/5 (80%) myeloid lineage-related genes were enriched in CS-exposed compared to RA-exposed bleomycin-treated mice at day 7 and 21 respectively (**Table S3**; **Table S4**). These transcriptional changes, including the upregulation of the CD11b-encoding gene *Itgam*, were likely related to the observed expansion of all $CD11b^+$ subpopulations at day 7 in CS-exposed bleomycin-treated mice (**Figure 5B**). This compositional phenotype was not maintained in CS-exposed bleomycin-treated mice at day 21, with only IM2 remaining expanded (**Figure 5C**). In contrast, at day 21, Res-AM and Mo-AM populations were decreased and IM1/IM3 were equivalent in CS-exposed compared to RA-exposed bleomycin-treated mice (**Figure 5C**).

These alterations in macrophage composition at day 7 and 21 were associated impaired fibrogenesis by day 21 as determined by biomechanical, transcriptional and histological measurements. CS-exposed compared to RA-exposed bleomycin-treated mice had reduced lung elastance (**Figure S5B**) at day 21. This decreased elastance was associated with the downregulation of 5/9 (55%) fibrotic/wound healing genes at day 7 and 3/9 (33%) at day 21 in CS-

exposed compared to RA-exposed bleomycin-treated mice (**Table S3**; **Table S4**). Notably, overall transcriptional changes were sufficient to define experimental groups by unsupervised hierarchical clustering analysis at day 7 but not at day 21, where clustering was split based on CS status (**Figure S5C-D**). These altered transcriptional and lung biomechanics were associated with attenuated expansion of α-SMA$^+$ cells in CS-exposed compared to RA-exposed mice (**Figure 5D**). Moreover, while the percent of collagenous area increased in RA-exposed bleomycin-treated mice compared to non-treated RA controls, collagen deposition was variable in CS-exposed bleomycin-treated mice and did not increase compared to controls (**Figure 5E**). Thus, trichrome staining suggests impaired collagen production in CS-exposed mice. Representative H&E stains are shown in (**Figure S5E**). Overall, these data suggest CS alters the transcriptional environment and macrophage composition at day 7 post bleomycin in a manner conductive to impaired fibrogenesis, as evidenced by decreased α-SMA$^+$ myofibroblasts, elastance and collagen deposition at day 21.

Macrophage function and polarisation is skewed by CS exposure. Given that we observed concurrent changes in macrophage composition and fibrotic outcome, we next sought to address whether CS specifically alters macrophage fibrogenic phenotype and function. M2-polarised, alternatively activated macrophages are proposed to contribute to tissue remodelling and fibrogenesis (21,30). Consequently, using CD38 as a marker for M1-like and CD206 for M2-like macrophages, we assessed the polarisation state of each macrophage subpopulation at day 7 and 21 post bleomycin. While polarised macrophages comprised less than 30% of each subpopulation, of those cells polarised, CD38$^+$

macrophages formed the greatest proportion at both day 7 and 21. CD38 expression was increased in all macrophage subpopulations of CS-exposed bleomycin-treated mice at day 7 (**Figure 6A**; **Figure S6A**). By day 21, polarised macrophages remained predominately $CD38^+$ but strikingly $CD206^+$ Res-AM decreased in CS-exposed compared to RA-exposed bleomycin treated mice (**Figure 6B**; **Figure S6B**). At both day 7 and day 21 CS-induced dual $CD38^+CD206^+$ expression, reflecting previous dual polarisation observations in CS only exposure models (31) (**Figure 6A-B**; **Figure S6A-B**). Of note, no difference in total cell number was observed between bleomycin-treated groups at either day 7 or 21 (**Figure S6C-D**). To explore the impact of CS on macrophage function further, adherent lung $CD45^+$ cells isolated following 12-weeks of CS or RA exposure were stimulated for 24-hours with a profibrotic cytokine mix (TGF-β1, IL-4, and IL-6). Comprising predominantly pulmonary macrophages, but not excluding monocytes or dendritic cells, we observed no difference in cell viability between experimental groups (**Figure S6E**). Arginase activity (as measured by urea production), a surrogate measure of alternatively-activated macrophage function, was equivalent in RA or CS-exposed cells following stimulation and demonstrating no loss in M2-like functionality (**Figure 6C**). In addition, while adherent $CD45^+$ cells produced soluble collagen, CS exposure did not alter production and therefore contribute to changes in collagen deposition (**Figure 6D**). However, CS exposure was sufficient to attenuate the induction of MMP9, a peptidase implicated in CS-mediated epithelial-mesenchymal transition and myofibroblast development in

fibrogenesis (32). In summary, CS exposure elicited a shift toward a M1-dominant phenotype and decreased MMP9 release.

DISCUSSION

Macrophages perform a central role in the pathogenesis of several CS-associated respiratory diseases including COPD and interstitial lung disease (1–3). However, the composition of pulmonary macrophage subpopulations following CS exposure is poorly understood. Using a mouse model of CS exposure, we showed increased $CD11b^{+}$ macrophage populations, including Mo-AM and IM1, -2 and -3, in CS-exposed mice. The expansion of Mo-AM and IM3 populations was IL-1α dependent and was associated with a transient decrease in monocyte and progenitor populations in the bone marrow, spleen, and lungs, at 12 weeks of CS. These compositional changes were exacerbated in a model of bleomycin-induced lung injury. Moreover, CS exposure increased M1-polarised macrophages and was associated with impaired MMP9 release. Ultimately, these macrophage compositional and functional changes were associated with decreased fibrogenesis and impaired tissue remodelling in CS-exposed mice.

IM populations are reported to be located in the lung parenchyma and associated with vascular integrity and antigen presentation (8,11). In CS-exposed mice, we observed all IM populations in the BAL. It is possible that the greater epithelial permeability in cigarette smokers (33,34) enables greater recovery of IM from CS-exposed mice. To note, these cells likely do not reflect a transitioning IM cell into a Mo-AM as these populations are reported to have

independent ontologies (10). Distinguishing IM and AM populations by histology is challenging due to the spectrum of cellular markers expressed which are shared between macrophage subpopulations. Further analysis is therefore warranted to determine whether IM1, -2 and -3 populations continue to reside in interstitial spaces upon CS exposure. The presence and the functional consequence of IM in the alveolar space warrants further investigation.

CS exposure caused a robust expansion of $CD11b^+$ (Mo-AM, IM1, -2, -3) populations in the lung. These expanded $CD11b^+$ populations have been previously reported to be derived from monocytes (10,17). We observed transient decreases in macrophage/monocyte progenitor populations in the bone marrow and decreased monocytes in the lung and spleen following CS exposure. Moreover, we observed increased total $BrdU^+$ Mo-AM and IM3 cell turnover in CS-exposed mice. It is therefore plausible these observations represent a CS-induced recruitment of monocytes which differentiate into Mo-AM and IM3 populations in the lung. However, targeted lineage tracing experiments are needed to confirm the ontogeny of these macrophage subpopulations in CS-exposed lungs. Res-AM numbers were unchanged by CS exposure with an equal balance between increased cell death and cell proliferation. This paradigm is supported by previous data that showed Res-AM have minimal postnatal recruitment and are self-maintained at steady state (12). Taken together, these data suggest that CS exposure promotes the expansion of $CD11b^+$ populations, and specifically Mo-AM and IM3, altering pulmonary macrophage composition.

The IL-1α axis has been shown to be vital in CS-induced inflammation (6,28,29). In *Il1a*$^{-/-}$ mice, we observed reduced Mo-AM and IM3. Notably, these populations had increased numbers positive for BrdU which suggested increased cell turnover. Overall, these data propose an IL-1α dependent recruitment of Mo-AM and IM3 populations to CS-exposed lungs. Furthermore, Res-AM expansion was also IL-1α dependent whereas IM1 and IM2 expansion was not. We speculate the smaller contribution of IL-1α to IM1 and IM2 populations is a consequence a proportion of yolk sac-derived to IM1 and IM2 populations. IM1 and IM2 populations share a cellular phenotype with self-maintained and long-lived yolk sac-derived IM cells11. Thus, we speculate long-lived yolk sac-derived IM cells are less dependent on IL-1α than foetal liver- or bone marrow-derived macrophage subpopulations.

Macrophages perform a vital role in the repair and regeneration of the tissue following damage (35). Using a model of bleomycin-induced lung injury, we observed attenuated tissue remodelling following CS exposure which was associated with decreased Res-AM and Mo-AM populations at peak fibrogenesis. Mo-AMs are necessary for fibrogenesis in mouse models of fibrosis (9,10); thus, a reduction in Mo-AM in CS-exposed compared to RA-exposed bleomycin-treated mice may represent an impairment in fibrogenesis in our model. In addition, IM1 which have been reported to protect against fibrosis (8), were expanded in CS-exposed mice and therefore may also contribute to an anti-fibrotic environment. Notably, CS exposure induced a greater number of M1-like compared to M2-like-polarised macrophages at both day 7 and 21 regardless of subpopulation. Lung transcriptional changes in

fibrotic/wound healing and M2-realted genes were most discordant at the day 7 timepoint between bleomycin-treated groups. This phenotypic shift was not associated with any difference in arginase activity suggesting macrophages remain capable of M2-like functional activity despite the increase in M1-like cells. Detailed investigation of the impact of CS on each macrophage subpopulation's function is needed to elucidate the precise mechanisms altered and that contribute to impaired tissue remodelling. Taken together, these data suggest that CS exposure alters pulmonary macrophage composition and polarisation, decreasing the accumulation of profibrotic macrophages early in fibrogenesis progression leading to an impaired tissue remodelling phenotype by day 21.

CS is well-known to compromise tissue repair through such processes as impaired myofibroblast differentiation (36). Specifically, MMP9 has been shown to contribute to TGF-β production (37) and epithelial-mesenchymal transition (32,38), processes central to myofibroblast differentiation (39). We observed impaired MMP9 expression in isolated adherent lung $CD45^+$ cells from 12-week CS-exposed mice. These data suggest an impaired, or delayed, ability for CS-exposed adherent $CD45^+$ cells to contribute to $\alpha\text{-}SMA^+$ myofibroblast expansion. It is plausible the CS-mediated reduction in $\alpha\text{-}SMA^+$ myofibroblasts, a major collagen producing cell (40), is critical in the impaired tissue remodelling and repair response observed in this bleomycin-induced lung injury model. Further investigation of processes that contribute to CS-induced impaired myofibroblast expansion in tissue remodelling is warranted.

In summary, we showed that CS altered pulmonary macrophage composition, increasing $CD11b^{+}$ subpopulations, including Mo-AM and IM1-2 and -3, at multiple CS exposure timepoints. The expansion of Mo-AM and IM3 was dependent on IL-1α and likely reflective of increased cell recruitment. Compositional changes were associated with predominately M1-like macrophages, attenuated MMP9 release and decreased fibrogenesis in a model of bleomycin-induced lung injury. Taken together, these data propose that CS exposure skews pulmonary macrophage subpopulation composition and function predisposing the host to impaired tissue remodelling following lung injury.

REFERENCES

1. Traves, S. L., Smith, S. J., Barnes, P. J. & Donnelly, L. E. Specific CXC but not CC chemokines cause elevated monocyte migration in COPD: a role for CXCR2. J. Leukoc. Biol. 76, 441–450 (2004).

2. Sumitomo, R. et al. M2 tumor-associated macrophages promote tumor progression in non-small-cell lung cancer. Exp. Ther. Med. 38, 4490–4498 (2019).

3. Prasse, A. et al. A vicious circle of alveolar macrophages and fibroblasts perpetuates pulmonary fibrosis via CCL18. Am. J. Respir. Crit. Care Med. 173, 781–792 (2006).

4. Gaschler, G. J. et al. Cigarette smoke exposure attenuates cytokine production by mouse alveolar macrophages. Am. J. Respir. Cell Mol. Biol. 38, 218–226 (2008).

5. Morissette, M. C., Shen, P., Thayaparan, D. & Stämpfli, M. R. Disruption of pulmonary lipid homeostasis drives cigarette smoke-induced lung inflammation in mice. Eur. Respir. J. 46, 1451–60 (2015).

6. Nikota, J. K. et al. Cigarette smoke primes the pulmonary environment to IL-1α/CXCR-2-dependent nontypeable Haemophilus influenzae-exacerbated neutrophilia in mice. J. Immunol. 193, 3134–45 (2014).

7. Dewhurst, J. A. et al. Characterisation of lung macrophage subpopulations in COPD patients and controls. Sci. Rep. 7, 1–12 (2017).

8. Chakarov, S. et al. Two distinct interstitial macrophage populations coexist across tissues in specific subtissular niches. Science (80-.). 363, (2019).

9. Misharin, A. V. et al. Monocyte-derived alveolar macrophages drive lung fibrosis and persist in the lung over the life span. J. Exp. Med. 214, 2387–2404 (2017).

10. Joshi, N. et al. A spatially restricted fibrotic niche in pulmonary fibrosis is sustained by M-CSF/M-CSFR signalling in monocyte-derived alveolar macrophages. Eur. Respir. J. 55, (2020).

11. Ural, B. B. et al. Identification of a nerve-associated, lung-resident interstitial macrophage subset with distinct localization and immunoregulatory properties. Sci. Immunol. 5, 1–15 (2020).

12. Tan, S. Y. S. & Krasnow, M. A. Developmental origin of lung macrophage diversity. Development 143, 1318–1327 (2016).

13. Guilliams, M. et al. Alveolar macrophages develop from fetal monocytes that differentiate into long-lived cells in the first week of life via GM-CSF. J. Exp. Med. 210, 1977–92 (2013).

14. Hashimoto, D. et al. Tissue-resident macrophages self-maintain locally throughout adult life with minimal contribution from circulating monocytes. Immunity 38, 792–804 (2013).

15. Gibbings, S. L. et al. Transcriptome analysis highlights the conserved difference between embryonic and postnatal-derived alveolar macrophages. Blood 126, 1357–1366 (2015).

16. Nayak, D. K. et al. Long-Term Persistence of Donor Alveolar Macrophages in Human Lung Transplant Recipients That Influences Donor-Specific Immune Responses. Am. J. Transplant. 16, 2300–2311 (2016).

17. Gibbings, S. L. et al. Three Unique Interstitial Macrophages in the Murine Lung at Steady State. Am J Respir Cell Mol Biol 57, 66–76 (2017).

18. Xiong, Z., Leme, A. S., Ray, P., Shapiro, S. D. & Lee, J. S. CX3CR1+ Lung Mononuclear Phagocytes Spatially Confined to the Interstitium Produce TNF- and IL-6 and Promote Cigarette Smoke-Induced Emphysema. J. Immunol. 186, 3206–3214 (2011).

19. Henson, P. M. et al. Deletion of c-FLIP from CD11b high Macrophages Prevents Development of Bleomycin-induced Lung Fibrosis. Am. J. Respir. Cell Mol. Biol. 58, 66–78 (2018).

20. McGovern, T. K., Robichaud, A., Fereydoonzad, L., Schuessler, T. F. & Martin, J. G. Evaluation of respiratory system mechanics in mice using the forced oscillation technique. J. Vis. Exp. 75, (2013).

21. Ayaub, E. A. et al. Overexpression of OSM and IL-6 impacts the polarization of pro- fibrotic macrophages and the development of bleomycin-induced lung fibrosis. Sci. Rep. 7, 1–16 (2017).

22. Wilson, A. M. et al. Lipid and smoker's inclusions in sputum macrophages in patients with airway diseases. Respir. Med. 105, 1691–1695 (2011).

23. Botelho, F. M. et al. Innate immune processes are sufficient for driving cigarette smoke-induced inflammation in mice. Am. J. Respir. Cell Mol. Biol. 42, 394–403 (2010).

24. Swirski, F. K. & Al., E. Identification of Splenic Reservoir Monocytes and Their Deployment to Inflammatory Sites. Science (80-.). 325, 612–616 (2009).

25. Oguro, H., Ding, L. & Morrison, S. J. SLAM family markers resolve functionally distinct subpopulations of hematopoietic stem cells and multipotent progenitors. Cell Stem Cell 13, 102–116 (2013).

26. Hettinger, J. et al. Origin of monocytes and macrophages in a committed progenitor. Nat. Immunol. 14, 821–830 (2013).

27. Kumar, R., Fossati, V., Israel, M. & Snoeck, H.-W. Lin − Sca1 + Kit − Bone Marrow Cells Contain Early Lymphoid-Committed Precursors That Are Distinct from Common Lymphoid Progenitors . J. Immunol. 181, 7507–7513 (2008).

28. Botelho, F. M. et al. IL-1α/IL-1R1 expression in chronic obstructive pulmonary disease and mechanistic relevance to smoke-induced neutrophilia in mice. PLoS One 6, e28457 (2011).

29. Pauwels, N. S. et al. Role of IL-1 a and the Nlrp3/caspase-1/IL-1 b axis in cigarette smoke-induced pulmonary inflammation and COPD. Eur. Respir. J. 38, 1019–1028 (2011).

30. Gibbons, M. A. et al. Ly6C hi monocytes direct alternatively activated profibrotic macrophage regulation of lung fibrosis. Am. J. Respir. Crit. Care Med. 184, 569–581 (2011).

31. Shaykhiev, R. et al. Smoking-Dependent Reprogramming of Alveolar Macrophage Polarization: Implication for Pathogenesis of Chronic Obstructive Pulmonary Disease. J Immunol 183, 2867–2883 (2009).

32. Agraval, H. & Yadav, U. C. S. MMP-2 and MMP-9 mediate cigarette smoke extract-induced epithelial-mesenchymal transition in airway epithelial cells via EGFR/Akt/GSK3β/β-catenin pathway: Amelioration by fisetin. Chem. Biol. Interact. 314, (2019).

33. Burns, A. R., Hosford, S. P., Dunn, L. A., Walker, D. C. & Hogg, J. C. Respiratory epithelial permeability after cigarette smoke exposure in guinea pigs. J. Appl. Physiol. 66, 2109–2116 (1989).

34. Jones, J. G. et al. Increased Alveolar Epithelial Permeability in Cigarette Smokers. Lancet 315, 66–68 (1980).

35. Puttur, F., Gregory, L. G. & Lloyd, C. M. Airway macrophages as the guardians of tissue repair in the lung. Immunol. Cell Biol. 97, 246–257 (2019).

36. Silva, D. et al. Effects of cigarette smoke and nicotine on cell viability, migration and myofibroblastic differentiation. J Periodont Res 47, 599–607 (2012).

37. Lee, C. G. et al. Interleukin-13 Induces Tissue Fibrosis by Selectively Stimulating and Activating Transforming Growth Factor Beta 1. J Exp Med 194, 809–821 (2001).

38. Lin, C. et al. Matrix metalloproteinase-9 cooperates with transcription factor Snail to induce epithelial – mesenchymal transition. Cancer Sci. 102, 815–827 (2011).

39. Willis, B. C., Roland, M. & Borok, Z. Epithelial Origin of Myofibroblasts during Fibrosis in the Lung. Proc Am Thorac Soc 3, 377–382 (2006).

40. Tsukui, T. et al. Collagen-producing lung cell atlas identifies multiple subsets with distinct localization and relevance to fibrosis. Nat. Commun. 11, 1–16 (2020).

	Res-AM	Mo-AM	IM1	IM2	IM3
CD64/MertK	+	+	+	+	+
CD11c	+	+	-	-	+
CD11b	-	+	+	+	+
SiglecF	+	+/-	-	-	-
MHCII	+/-	-	-	+	+

Table 1. Cell surface expression of pulmonary macrophage subpopulations. Expression profile for macrophage subpopulations, based on Gibbings *et al.*, used for flow cytometry analysis. Cells express marker (+), cells do not express (-), and cells have a spectrum of expression (-/+).

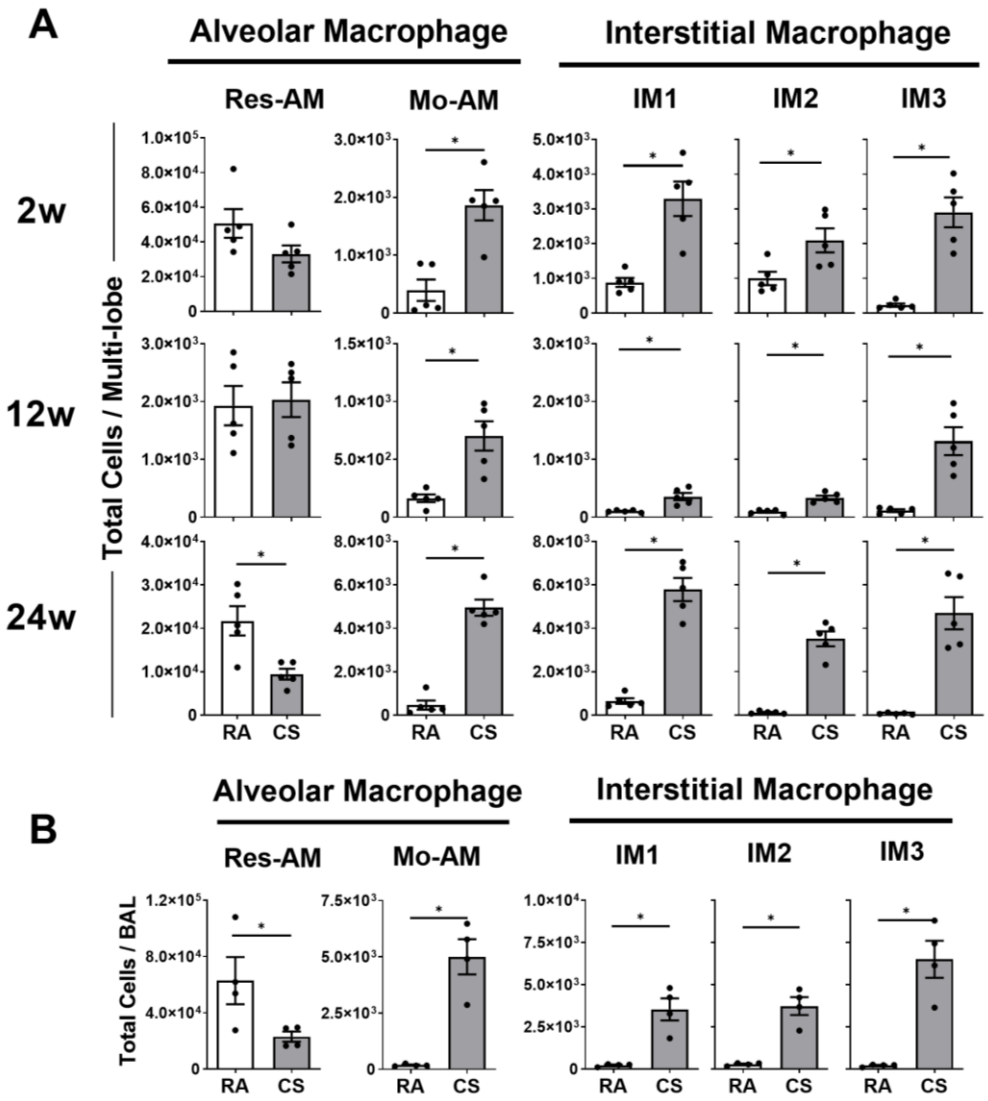

Figure 1. Cigarette smoke exposure alters pulmonary macrophage subpopulation composition expanding CD11b^{+} populations. Female C57BL/6 mice were RA or CS-exposed for 2- to 24-weeks. Data show total numbers of Res-AM, Mo-AM, IM1, IM2, and IM3 populations in **(A)** lung tissue and **(B)** bronchoalveolar lavage (BAL). Data show mean ± SEM, n = 5. Unpaired t test with Welch's correction. RA – room air. CS – cigarette smoke

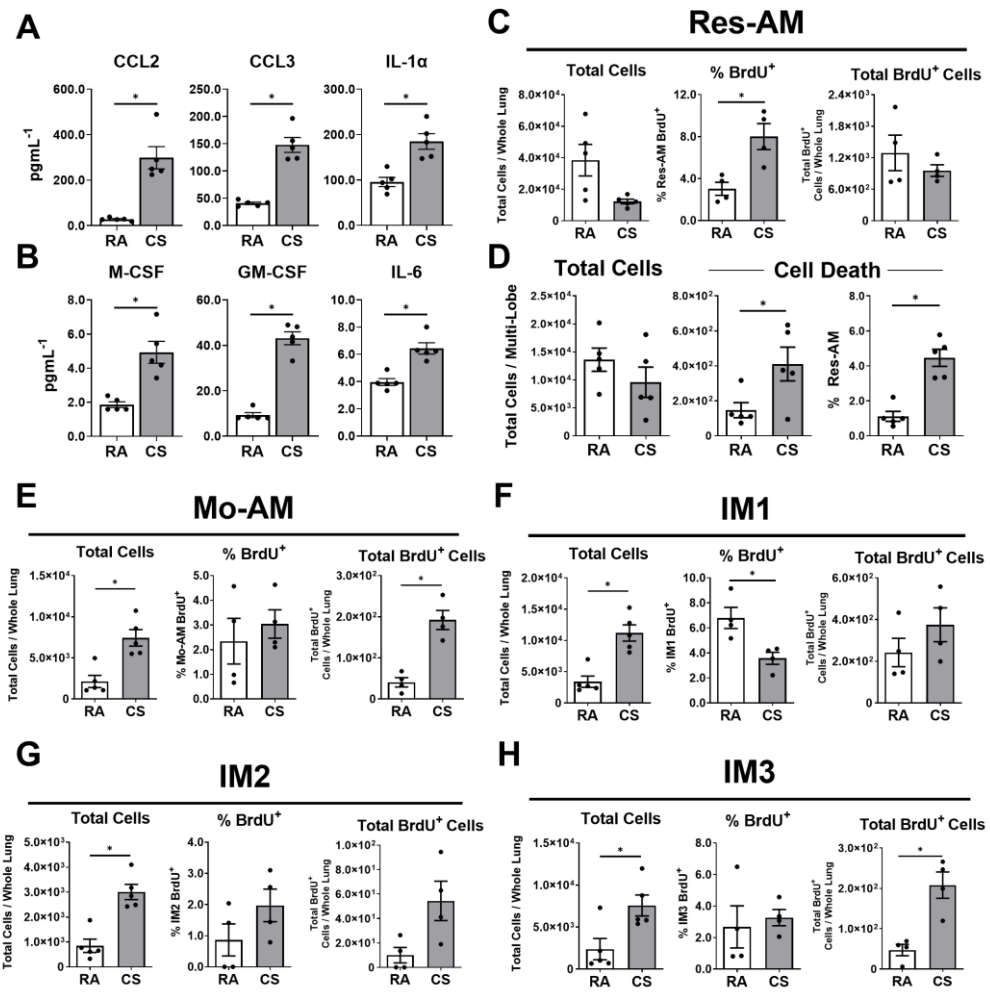

Figure 2. CD11b$^+$ macrophages are recruited to the lung during cigarette smoke exposure. Female C57BL/6 mice were RA or CS-exposed for 12-weeks. Lung homogenate **(A)** immune mediators (CCL2, CCL3, and IL-1α) and **(B)** monocyte differentiation and macrophage survival factors (M-CSF, GM-CSF, and IL-6). BrdU was used to assess macrophage subpopulation turnover in the lung at 6-weeks CS. Data show **(C)** total cells, % BrdU$^+$ and total BrdU$^+$ Res-AM and **(D)** total cells, total dead and % dead Res-AM. Shown in **(E)** Mo-AM, **(F)** IM1, **(G)** IM2, and **(H)** IM3 are total cells, % positive and total BrdU$^+$ cells. Data show mean ± SEM, n = 4 - 5. Unpaired t test with Welch's correction. RA – room air. CS – cigarette smoke

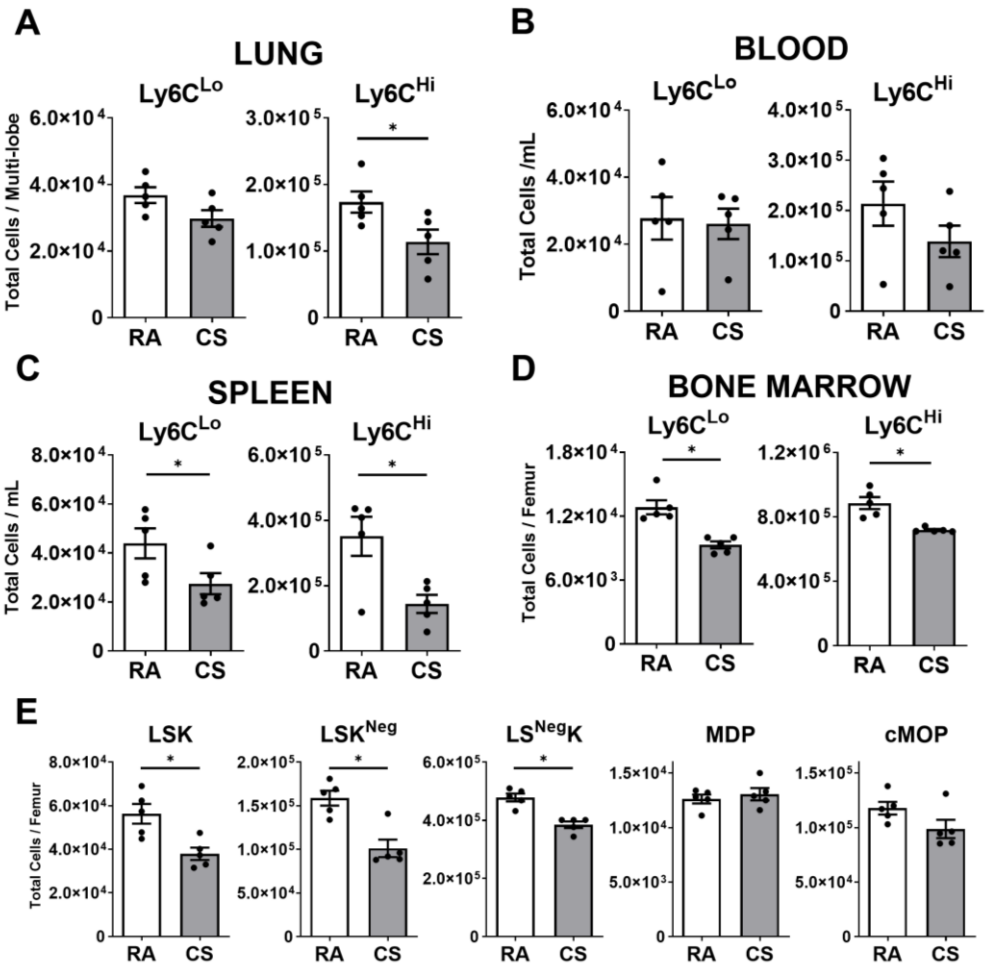

Figure 3. Macrophage progenitor cells are transiently decreased at 12-weeks of cigarette smoke exposure. Female C57BL/6 mice were RA or CS-exposed for 12-weeks. Data show total numbers of Ly6C^{Lo} and Ly6C^{Hi} monocyte populations in (**A**) lungs, (**B**) blood, (**C**) spleen, and (**D**) bone marrow. Shown in (**E**) total numbers of macrophage progenitor cells in the bone marrow (lineage-negative Sca1 c-Kit (LSK), monocyte-macrophage dendritic cell progenitor (MDP), common monocyte progenitor (cMoP)). Data show mean ± SEM, n = 5. Unpaired t test with Welch's correction. RA – room air. CS – cigarette smoke

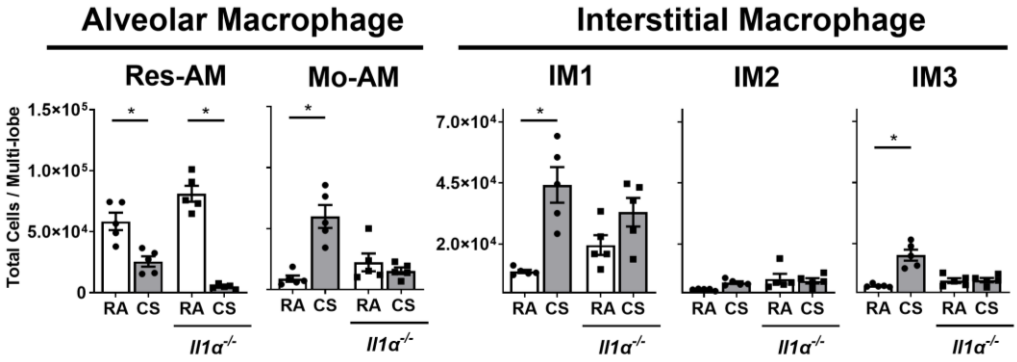

Figure 4. Macrophage expansion in cigarette smoke-exposed lung is IL-1α dependent. Data show total lung Res-AM, Mo-AM, IM1, -2 and -3 populations in *Il1a*$^{-/-}$ and C57BL6 wild type control mice at 8-weeks CS. Data show mean ± SEM, n = 5. Two-way ANOVA with Tukey's multi-comparison test. RA – room air. CS – cigarette smoke

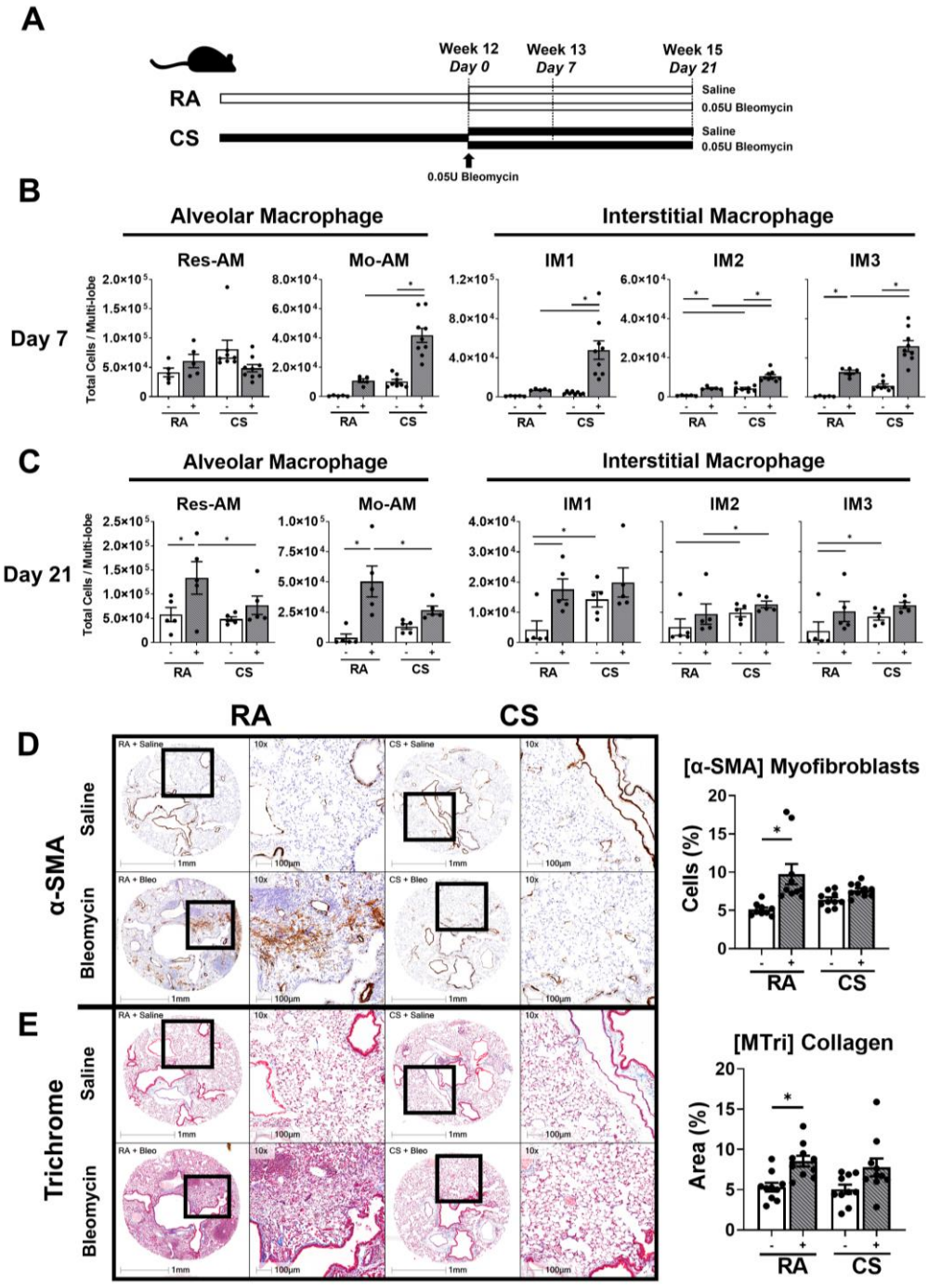
A
Week 12
Day 0
Week 13
Day 7
Week 15
Day 21
RA
Saline
0.05U Bleomycin
CS
Saline
0.05U Bleomycin
0.05U Bleomycin
B
Alveolar Macrophage
Interstitial Macrophage
Res-AM
Mo-AM
IM1
IM2
IM3
Day 7
Total Cells / Multi-lobe
RA
CS
C
Alveolar Macrophage
Interstitial Macrophage
Res-AM
Mo-AM
IM1
IM2
IM3
Day 21
Total Cells / Multi-lobe
RA
CS
D
RA
CS
α-SMA
Saline
Bleomycin
[α-SMA] Myofibroblasts
Cells (%)
RA
CS
E
Trichrome
Saline
Bleomycin
[MTri] Collagen
Area (%)
RA
CS

Figure 5. Skewed macrophage subpopulation composition is associated with decreased fibrogenesis. (A) Schematic of CS exposure with bleomycin instillation. C57BL/6 female mice were administered bleomycin (0.05U/mouse) (grey bars) or saline control (open bars) following 12-weeks of RA or CS exposure. Res-AM, Mo-AM, IM1, IM2, and IM3 populations in lung tissue following **(B)** 7 days or **(C)** 21 days of bleomycin administration. Data show representative image and HALO quantification for **(D)** α-SMA and **(E)** Masson's trichrome. Data show mean ± SEM, n = 5 - 10. Two-way ANOVA with Tukey's multi-comparison test. RA – room air. CS – cigarette smoke.

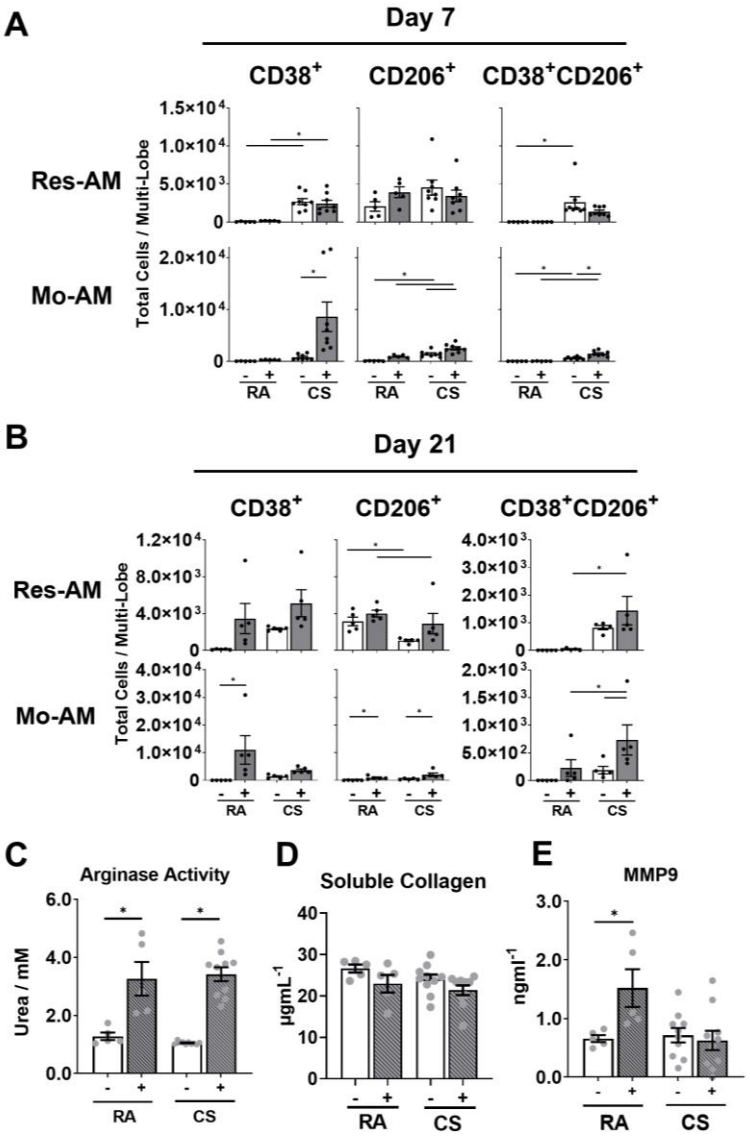

Figure 6. Macrophage subpopulation function and polarisation is altered by cigarette smoke exposure. C57BL/6 female mice were administered bleomycin (0.05U/mouse) (grey bars) or saline control (open bars) following 12-weeks of RA or CS exposure. Total number of Res-AM and Mo-AM expressing CD38, CD206 and CD38/CD206 in lung tissue following **(C)** 7 days or **(D)** 21 days post bleomycin administration. Adherent lung $CD45^+$ cells isolated from 12-week RA- or CS-exposed C57BL/6 cell supernatant **(C)** urea production, **(D)** soluble collagen and (**E**) MMP9 release following TGF-β1, IL-4, IL-6 stimulation. Data show mean ± SEM, n= 5-10. Two-way ANOVA with Tukey's multi-comparison test. RA – room air. CS – cigarette smoke.

Antibody Specificity	Conjugate	Clone	Supplier
CD3	APCeFlour780	17A2	eBioscience
CD11b	Pe Dazzle 594	M1/70	Biolegend
CD11c	BV650	N418	Biolegend
CD19	APCeFlour780	eBio1D3	eBioscience
CD24	BV421	M1/69	Biolegend
CD45	AlexaFluor700	30-F11	Biolegend
CD64	PeCy7	X54-5/71	Biolegend
EpCAM	APC Cy7	G8.8	Biolegend
LIVE/DEAD™	Fixable Yellow Stain		Thermo Fisher Scientific
Ly6C	BV711	HK1.4	Biolegend
Ly6G	APC Cy7	1A8	Biolegend
MerTk	APC	2B10C42	Biolegend
MHCII	PerCp Cy5.5	M5/114.15.2	Biolegend
NK1.1	APC Cy7	PK136	Biolegend
SiglecF	Pe	E50-2440	BD Pharmingen
SiglecF	BV421	S17007L	Biolegend
CD38	Pe	90	Biolegend
CD206	BV785	C068C2	Biolegend
CD115	BV421	AF598	Biolegend
CD115	PE/Cy7	AF598	Biolegend
CD117	APC	2B8	Thermo Fisher Scientific
CD135	BV421	A2F10	Biolegend
Sca1	BV650	D7	Biolegend
BrdU	APC		BD Biosciences

Table S1. Flow cytometry panel. A panel of surface and intracellular markers to examine the myeloid cells in mouse lung, blood, spleen and bone marrow.

Wound healing/Fibrogenesis	**Myeloid**	**M1**	**M2**
Fgf2	*Itgam*	*Nos2*	*Arg1*
Pdgfa	*Itgax*	*Tnf*	*Mrc1*
Tgfb1	*Ccl2*	*IL1b*	*IL4ra*
Lrrc32	*IL-10*	*IL1a*	*IL6ra*
Vegfa	*Cxcl1*		*Osmr*
Fn1			*IL6*
Col1a1			*Osm*
Col3a1			
Timp1			

Table S2. NanoString custom designed fibrogenesis panel. A panel to assess the expression of genes related to wound healing/fibrogenesis, myeloid, M1 and M2 macrophage polarisation.

		RA Bleo - RA Saline	CS Bleo - CS Saline	CS Bleo - RA Bleo	CS Saline - RA Saline
Fibrosis/wound healing	*Fgf2*	1.46	1.18	-1.32	-
	Pdgfa	-1.33	-	1.17	-
	Tgfb1	-1.11	-1.08	1.11	-
	Lrrc32	-	-1.37	-	-
	Vegfa	-1.28	-	-	-1.19
	Fn1	2.82	1.84	-1.48	-
	Col1a1	2.71	2.13	-1.42	-
	Col3a1	2.45	2.16	-1.38	-1.22
	Timp1	11.18	3.73	-1.81	1.65
Myeloid	*Itgam*	-	1.36	1.83	1.44
	Itgax	1.34	-	1.67	2.68
	Ccl2	11.55	1.70	-	7.41
	Il10	-3.67	-3.49	-	-
	Cxcl1	2.36	-	2.14	7.64
M1	*Nos2*	1.81	1.43	-	-
	Tnf	1.72	-	1.50	2.79
	Il1b	-1.81	-	-	-1.41
	Il1a	-	-	1.71	1.75
M2	*Arg1*	4.53	3.14	-1.76	-
	Mrc1	-	-1.35	-	1.55
	Il4ra	1.31	1.21	-1.15	-
	Il6ra	-1.83	-1.58	-	-
	Osmr	1.62	1.12	-	1.34
	Il6	2.72	-	-	1.93
	Osm	1.39	-	-	1.40

Table S3. mRNA differential expression of fibrogenesis-associated genes at day 7 post bleomycin. Expression of genes related to wound healing/fibrogenesis, myeloid, M1 and M2 macrophage polarisation. Shown are genes significantly differentially expressed at day 7. Limma package, R.

		RA Bleo - RA Saline	CS Bleo - CS Saline	CS Bleo - RA Bleo	CS Saline - RA Saline
Fibrosis/wound healing	*Fgf2*	-	-	-	-
	Pdgfa	-	1.17	-	-
	Tgfb1	-	-	-	1.17
	Lrrc32	-	-	-	-
	Vegfa	-	-	-	-1.45
	Fn1	1.29	-	-1.25	-
	Col1a1	1.65	-	-1.44	-
	Col3a1	2.15	-	-1.52	-
	Timp1	1.69	-	-	2.14
Myeloid	*Itgam*	-1.27	-	1.67	1.30
	Itgax	1.30	-	1.91	2.52
	Ccl2	-	-	7.82	8.78
	Il10	-	-	-	4.04
	Cxcl1	-	-	6.37	4.15
M1	*Nos2*	2.06	-	-	-
	Tnf	-	-	1.93	1.95
	Il1b	-1.40	-	-	-2.27
	Il1a	-	-	1.89	1.99
M2	*Arg1*	-	1.59	-	-2.09
	Mrc1	-	-	1.52	1.68
	Il4ra	-	-	-	-
	Il6ra	-1.58	-	-	-1.34
	Osmr	-	-	-	-
	Il6	-	-	-	-
	Osm	-	-	-	-1.44

Table S4. mRNA differential expression of fibrogenesis-associated genes at day 21 posy bleomycin. Expression of genes related to wound healing/fibrogenesis, myeloid, M1 and M2 macrophage polarisation. Shown are genes significantly differentially expressed at day 21. Limma package, R.

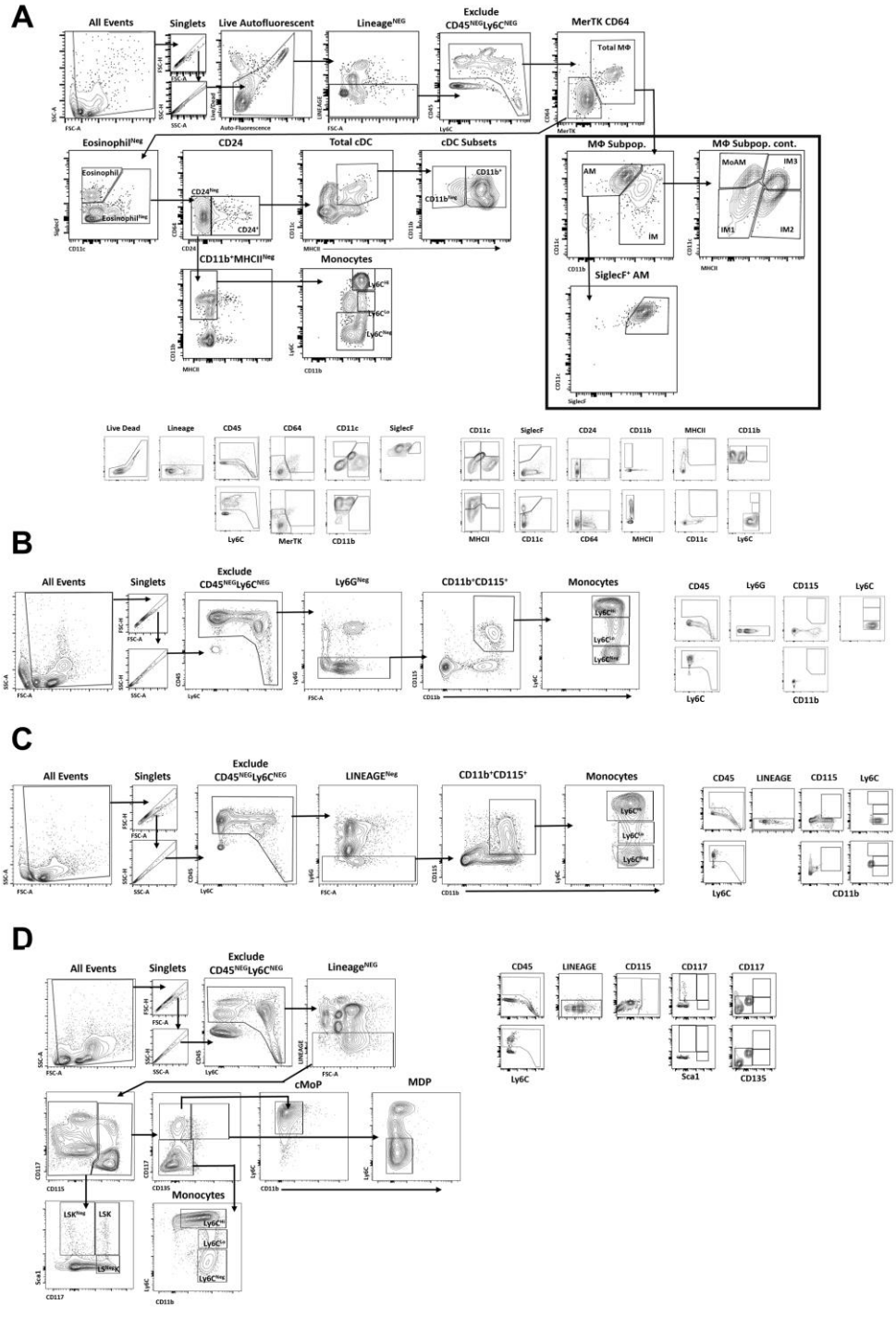
A
All Events
Singlets
Live Autofluorescent
Lineage^NEG
Exclude CD45^NEG Ly6C^NEG
MerTK CD64
Total MΦ
Eosinophil^Neg
CD24
Total cDC
cDC Subsets
MΦ Subpop.
MΦ Subpop. cont.
AM
IM
MoAM
IM3
IM1
IM2
SiglecF+ AM
CD11b+MHCII^Neg
Monocytes
Live Dead
Lineage
CD45
CD64
CD11c
SiglecF
CD24
CD11b
MHCII
Ly6C
MerTK
B
All Events
Singlets
Exclude CD45^NEG Ly6C^NEG
Ly6G^Neg
CD11b+CD115+
Monocytes
CD45
Ly6G
CD115
Ly6C
CD11b
C
All Events
Singlets
Exclude CD45^NEG Ly6C^NEG
LINEAGE^Neg
CD11b+CD115+
Monocytes
CD45
LINEAGE
CD115
Ly6C
D
All Events
Singlets
Exclude CD45^NEG Ly6C^NEG
Lineage^NEG
cMoP
MDP
Monocytes
CD45
LINEAGE
CD115
CD117
CD135
Sca1

Figure S1. Monocyte and macrophage subpopulations gating strategies. (**A**) Lungs were enzymatically digested and stained for flow cytometry. Diagrams showing gating strategies used to isolate total macrophage populations identified as Live Autofluorescent $(FITC)^{+/-}Lineage^{Neg}CD45^{+}MertK^{+}CD64^{+}$. We further distinguished $CD11c^{+}CD11b^{Neg}SiglecF^{Hi}$ resident alveolar macrophages (Res-AMs), $CD11c^{+}CD11b^{+}MHCII^{Neg}$ monocyte-derived alveolar macrophages (Mo-AMs), $CD11c^{Neg}CD11b^{+}MHCII^{Neg}$ interstitial macrophage 1 (IM1), $CD11c^{Neg}CD11b^{+}MHCII^{+}$ (IM2), $CD11c^{+}CD11b^{+}MHCII^{+}$ (IM3) plus $Ly6C^{Lo}$, $Ly6C^{Hi}$ monocyte subsets. Blood (**B**) and spleen (**C**) monocyte populations were determined as $CD45^{+}Ly6G^{Neg}CD11b^{+}CD115^{+}$ then $Ly6C^{Lo}$ and $Ly6C^{Hi}$. (**D**) Bone marrow monocytes and progenitors were defined as $CD45^{+}Lineage^{Neg}$. Subsequently monocytes defined as $CD11b^{+}CD115^{+}CD117^{Neg}CD135^{Neg}$ then $Ly6C^{Lo}$ and $Ly6C^{Hi}$. Myeloid progenitors were defined as $CD115^{+}CD117^{+}CD135^{Neg}CD11b^{Neg}Ly6C^{Hi}$ common monocyte progenitor (cMoP), $CD115^{+}CD117^{+}CD135^{+}CD11b^{Neg}Ly6C^{Neg}$ monocyte-macrophage dendritic cell progenitor (MDP) plus $CD115^{Neg}CD117^{+}Sca1^{Hi}$ Sca1 c-Kit (LSK), $CD115^{Neg}CD117^{+}Sca1^{Neg}$ ($LS^{Neg}K$) and $CD115^{Neg}CD117^{Neg}Sca1^{+}$ (LSK^{Neg}). Fluorescence minus one (FMO) was used to gate each of the population of interest.

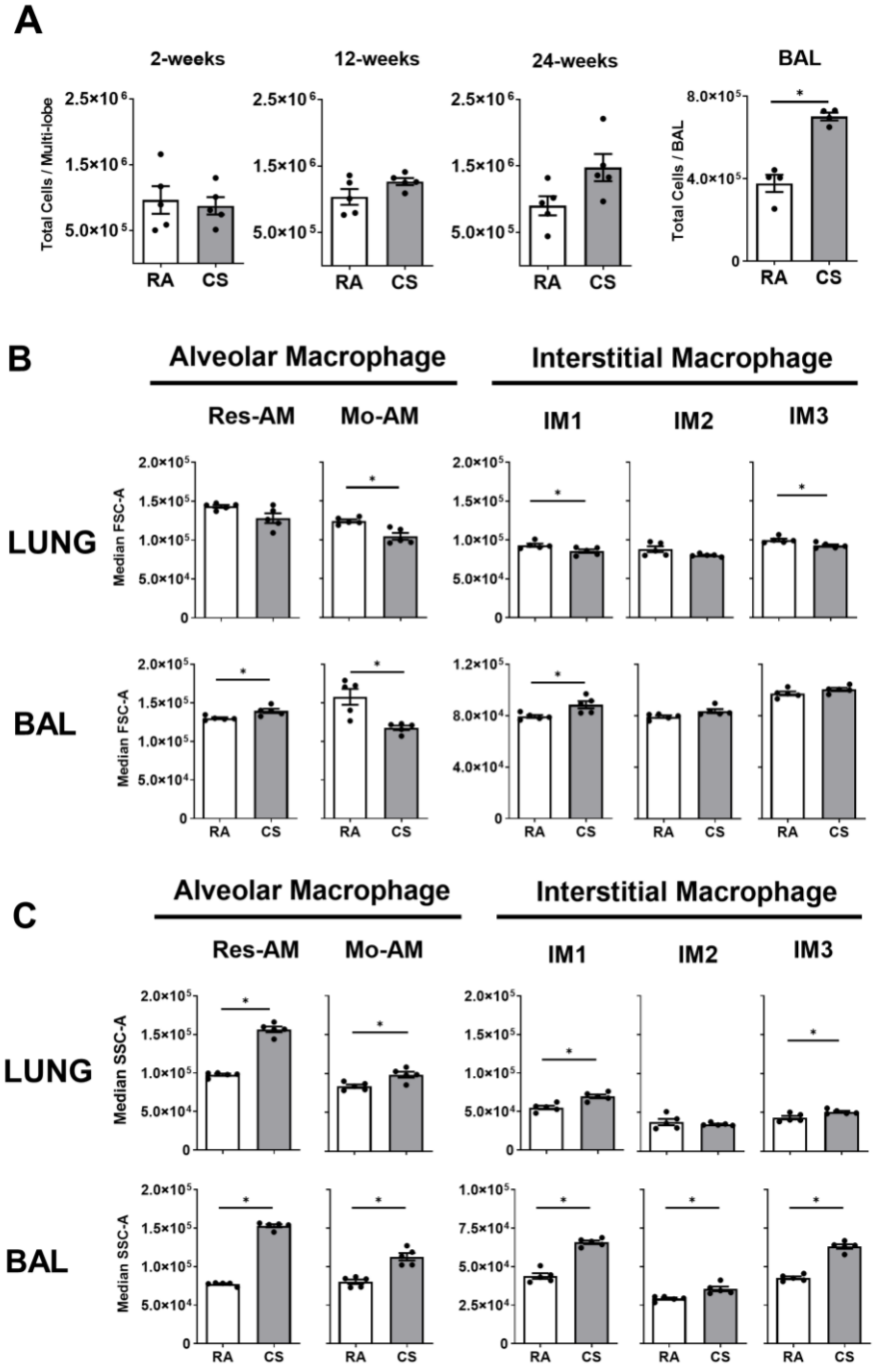

Figure S2. Macrophage size and granularity following cigarette smoke exposure. Data show total numbers of **(A)** lung (2-, 12-, 24-weeks) and BAL (8-weeks) cells following CS exposure. **(B)** Res-AM, Mo-AM, IM1, IM2, and IM3 population size measured by forward scatter (FSC). **(C)** Res-AM, Mo-AM, IM1, IM2, and IM3 population granularity measured by side scatter (SSC). Data show mean ± SEM, n = 5. Unpaired t test with Welch's correction. RA – room air. CS – cigarette smoke.

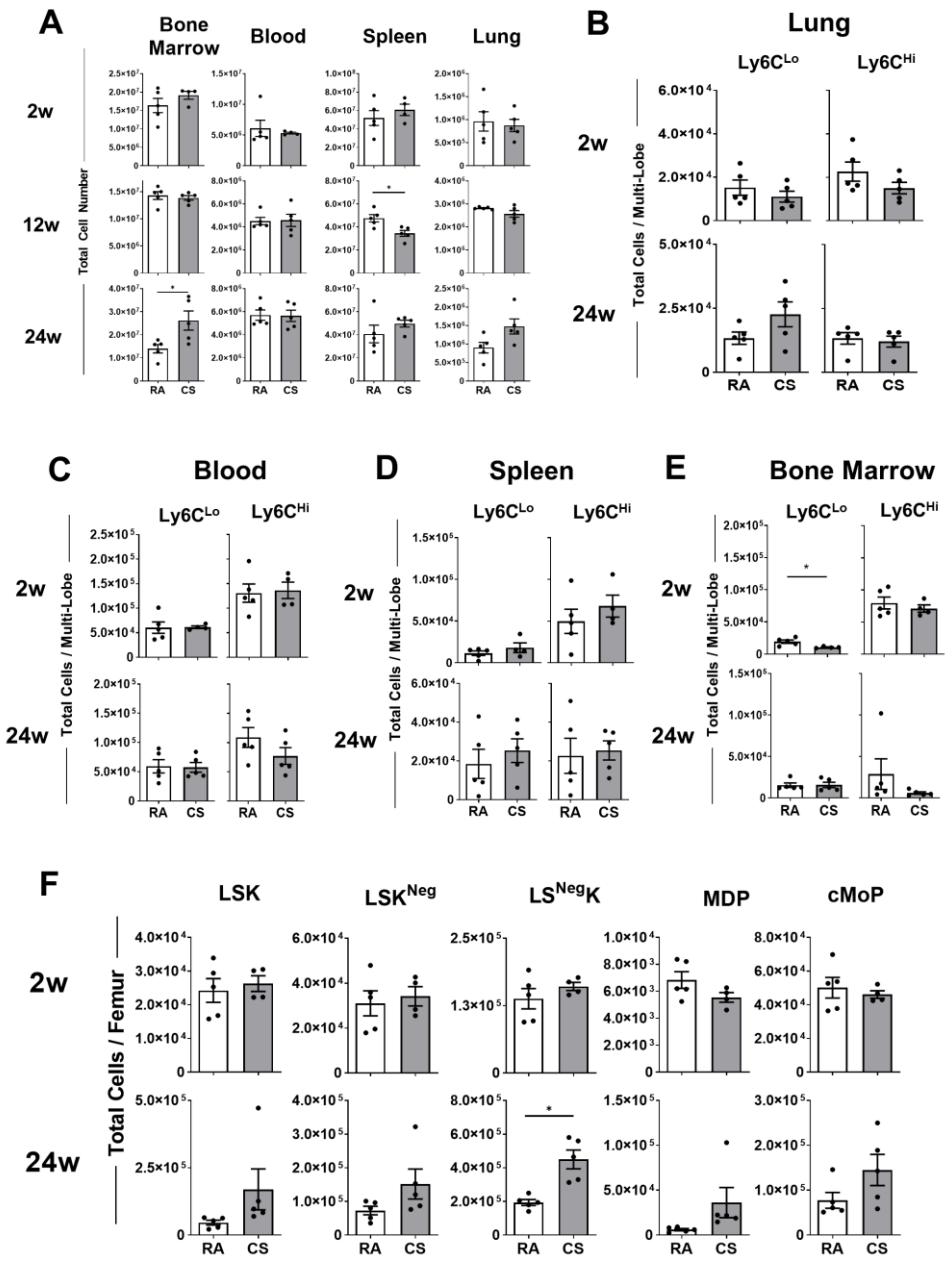

Figure S3. Progenitor and monocyte populations at 2, 12 and 24-weeks following cigarette smoke exposure. Female C57BL/6 mice were RA or CS-exposed for 2, 12, or 24-weeks. Data show total cell numbers in (**A**) lung, blood, spleen, and bone marrow. Data also show total numbers of Ly6C^{Lo} and Ly6C^{Hi} monocyte populations in (**B**) lung, (**C**) blood, (**D**) spleen, and (**E**) bone marrow and (**F**) total numbers of macrophage progenitor cells in the bone marrow (lineage-negative Sca1 c-Kit (LSK), monocyte-macrophage dendritic cell progenitor (MDP), common monocyte progenitor (cMoP)). Data shown mean ± SEM, n= 4 - 5. Unpaired t test with Welch's correction.

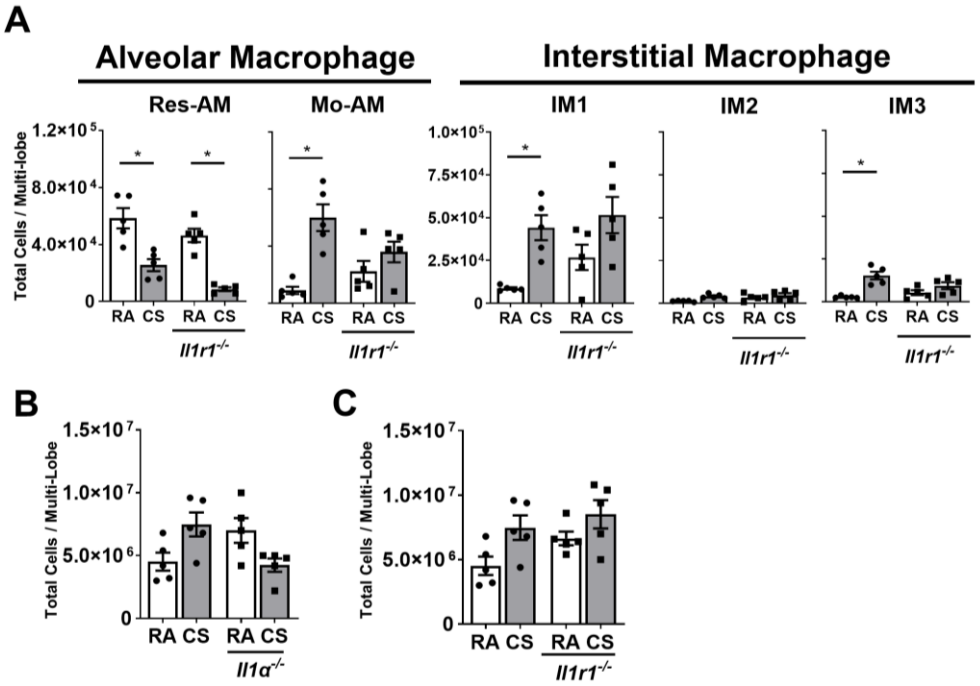

Figure S4. Pulmonary macrophages are expanded via IL1α during cigarette smoke exposure. Female C57BL/6, *Il1a*$^{-/-}$ and *Il1r1*$^{-/-}$ mice were RA or CS-exposed for 8-weeks. **(A)** Data show total Res-AM, Mo-AM, IM1, -2, -3 numbers in *Il1r1*$^{-/-}$ mice and C57BL/6 wildtype controls. Total cell number in **(B)** *Il1a*$^{-/-}$ and **(C)** *Il1r1*$^{-/-}$ mice plus C57BL6 wildtype controls. Data show mean ± SEM, n = 5. Two-way ANOVA with Tukey's multi-comparison test. RA – room air. CS – cigarette smoke.

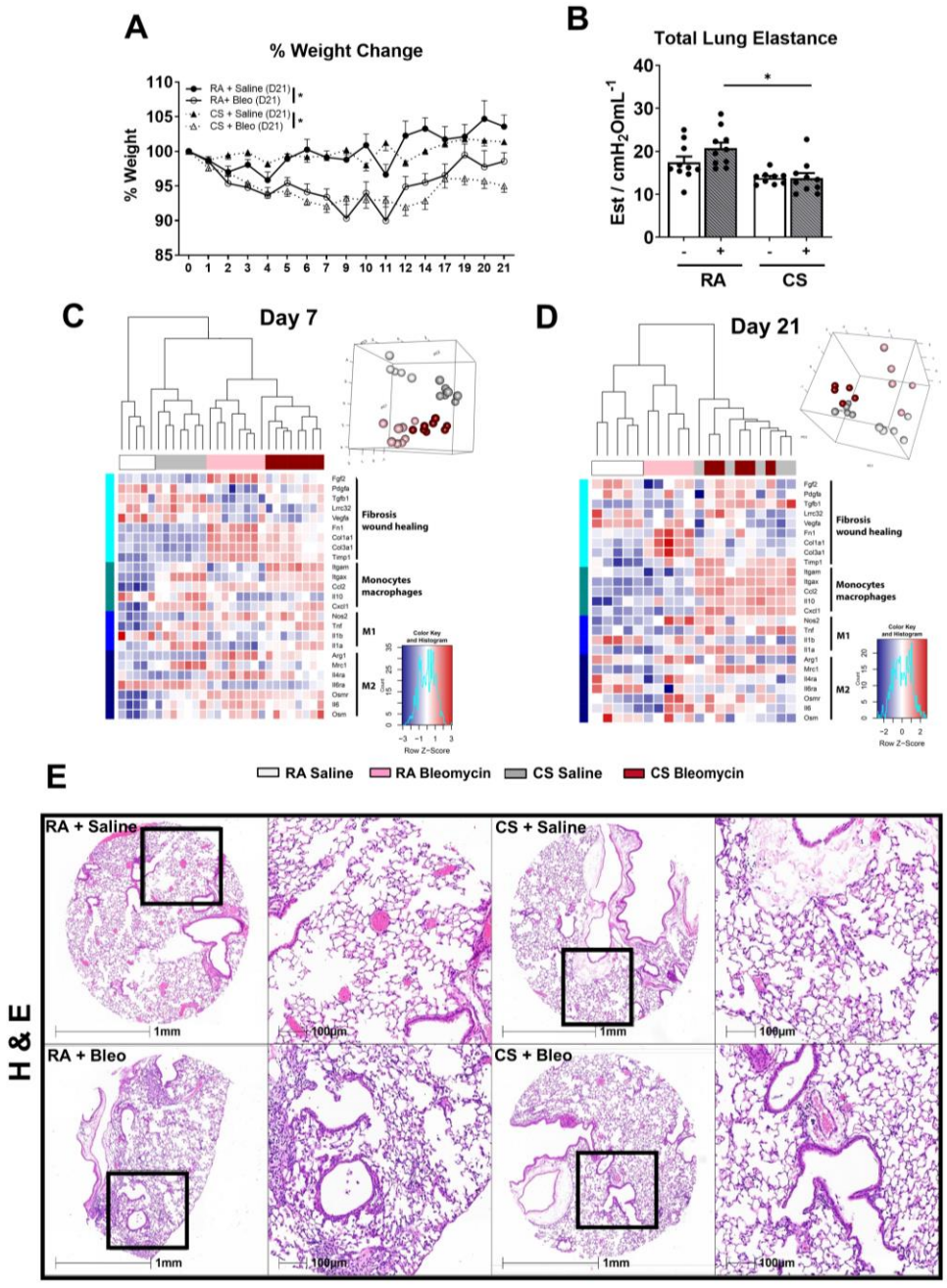
A
% Weight Change
% Weight
RA + Saline (D21)
RA+ Bleo (D21)
CS + Saline (D21)
CS + Bleo (D21)
B
Total Lung Elastance
Est / cmH2OmL-1
RA
CS
C
Day 7
D
Day 21
Fibrosis wound healing
Monocytes macrophages
M1
M2
Row Z-Score
E
RA Saline
RA Bleomycin
CS Saline
CS Bleomycin
H & E
RA + Saline
CS + Saline
RA + Bleo
CS + Bleo
1mm
100µm

Figure S5. Fibrotic measurements at day 21 of bleomycin instillation. C57BL/6 female mice were administered bleomycin (0.05U/mouse) or control saline following 12-weeks of RA or CS exposure. Mice were monitored 21 days prior to flexiVent® lung measurements and tissue harvest. **(A)** Body weight was measured daily and shown as percentage change in body weight. **(B)** Total lung elastance, a functional parameter derived from the pressure-driven pressure–volume loops, measured at day 21. Principal component analysis and heatmaps defined by 25 mouse genes from lung homogenate assessed by NanoString at **(C)** day 7 and **(D)** day 21. **(E)** Representative images for H&E-stained sections. Data show mean ± SEM, n= 4-10. Two-way ANOVA with Tukey's multi-comparison test. RA – room air. CS – cigarette smoke.

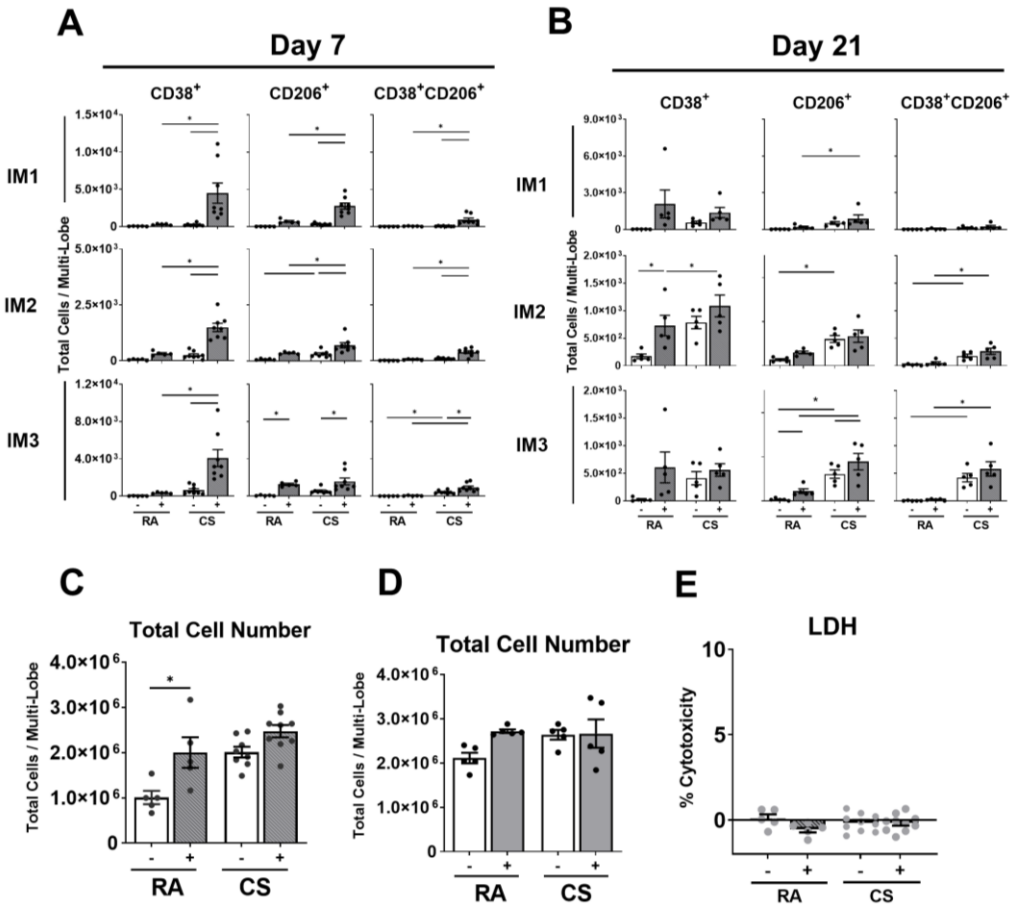

Figure S6. CD38$^+$ macrophages are increased in cigarette smoke-exposed bleomycin-treated mice. C57BL/6 female mice were administered bleomycin (0.05U/mouse) or control saline following 12-weeks of RA or CS exposure. Graphs demonstrate total numbers of IM1, IM2, and IM3 populations expressing CD38, CD206 and CD38/CD206 in lung tissue following **(A)** 7 days or **(B)** 21 days of bleomycin administration. Total lung cell counts **(C)** day 7 and **(D)** day 21. Adherent lung CD45$^+$ lactose dehydrogenase release in *ex vivo* TGF-β1, IL-6 and IL-4 stimulated cell supernatant from **(E)** 12-week room air (RA)- or cigarette smoke (CS)-exposed mice. Shown mean ± SEM, n = 4 - 10. Two-way ANOVA with Tukey's multi-comparison test. RA – room air. CS – cigarette smoke.

CHAPTER V: DISCUSSION

5.1. Summary of results

The work in this thesis focused on the impact of cigarette smoke on immune components of respiratory disease. Data in this thesis address two areas of focus. The first area of focus centred on (auto)antibodies in COPD. The intent of these studies was to assess whether autoantibodies could serve as a biomarker of disease progression. The second focus of this work assessed the effect of cigarette smoke on pulmonary macrophage composition and the subsequent impact on lung remodelling. This study sought to identify the specific macrophage subpopulations that lead to cigarette smoke-associated respiratory disease.

5.1.1. (Auto)antibodies in patients with COPD

The presence of autoantibodies has been proposed as a contributor to progressive lung function decline in COPD, even in individuals who have quit smoking cigarettes[179]. Given the variability in serum autoantibody levels in patients with COPD[180–182], we assessed sputum autoantibodies as a direct measurement from the respiratory tract. Sputum, mucosal expectorate from the lungs, is a non-invasive method to sample the respiratory tract and has been previously used to study asthma and infectious disease[231–234]. However, prior to this study little was known regarding the presence of sputum antibodies or autoantibodies in patients with COPD. Consequently, we first addressed whether antibodies were detectable in the sputum of patients with COPD.

In two independent COPD cohorts, we assessed the presence of total antibodies in cigarette smokers and patients with COPD. These cohorts were comprised of one single centre cohort based at GIRH and the second was a multicentre cohort spanning clinics in North America and Europe (ADEPT). In total, we assessed 251 sputum supernatants for the presence of total IgM, IgG and IgA. IgA was the most abundant antibody class in sputum samples reflecting its high abundance at mucosal surfaces[129]. IgG and IgM were also detectable in samples but at lower levels than IgA. These data validated the use of sputum as a matrix with which to assess the presence of antibodies in patients with COPD.

The recovered sputum IgM and IgA yield was variable between the ADEPT and GIRH cohorts. Notably, these cohorts had procedural differences in sputum processing. The ADEPT cohort followed the protocol outlined by Pizzichini *et al.*[229] which used DTT as a mucolytic whereas the GIRH cohort was processed according to a protocol outlined by Bafadhel *et al.*[230] PBS method. In **Appendix Figure 1A.**, we showed that in matched samples processed concurrently in either DTT or PBS that the presence of DTT did not alter the recovery of either IgG or IgM using a direct ELISA system. In contrast, DTT processing increased IgA recovery from the sputum. The increased IgA yield is possibly attributable to improved IgA release from the mucus plug akin to dithioerythritol (**DTE**), an optical isomer of DTT, which increased inflammatory cell and cytokine release from mucus plugs[243]. Next, we assessed the ability to detect a fixed concertation of Ig in each processing buffer to assess buffer interference. PBS or DTT processing buffer was not associated with differences in spike recovery (**Appendix Figure 1B.**). This suggested in this

direct ELISA system there was no interference from DTT in sample detection. In contrast, in the sandwich ELISA system employed in **Chapter II**, DTT interference did contribute to differences between cohorts. Using a spike protocol, DTT interfered with Ig standard binding signal for IgM (54.7% reduction), IgA (7.7% reduction) while IgG standard binding signal increased 15.5% (**Appendix Table 1.**). Thus, sputum processing buffers do not adversely affect antibody recovery but DTT interference does likely contribute to antibody recovery variability in a sandwich ELISA system.

Cigarette smoke[137–139] and COPD status[165,167,168] are associated with altered antibody levels; but, to date, no studied has assessed cigarette smoke's impact on sputum antibodies. We demonstrated that patients with COPD had decreased total sputum IgA independent of current smoking status. This is in agreement with previous histological and BAL analysis in COPD which observed decreases in IgA[167–169]. Of note, individuals with antibody deficiencies have increased respiratory infections[244] and airway remodelling[168,169]. In patients with COPD who currently smoked cigarettes, we observed decreased total sputum IgM and IgG in mild to moderate COPD but not severe or very severe COPD subjects. Thus, mild to moderate patients with COPD who currently smoke had reduced IgM/G and may consequently be at a heightened risk of infection compared to patients who have quit cigarette smoking.

Following the successful detection of sputum antibodies in patients with COPD, we used an autoantigen array to investigate sputum autoantibody levels in the ADEPT and GIRH cohorts. Serum autoantibodies were also assessed to facilitate comparison with previous studies and to assist in our interpretation of

sputum autoantibody levels. Patients with COPD had decreased IgG sputum autoantibodies compared to healthy controls but not asymptomatic smokers. In contrast, select IgG and IgM serum autoantibodies were differentially expressed compared to asymptomatic smokers in the GIRH cohort. No change in serum autoantibodies was observed in the ADEPT cohort. This differential expression of sputum and serum autoantibodies was not sufficient to identify patients with COPD from control groups based on unbiased clustering approaches. This suggests that COPD subjects had an overall autoantibody repertoire similar to asymptomatic smokers and healthy controls. Using a rigorous autoantigen array platform, we showed no conserved change in serum autoantibodies between two independent cohorts. Moreover, patients with COPD were not identifiable from an autoantibody profile from individuals without disease. Thus, autoantibodies do not provide a suitable biomarker for disease pathogenesis.

Growing evidence suggests a link between B cells and emphysema in patients with COPD[163]. In previous studies, increased serum autoantibody have been associated with emphysema providing a functional link between B cells and airspace enlargment[181,186,189]. In this study, we identified a weak correlation between select serum autoantibodies and emphysema in the GIRH cohort. We report AT IgM serum autoantibodies were weakly correlated with airspace enlargement in the GIRH cohort, validating observations by Nunez *et al.* of increased AT autoantibodies and worsening DL_{CO}[181]. However, we did not observe an association between airspace enlargement and autoantibodies in the ADEPT cohort. Ultimately, within patients with COPD, serum and not sputum

autoantibody titres weakly correlated with a measure of airspace enlargement but this finding was not validated between cohorts.

5.1.2. Impact of cigarette smoke on macrophage subpopulation composition and function

Macrophages are proposed to orchestrate the immunopathology associated with cigarette smoke-associated respiratory diseases such as COPD[245] and IPF[41]; however, the composition of macrophage subpopulations following cigarette smoke exposure is not fully understood. Using a mouse model of cigarette smoke exposure, we observed increased monocyte-derived $CD11b^+$ macrophage populations, Mo-AM and IM1, -2, and -3, in cigarette smoke-exposed mice. Notably, the increase in $CD11b^+$ macrophage subpopulations remained elevated even following 4- and 16-weeks of cigarette smoking cessation (**Appendix Figure 2.**). Thus, all $CD11b^+$ macrophage populations were increased following cigarette smoke exposure.

CD11b is an integrin used for cell adhesion by monocytes, macrophages and other granulocytes[246]. Given that CD11b is also used for cell migration, we assessed the origin of $CD11b^+$ macrophage populations. First, we assessed bromodeoxyuridine (**BrdU**) incorporation as a method to measure cell turnover demonstrating that the expansion of these cell populations was likely a result of monocyte recruitment. Specifically, the expansion of Mo-AM and IM3 was IL-1α dependent. We observed a smaller contribution of IL-1α to the expansion of IM1 and IM2 populations, which suggests a plausible involvement of self-renewing yolk sac-derived IM to these subpopulations[44]. Despite increased expansion of $CD11b^+$ populations, we observed only transient changes in

macrophage progenitor cells in the bone marrow and the blood of cigarette smoke-exposed mice. Cigarette smoke exposure was associated with the expansion of $CD11b^+$ macrophage populations likely via increased cell recruitment from the bone marrow.

To explore the functional consequences of altered macrophage subpopulation composition following cigarette smoke exposure, we used a model of concurrent bleomycin-induced lung injury to study tissue repair and remodelling. In cigarette smoke-exposed animals, bleomycin administration elicited less fibrogenesis as measured by decreased α-smooth muscle actin, collagen disposition and total lung elastance at day 21. This was associated with decreased Res-AM and Mo-AM populations at day 21 in cigarette smoke-exposed bleomycin-treated animals compared to room air-exposed bleomycin-treated mice. Notably, Mo-AM are reported to be a major contributor to aberrant fibrogenesis leading to fibrosis development in models of asbestos and bleomycin-induced lung injury[39,41]. Concurrent cigarette smoke exposure and bleomycin administration altered the composition of pulmonary macrophages beyond either insult individually and resulted in impaired fibrogenesis.

To further explore the contribution of cigarette smoke-exposed macrophages to tissue repair and fibrogenesis, we assessed macrophage polarisation and function. Prior to fibrogenesis, during the inflammatory phase of injury, we demonstrated a decrease in wound healing genes in the lung and a shift toward a predominant "M1" macrophage polarisation response. Thus, prior to fibrogenesis initiation the immune environment was skewed toward a proinflammatory rather than remodelling phenotype. *Ex vivo* analysis of

adherent $CD45^+$ lung cells stimulated with a profibrotic cytokine cocktail showed cigarette smoke-exposed cells had decreased matrix metalloproteinase-9 (**MMP9**) release. MMP9 is reported to contribute to TGF-β production[247] and epithelial-mesenchymal transition[248,249], processes leading to myofibroblast differentiation and aberrant tissue remodelling[250]. Overall, cigarette smoke exposure altered the composition of macrophages in the lung, recruiting M1-like $CD11b^+$ monocyte-derived subpopulations during the inflammatory phase of bleomycin injury. This composition change and associated impaired MMP9 release likely contributed to an impaired fibrogenesis response. Taken together these data demonstrated that cigarette smoke-induced changes to macrophage composition and function predispose cigarette smokers to impaired wound healing and repair following injury.

5.2. Clinical implications

Current or having a history of cigarette smoking is associated with multiple respiratory diseases including COPD and IPF[2,3]. These respiratory diseases are characterised by accelerated lung function decline and poor quality of life, even after quitting cigarette smoking. A better understanding of the impact of cigarette smoke on the immune system will shed light on novel intervention strategies to halt disease progression.

5.2.1. Current smoking status influences sputum antibody levels

Determining an individual's smoking history is key when gathering patient information as it provides the attending physician an important indicator of patient risk of developing disease. In this regard, cigarette smoking predisposes

individuals to increased bacterial colonisation and viral infection which can lead to, or exacerbate, disease pathologies[29,31]. Antibodies perform a vital role in the neutralisation of pathogens and preventing infection[130] but cigarette smoke has been demonstrated to decreased serum IgG antibodies[137–140], as well as impair the induction of salivary IgG and IgM responses[141]. We demonstrated that current smoking status was associated with decreased sputum IgM in both the ADEPT and GIRH cohort. IgM is present on naïve B cells and contributes to the adaptive immune response and protection against inhaled pathogens[129]. Consequently, decreased IgM in cigarette smokers may predispose individuals to greater risk of infection and colonisation. Specifically, reduced IgM levels are associated with *Streptococcus pneumoniae* infection and septicemia[251] as well as diseases such as bronchitis, bronchiectasis, and pneumonia[252]. Notably, these pathologies are also associated with COPD[149]. In addition, cigarette smoke has been observed to attenuate upper respiratory tract immune responses leading to *S. pneumoniae* colonisation and dissemination[31,253]. It is plausible this increased dissemination into the lower airways remains uncontrolled through reduced IgM levels in current cigarette smokers, leading to the development of bronchitis and invasive pneumococcal disease.

Current smoking status was further associated with decreased sputum IgM and IgG in mild to moderate COPD, but not in more severe disease. The mechanisms that lead to a decrease in antibody levels in patients with mild COPD who smoke is not known. Of note, the observed decreases were not associated with age, sex, or ICS dose. A possible mechanism resulting in this phenomenon is the transient decrease in T cell-mediated help in mild COPD[254].

Decreases in T cell-mediated immunity may limit the ability of B cells to proliferate and produce antibodies. Alternatively, the absolute number of B and T cells that accumulate with worsening disease[54,161] may compensate for any impaired mechanisms in patients with severe COPD and thus result in the recovery of antibody levels. Given the role of antibodies in host defence and the predisposition of cigarette smokers to infectious disease[255], this work highlights the importance of understanding smoking history when analysing antibody levels in COPD. These data suggest that targeted antibody therapies such as intravenous immunoglobulin delivery could be of particular use in treating infectious disease in current cigarette smokers.

Total sputum IgA was decreased in severe COPD subjects; however, current smoking status did not adversely alter IgA. Mechanisms resulting in IgA reduction in COPD likely mask decreases that are observed by cigarette smoking alone. For instance, the reduction in sputum IgA in patients with COPD may be in part a result of decreased pIgR, the receptor involved in IgA transcytosis into the alveolar space[167]. Notably, COPD is also associated with increased expression of TGF-β[256]. This has a two-fold impact upon IgA release. Firstly, TGF-β is involved in IgA class switching[257] and will preferentially result in increased IgA production as compared to other antibody classes. However, secondly, increased TGF-β is also negatively correlated with bronchial expression of pIgR in COPD[258] and thus will impair transcytosis mechanisms. Taken together, increased TGF-β and decreased pIgR expression in COPD suggest a mechanism which supports why lymphoid follicles are associated with IgA production[259] but overall there is an impairment in the transcytosis of IgA

into the alveolar space. Subsequently, we propose airway remodelling processes in COPD limit the ability to transcytosis IgA masking any cigarette smoke-only impairment of antibody production. Overall, cigarette smoking and disease severity-related decreases in antibodies in patients with COPD offer the potential for opportunistic infections, as demonstrated by increased bacterial infection in IgA deficient areas in COPD lung sections[168], to enter the respiratory tract and exacerbate disease.

Reduced total sputum IgM and IgG antibodies in current cigarette smokers did not translate to decreased sputum IgM/G autoantibodies. Total IgM and IgG autoantibody levels as well as total IgG/M ANA and AT levels were unchanged based on current smoking status. We speculate that the cellular source of autoantibodies may differ from that of the majority of antibodies present in the lung. B-1 cells are known to spontaneously release nAb which can have self-reactive properties[119,120]. This innate-like, T cell independent property may bypass the cell-to-cell interactions necessary for B-2 antibody generation and release. Consequently, while affecting B-2 mediated antibody responses, the transient decreases in T cells observed in COPD[254] leaves the B-1 compartment unaffected. These data suggest sputum autoantibody generation is isolated from other B cell processes in the lung.

5.2.2. Health consequences of altered (auto)antibodies in COPD

Recent data demonstrated that a subset of patients who experience frequent exacerbations had antibody deficiencies[172,173]. In particular, serum IgG deficiencies in patients with COPD have been linked to increased hospitalisation rates[260]. In this study, we did not observe a relationship between total sputum

IgM, IgG and IgA and increased hospitalisation rates (**Appendix Figure 3.**). We stratified subjects based on lung function only and did not undertake subgroup analysis based on specific endotypes in order to maintain statistical power. These data proposes that antibody levels are not a reliable marker of AECOPD risk without further stratification of patient populations.

Autoantibodies in COPD are proposed to offer insight into exacerbation risk. Clustering based approaches have identified two COPD endotypes with differences in autoantibodies, lung function, symptomatic scoring and blood cellular profiles, that were negatively or positively associated with AECOPD[261]. Based on a criteria of ≥ 1 hospitalisation in the past year, we did not observe either a positive or negative association between sputum or serum autoantibodies and AECOPD in GOLD-defined groups. In conjunction with Liang *et al.*[261] this study demonstrated that any association between autoantibodies and AECOPD is specific to select patient endotypes and is not a robust reflection of autoantibody levels in GOLD stages. Taken together, these data do not support the use of sputum autoantibodies to predict frequent exacerbations in the general COPD population. However, in defined COPD endotypes autoantibodies may act a biomarker to predict those at risk of frequent AECOPD and thus, allow pre-emptive treatment to lessen the burden on health care resources.

To date, investigators have proposed that autoantibodies in COPD contribute to airspace enlargement. This hypothesis is supported by a positive correlation between an increase of specificities that bind extracellular matrix components with worsening of gas exchange, as measured by DL_{CO}[181]. Lung

tissue sections from emphysema-dominant patients stained more strongly for deposited IgG than chronic bronchitis-dominant subjects[186]. Moreover, complement deposition, representative of a downstream process of antibody binding, has been reported in lung tissue sections of patients with COPD[180]. We observed weak positive correlation between serum IgM autoantibodies and % LAA-950 in the GIRH cohort. Notably, serum IgM AT specificities were more strongly positively correlated than IgM ANA with % LAA-950. These data support, albeit weakly, a link between AT expression and tissue destruction.

The weak correlation between AT expression and airspace enlargement was not observed in the ADEPT cohort which assessed emphysema using DL_{CO}, rather than % LAA-950. The differences between ADEPT and GIRH cohorts likely reflect the greater sensitivity of % LAA-950 as a densitometry measurement based directly on CT scans as compared to an indirect assessment of gas exchange via DL_{CO}. Overall, these surrogate emphysema measurements suggest that any link between autoantibodies and emphysema is weak in a general COPD population. Thus, for functional studies, precise patient endotypes are needed to explore whether sputum autoantibodies are a causative agent or a consequence of tissue destruction.

In the context of health, autoantibodies are typically assumed to be detrimental causing type II and III hypersensitivity reactions; however, autoantibodies have been shown to contribute to protective homeostatic processes[192,200,201]. This study detected sputum and serum autoantibodies in asymptomatic smokers and healthy controls alongside patients with COPD. This supports the notion that autoantibodies are part of a healthy immune system

and not simply a negative indicator of health. Consequently, any loss of autoantibodies and therefore the homeostatic role performed, has several implications for COPD pathogenesis. Our data demonstrated 16% of IgG sputum autoantibodies were downregulated compared to healthy controls. Moreover, of the differentially expressed serum autoantibodies the largest fold changes were observed in specificities that decreased. Therefore, autoantibody loss must be considered alongside the impact of increased autoantibodies and hypersensitivity reactions on disease pathogenesis.

The best studied autoantibodies in relation to protective phenotypes are nAb and, in particular, specificities that target anti-nuclear antigens. For instance, autoantibodies are known to mediate apoptotic cell clearance (efferocytosis) via anti-nuclear antigens on the cell surface[205,262]. Efferocytosis is a critical process in the removal of apoptotic bodies from the local environment. Notably, in patients with COPD there is increased epithelial apoptosis[193] which require efferocytotic clearance. The failure to effectively remove these apoptotic cells can lead to secondary necrosis and release of proinflammatory damage-associated molecular patterns (**DAMPs**)[263]. DAMP release, and recognition through pattern recognition receptors on innate immune cells, can promote prolonged inflammation[264]. Consequently, the loss of ANA specificities may lead to the accumulation of necrotic cells and the release of DAMPs contributing to a chronic inflammatory environment.

In addition to sources of anti-nuclear antigens from apoptosis, cigarette smoke induces increased neutrophil infiltration and NETosis[96,193]. Neutrophil extracellular traps (**NET**s) expose several anti-nuclear antigens to the immune

system[265]. Autoantibodies targeting NET components and apoptotic bodies have previously been observed in patients with COPD[186] and were decreased in this study. For instance, in both the ADEPT and GIRH cohorts, anti-histone and -SmD autoantibodies decreased. These specificities target autoepitopes presented on the cell surface during apoptosis[263,266] and in the chromatin structure released by neutrophils in NET formation[263]. In this regard, we showed a decreasing trend in the ability of sputum from patients with COPD to opsonise dying cells (**Appendix Figure 4.**). Therefore, decreased autoantibodies may lead to the failed ability to remove apoptotic bodies and contribute to chronic inflammation in patients with COPD. The role of autoantibodies in the removal of cellular debris and tissue homeostatic processes must be considered in addition to hypersensitivity reactions in disease.

We showed that clustering on autoantibodies was not sufficient to define COPD status. This demonstrates that cigarette smokers, subjects at higher risk of disease onset, and healthy controls had indistinguishable autoantibody profiles compared to those of COPD subjects. However, this does not preclude the possibility that patients with COPD may develop autoantibodies against alternative autoepitopes or generate a T cell-meditated autoimmune component. Secondly, this unbiased autoantibody-driven clustering suggests that the differentially expressed autoantibodies in COPD are not a causative agent, but rather a consequence of disease. We speculate that if autoantibodies were a vital part of disease pathogenesis, then autoantibody specificities would be strongly conserved between patients and cohorts, as seen in autoimmune disease cohorts. Instead, specificities varied between COPD cohorts and had minimal

differential expression compared to controls. Thus, differentially expressed autoantibodies may contribute to chronic inflammation and disease progression but are likely a consequence of the inflammatory environment and not a primary factor in the development of COPD. Ultimately, these data suggest that autoantibodies, whether sputum or serum, are not a reliable biomarker to identify patients with COPD.

5.2.3. Impaired fibrogenesis and tissue remodelling following cigarette smoke exposure

Macrophages accumulate in the lungs of patients with cigarette smoke-associated diseases such as COPD and IPF[54,222] and are considered key in disease pathogenesis. Increasingly, studies are focusing on different pulmonary macrophage subpopulations and how each independent population influences respiratory disease. To date, the manner in which cigarette smoke exposure alters the composition of macrophage subpopulations is not fully understood. Studies in COPD showed IM to be more proinflammatory, but less phagocytic, than AM but have yet to investigate the contribution of different subpopulations to this phenotype[45]. We observed an increase of $CD11b^+$ populations in lung tissue with IM1, -2, -3 and Mo-AM populations increased at 2-, 12- and 24-weeks of exposure. These populations decreased following smoking cessation but trended to be elevated compared to room air mice. Notably, Res-AM populations were not expanded and displayed a decreasing trend at multiple cigarette smoke exposure timepoints. The increase in IM populations supports previous data by Xiong *et al.* that demonstrated an accumulation of interstitial CX_3CR1^+ mononuclear phagocytes, a marker shown to be expressed on IM1, -

2 and -3[41,42], in cigarette smoke-exposed mice[65]. The increase in IM and Mo-AM populations, both linked to a proinflammatory phenotype[39,41,42,45], in cigarette smoke-exposed mice suggests the expansion of all $CD11b^+$ macrophage populations need to be closely monitored in patients.

The function of the different macrophage subpopulations following cigarette smoke exposure is yet to be elucidated. Notably, impaired macrophage phagocytosis is observed in cigarette smokers and patients with COPD[58,59]. The altered macrophage composition following cigarette smoke exposure may contribute to these clinical observations. IM subpopulations are reported to have decreased phagocytic ability than AM[42]. Of note, while Res-AM granularity increased 160% and 198% in the lung and BAL respectively following cigarette smoke exposure. Smaller increases in granularity were observed in $CD11b^+$ populations suggestive of less phagocytic uptake in these subpopulations. As a proportion of the total pulmonary macrophage population, cigarette smoke exposure led to an increase in IM populations. This suggests an increased odds of IM populations to be sampled from lung sections and contribute to a perceived decrease in phagocytic ability of cigarette smoke-exposed macrophages. These data highlight a need to carefully characterise macrophage ontogeny to better delineate functional consequences to insult.

Macrophages perform a vital role in the repair and regeneration of the tissue following damage[267,268]. Using a bleomycin model, we evaluated the impact of cigarette smoke on the ability of macrophages to facilitate tissue remodelling. Notably, $CD11b^+$ macrophages[211] and specifically Mo-AM[39,41] have been reported to be necessary for aberrant tissue remodelling processes.

Given, that cigarette smoke increases Mo-AM, a cell type associated with aberrant fibrogenesis and fibrosis[39,41,211], we expected exacerbated fibrogenesis. In contrast, we observed attenuated fibrogenesis in cigarette smoke-exposed mice. Notably, bleomycin hydrolase, which inactivates bleomycin, has a relative low expression in the lungs compared to other tissues and decreased fibrogenesis likely does not represent an increase in bleomycin metabolism in the lungs[269,270]. Indeed, Mo-AM were decreased in cigarette smoke-exposed bleomycin-treated mice as compared to room air-exposed bleomycin-treated mice at day 21. Leading to this timepoint, we observed a decrease in wound healing genes and increased IM1 populations in bleomycin-treated mice at day 7. IM1s perform a role in maintaining vascular integrity and thus may actively inhibit early aberrant tissue remodelling in cigarette smokers[43]. Thus, cigarette smoke attenuated profibrotic macrophage subpopulation expansion, expanded macrophage subpopulation with antifibrotic capacity and was associated with impaired fibrogenesis. These data highlight that composition changes in macrophage populations induced by cigarette smoke during the course of fibrogenesis may contribute to impaired wound healing observed in cigarette smokers following injury[271].

To complement our investigation of macrophage subpopulation composition during fibrogenesis, we assessed macrophage polarisation status. While macrophage polarisation is a spectrum whereby “M1” and “M2” expression markers are observed in fibrotic disease[41], “M2” markers such as CD206 are linked strongly to wound healing responses[272]. Total alternatively-activated $CD11b^{+}$ $CD206^{+}$ M2-like macrophages increased at day 7 and 21 in

cigarette smoke-exposed bleomycin treated mice. In contrast, total Res-AM $CD206^+$ populations were unchanged at day 7 and decreased at day 21. Notably, cigarette smoke-induced a predominant shift toward a M1-like profile at both day 7 and 21 post bleomycin in all subpopulations. This profile is suggestive of a proinflammatory rather than remodelling-like phenotype[49] and consequently may contribute to the decreased fibrogenesis observed. Despite the predominate shift toward an M1-like profile, *ex vivo* analysis of adherent $CD45^+$ lung cells observed no difference in collagen or urea production in TGF-β, Il-4 and Il-6 stimulated room air or cigarette smoke exposed cells. Urea production is a functional measure of arginase activity, a M2-like function. This suggests in this model that cigarette smoke exposure does impair M2-like functions. This study does not preclude that other M2-like functions may be impaired or that the presence of increased number of M1-like macrophages support a proinflammatory response capable of extracellular matrix breakdown. In this regard, the induction of M1-like macrophages may serve as a balance to any aberrant remodelling stimulated by bleomycin.

One mechanism which macrophages can directly affect the remodelling process is the accumulation of myofibroblasts, cells key to collagen secretion and protecting the tissue from mechanical stress[273]. In cigarette smoke-exposed bleomycin-treated mice, α-smooth muscle $actin^+$ cells (myofibroblasts) were decreased compared to room air bleomycin-treated mice. This decrease in myofibroblasts was associated with decreased expression of MMP9 by $CD45^+$ adhered cells. MMP9 performs a central role in TGF-β production[247] and epithelial-mesenchymal transition[248,249] which mediate myofibroblast

differentiation[250]. Notably MMP9 is shown to be increased in IPF[274] and MMP9-deficency shown to confer protection against renal fibrosis[275]. Thus, these data suggest that decreased macrophage-associated MMP9 may limit fibrogenesis in cigarette smokers and led to impaired wound healing following injury.

The attenuated fibrogenesis observed in cigarette smoke-exposed mice sheds light on processes occurring in IPF patients who continue to smoke. Multiple IPF studies have reported better patient survival rates in current smokers compared to non-smokers[218,219]. This could be interpreted as a "healthy" smoker affect but the skewed macrophage composition and polarisation observed in our model offers insight into a dichotomous cigarette smoke effect on fibrogenesis. Cigarette smoke beyond doubt causes frequent microinjuries to the epithelium likely via excessive oxidant activity, resulting in expanded profibrotic Mo-AM populations which plausibly increase the odds of fibrotic lesion development. However, with sustained cigarette smoke exposure the expansion of anti-fibrotic IM1 subpopulation and a proportional loss of Mo-AM compared to those who do not smoke may lead to a slower disease progression. Therefore, we speculate while those subjects that continue to smoke cigarettes appear to have marginal improvements in morbidity this represents a slower disease onset.

5.3. Limitations and future direction

5.3.1. COPD endotypes and patient characteristics

One of the main objectives of this study was to assess the presence of autoantibodies in COPD to identify subjects at risk of developing disease or those with disease who are at risk of accelerated lung function decline. To this end, we performed a comprehensive retrospective analysis of matched serum and sputum autoantibodies in 224 individuals across three continents. As part of the ADEPT cohort controls, we assessed healthy controls as well as asymptomatic smokers. These healthy control subjects had no history of respiratory diseases and had quit smoking for at least one year prior to study enrolment. A similar control group was not recruited in the GIRH autoantibody cohort. Subsequently, the decreased expression of IgG sputum autoantibodies observed in the ADEPT cohort could not be validated. To note, patients with COPD had the same sputum autoimmune profile as GIRH and ADEPT asymptomatic smokers and ADPET healthy controls. This suggests that patients with COPD would not have a differing sputum autoantibody profile from additional healthy controls; however, further investigation of sputum autoantibodies in healthy individuals is warranted to fully understand consequences of decreased sputum autoantibodies in COPD.

Sex differences are important to consider in disease pathogenesis. There is increasing evidence that demonstrates that sex differences are implicated in immune pathologies. For example, women are more likely to develop autoimmune disease than men[276]. The GIRH cohort included only male subjects. Therefore, this study may underrepresent differentially expressed

autoantibodies in the GIRH cohort. However, the ADEPT cohort was well represented by both men and women and no association between total sputum antibody levels or any autoantibodies and sex was observed. Furthermore, to address any sex differences, the analysis in **chapter III** was undertaken using regression analysis to adjust for sex and consequently, we evaluated and corrected for any influence of sex upon autoantibody measurements.

Personalised medicine and the drive to determine patient specific endotypes is becoming increasingly important in modern medicine. COPD is a complex disease that is diagnosed using lung function and symptomatic score. Specific disease endotypes, such as emphysema-dominant, chronic bronchitis-dominant, or exacerbation history provide greater resolution in immune mechanisms in COPD. Previous studies showed increased serum autoantibodies associated particularly with patients with emphysema-dominant COPD[181,186]. In the ADEPT cohort, there was no association between autoantibodies and DL_{CO} in either the sputum or serum. In contrast, we reported a weak association between serum IgM AT and % LAA-950 in the GIRH cohort. The difference observed in cohorts may reflect the inability to confirm the presence of emphysema and stringently stratify subjects. Consequently, stratifying heterogenous diseases such as COPD into precise pathologies, such as emphysema- or chronic bronchitis-dominant, is of benefit to future COPD studies and should become standard practice. To this end, stratification of subject endotypes based on exacerbation status is needed to fully understand the contribution of specific sputum autoantibody profiles to increased or reduced AECOPD events. Together, a systematic breakdown of COPD endotypes is

needed and will aid investigation of immune processes and thus assist the design of future treatments.

5.3.2. IgA assessment

There is an emerging literature regarding the role of IgA in COPD pathogenesis. Strikingly, in addition to data from this thesis, several studies reported decreased total IgA in COPD[166,168,169]. Decreased IgA has been shown to enable endogenous bacteria to recruit monocyte-derived dendritic cells into the airways[169]. It is this increase in monocyte-derived dendritic cells that can then mediate aberrant T cell responses, thus leading to airway remodelling[169]. These data and ours, seem in contrast to studies that observed increases in lymphoid follicle-associated IgA[259]. An investigation to address this dichotomy of increased lymphoid follicle associated IgA but decreased airway IgA[167,259] is needed.

COPD autoantibody studies have focused on serum IgG and IgM[180,184,186]. These isotypes are commonly assessed in studies of autoimmune disease. Thus, we aimed to validate the presence of serum IgG and IgM autoantibodies and expand on these analyses in the sputum. Studies are also now warranted to investigate the presence of IgA autoantibodies in COPD. To note, the role of IgA autoantibodies in autoimmune disease as a whole is currently not well understood. As IgA is associated with the mucosal surface barrier protection, the assessment of sputum IgA autoantibodies in autoimmune disease offers opportunities to better understand respiratory diseases.

5.3.3. Cigarette smoke-modified neoepitopes and neo-autoantibodies

The autoantigen array used in this work provided a validated platform to measure a broad assortment of common autoantibodies. Cigarette smoke is a complex insult and can induce modifications including, but are not limited to, citrullination, carbonylation and carbamylation[277–279]. It is plausible that development of anti-neoepitope antibodies may contribute to chronic inflammation in COPD. In matched serum and sputum samples from the ADEPT cohort, we reported no difference in IgG anti-cyclic citrullinated peptides or IgG/IgA anti-cyclic citrullinated peptides, between patients with COPD and asymptomatic smoker or healthy controls (**Appendix Figure 5.**). Further investigation of neoepitopes caused by cigarette smoked-related oxidants which can induce carbonyl adducts or carbamylation are needed. Carbamylation may prove an optimal start as myeloperoxidase, a molecule known to be elevated in COPD, is the main trigger for homocitrulline development and neo-autoantigen generation[155,280]. In summary, to comprehensively assess autoantibodies in COPD, cigarette smoke-modified epitopes and neo-autoantibody generation require further investigation.

5.3.4. T cell-mediated autoimmunity

This thesis focused on the presence of autoantibodies as a measure of autoimmunity in COPD. This approach was taken to address the variable expression of autoantibodies in the serum of patients with COPD[180–182]. Moreover, offer insight to the a potential functional link between B cell-rich lymphoid follicles in the small airways[161] and emphysema[162]. Ultimately, this study found limited evidence of differential expression of autoantibodies in

COPD. However, B cells only represent one arm of the adaptive immune response, with T cells also potential contributors to autoimmune disease. For instance, programmed death receptor (**PD**)-1 and corresponding programmed death receptor ligand (**PD-L**)1 provide a mechanism to regulate the immune response, and in particular perform a key role in inhibiting T cell activation[281]. In the peripheral blood and lung tissue samples of patients with COPD, $CD4^+$ and $CD8^+$ T cells have increased PD-1 expression[108,282]. In contrast, data suggest that PD-L1 expression on antigen presenting cells is reduced in COPD[108,283]. An imbalance in PD-1/PD-L1 homeostasis may perform a pivotal role the development of autoreactive T cells leading to type IV hypersensitivities. These cell-mediated reactions have the potential to contribute to the chronic inflammation in patients with COPD.

5.3.5. Cigarette smoke-associated antibody decreases

In current cigarette smokers with mild to moderate COPD, total sputum IgM and IgG was decreased; however, IgM and IgG sputum autoantibodies were not changed. The mechanism underlying the impact of cigarette smoke on sputum total antibodies but not autoantibodies is not known. Given that T cells are transiently decreased in COPD[254] and that B-1 cells spontaneously release nAb in the absence of T cell help[119,120], studies focusing on the cellular source of COPD autoantibodies are needed. These studies will elucidate the impact of cigarette smoke on the autoantibody development.

To complement studies to assess the source of autoantibodies in COPD, studies assessing the impact of cigarette smoke on autoantibody transport to the alveolar space are needed. Tissue remodelling processes in the lung are shown

to decrease pIgR expression and consequently reduce Ig transcytosis into the alveolar space[168,169,171]. Further investigation of the impact of tissue remodelling processes in current cigarette smokers is needed to elucidate mechanisms of airway antibody and autoantibody deficiency.

5.3.6. Macrophage subpopulation function

$CD11b^+$ macrophages are expanded following cigarette smoke exposure. The functional consequence of increased $CD11b^+$ macrophages in the context of respiratory disease development needs to be further assessed. Using a model of concurrent bleomycin-induced lung injury, we observed an attenuated fibrogenesis and tissue remodelling following cigarette smoke exposure. To further elucidate the impact of cigarette smoke on the function of macrophage subpopulations, transcriptional analysis of each subpopulation would provide a powerful method to probe differences in each subpopulation regardless of low recoverable cell numbers. This bleomycin model just represents one model to assess the impact of cigarette smoke on macrophage function. Given that cigarette smokers are susceptible to increased infections[255], alternative models with a focus on bacterial or viral stimuli would provide another relevant assessment of the functional impact of cigarette smoke on macrophages. Investigation of specific functional responses of each macrophage subpopulation in cigarette smoke-induced inflammation will enable future therapies to target the subpopulations responsible for disease pathogenesis while not ablating subpopulations needed to maintain tissue homeostasis.

Understanding the composition and function of macrophage subpopulations in COPD is of vital importance. Macrophages are central in

facilitating cigarette smoking-mediated immunopathology[245] and remain elevated following smoking cessation[54]. Blocking the expansion of pathogenic subpopulations and alleviating pathology would provide novel strategies to treat patients with COPD and other cigarette-associated respiratory diseases. Targeted approaches at blocking IM recruitment via chemokines such as CCL2, CCL3 or CX_3CL1 might pose novel intervention strategies to halt disease. Furthermore, we showed that IL-1α is an important component in the recruitment and proliferation of macrophage subpopulations following cigarette smoke exposure. Further studies in transgenic and conditional knockout models are required to better understand the contribution of each subpopulation to pathology. These studies would direct focused treatment of singular subpopulations aimed at halting pathology without compromising immunity. Future therapeutics aimed at blocking the expansion of $CD11b^+$ macrophage subpopulations may provide a new strategy to halt accelerated lung function decline.

5.4. Concluding remarks

In this thesis, we evaluated the impact of cigarette smoke on the immune cells and mediators. The first study (published in the *European Respiratory Journal*) demonstrated that sputum was a viable matrix to assess antibody levels in individuals with COPD. This study demonstrated that patients with severe COPD had decreases in sputum IgA. In addition, this study highlighted that current smoking status is associated with reduced IgM and IgG sputum antibodies in mild to moderate COPD. These data emphasise the need to assess

current cigarette smoking status when sampling respiratory matrixes such as sputa.

In the second study (published in the *American Journal of Physiology Lung Cellular and Molecular Physiology*), we observed that autoantibodies are present in the sputum and serum of patients with COPD. Despite COPD being a respiratory disease, a more diverse IgM and IgG autoantibody repertoire was observed in the serum than the sputum. With COPD status, a proportion of serum IgM and IgG autoantibodies were differentially expressed, but this expression was not strongly associated with any clinical parameter. Overall, we found an individual's autoantibody profile was not sufficient to determine COPD disease status. These data suggests that autoantibodies do not provide a reliable biomarker for COPD identification for disease interception therapies.

In the third study (in review at *Frontiers in Immunology*), we demonstrated that cigarette smoke exposure altered the composition of pulmonary macrophage subpopulations resulting in expansion of $CD11b^+$ populations. This expansion in $CD11b^+$ populations, specifically Mo-AM and IM3, was dependent on IL-1α. This altered macrophage composition was associated with attenuated fibrogenesis in a mouse model of bleomycin-induced lung injury. In summary, this study showed that cigarette smoke altered the composition of macrophage subpopulations in the lungs. These changes in composition were associated with impaired tissue remodelling and offered insight into impaired wound healing processes in cigarette smokers. Halting the accumulation of $CD11b^+$ macrophages following cigarette smoke exposure may

provide a mechanism to improve outcome in cigarette smoke-associated disease.

Overall, the work presented in this thesis explored the impact of cigarette smoke on the immunopathogenesis of respiratory disease. This work has increased the awareness of current cigarette smoking status on the assessment of total antibodies, demonstrating antibody decreases in current smokers. This sheds light on mechanisms which increase the susceptibility of cigarette smokers to infectious disease and COPD exacerbation. Moreover, this worked provided evidence that autoantibodies in COPD do not provide a reliable biomarker with which to identify individuals with disease. Lastly, we demonstrated that cigarette smoke exposure altered pulmonary macrophage subpopulation composition, increasing $CD11b^{+}$ subpopulations, and this was associated with impaired tissue remodelling. Overall, this thesis highlighted the determinantal impact of cigarette smoke on (auto)antibody levels and pulmonary macrophage composition.

APPENDIX

McMaster University

STEVEN CASS <casss@mcmaster.ca>

Request for Permission; PhD Thesis

European Respiratory Society Permissions <permissions@ersnet.org> Mon, Apr 12, 2021 at 5:42 AM
To: Steven Cass <casss@mcmaster.ca>

Dear Steven,

Thank you for your enquiry.

European Respiratory Society hereby grants you permission to reproduce the material as requested for your thesis (print and digital) and full acknowledgement must be given.

Current smoking status is associated with reduced sputum immunoglobulin M and G expression in COPD

Steven P. Cass, Yuqiong Yang, Jing Xiao, Joshua J.C. McGrath, Matthew F. Fantauzzi, Danya Thayaparan, Fengyan Wang, Zhenyu Liang, Fei Long, Christopher S. Stevenson, Rongchang Chen, Martin R. Stampfli

European Respiratory Journal 57 (2) 1902338; **DOI:** 10.1183/13993003.02338-2019 Published 4 February 2021

Material: Entire Article

Acknowledgement Wording: Reproduced with permission of the © ERS 2021: European Respiratory Journal 57 (2) 1902338; **DOI:** 10.1183/13993003.02338-2019 Published 4 February 2021

Copyright remains with © ERS 2021. These publications are copyrighted material and must not be copied, reproduced, transferred, distributed, leased, licensed, placed in a storage retrieval system or publicly performed or used in any way except as specifically permitted in writing by the publishers (European Respiratory Society), as allowed under the terms and conditions of which it was purchased or as strictly permitted by applicable copyright law. Reproduction of this is material is confined to the purpose and/or media for which permission is hereby given. Altering/Modifying Material: This is not permitted, however figures and illustrations maybe altered/adapted minimally to serve your work. Please be aware that the permission fee for the requested use of this material is waived in this instance but please be advised that your future requests for materials may attract a fee. This agreement is personal to you and may not be sublicense, assigned or transferred by you to any other person without our written permission. Any unauthorised distribution or use of this text may be a direct infringement of the publisher's rights and those responsible may be liable in law accordingly

"Green" open access and author archiving (where applicable)

Authors who do not wish to pay for their article to be published open access in the *ERJ* will still have their manuscripts made free to access via the *ERJ* online archive following the journal's 18-month embargo period. Authors also have licence to make their manuscripts available in an institutional (or similar) repository for public archiving, 12 months after final publication, provided the following requirements are met:

1) The final, peer-reviewed, author-submitted version that was accepted for publication is used (before copy-editing and publication).

2) A permanent link is provided to the version of the article published in the ERJ, through the dx.doi.org platform. For

example, if your manuscript has the DOI 10.1183/13993003.06543-2018, then the link you provide must be https://doi.org/10.1183/13993003.06543-2018

3) The repository on which the manuscript is deposited is not used for systematic distribution or commercial sales purposes.

4) The following required archiving statement appears on the title page of the archived manuscript: "This is an author-submitted, peer-reviewed version of a manuscript that has been accepted for publication in the European Respiratory Journal, prior to copy-editing, formatting and typesetting. This version of the manuscript may not be duplicated or reproduced without prior permission from the copyright owner, the European Respiratory Society. The publisher is not responsible or liable for any errors or omissions in this version of the manuscript or in any version derived from it by any other parties. The final, copy-edited, published article, which is the version of record, is available without a subscription 18 months after the date of issue publication."

For manuscripts with Europe PMC funding, the journal acknowledges that the author retains the right to provide a copy of the final, peer-reviewed author-supplied manuscript (before copy-editing and publication) for public archiving in compliance with the requirements of the funder, i.e. 6 months after final publication for authors with funding from Europe PubMed Central Funders Group members.

Kind regards,

Kay

ERS
Kay Sharpe
European Respiratory Society Permissions Editor
D +44 114 267 28 61
ERS 442 Glossop Road Sheffield S10 2PX United Kingdom
Central T +44 114 267 28 60 F +44 114 266 50 64 W ersnet.org

Note: I am only working 5-6 hours per day on a phased return and please be aware that processing requests could take between 3-5 days.

The ABSTRACTS from the ERS Virtual Congress from 2020 are now available at https://erj.ersjournals.com/content/56/suppl_64

In keeping with current recommendations relating to COVID-19, our offices in Lausanne, Brussels and Sheffield are now all closed as a precautionary measure. ERS and ELF staff will continue to work from home where possible

[Quoted text hidden]

THE AMERICAN PHYSIOLOGICAL SOCIETY ORDER DETAILS
Apr 29, 2021

This Agreement between Steven P Cass ("You") and The American Physiological Society ("The American Physiological Society") consists of your order details and the terms and conditions provided by The American Physiological Society and Copyright Clearance Center.

Order Number	501650911
Order date	Apr 29, 2021
Licensed Content Publisher	The American Physiological Society
Licensed Content Publication	Am J Physiol-Lung, Cellular, and Molecular Physiology
Licensed Content Title	Differential expression of sputum and serum autoantibodies in patients with chronic obstructive pulmonary disease
Licensed Content Author	Steven P Cass, Anna Dvorkin-Gheva, Yuqiong Yang, et al
Licensed Content Date	Apr 28, 2021
Licensed Content Volume	0
Licensed Content Issue	0
Type of Use	Thesis/Dissertation
Requestor type	author
Readers being charged a fee for this work	No
Format	print and electronic
Portion	full article
Will you be translating?	no
World Rights	no
Order reference number	
Title	CIGARETTE SMOKE IMPACT ON RESPIRATORY DISEASE IMMUNOPATHOLOGY
Institution name	McMaster Uniersity
Expected presentation date	Jul 2021
Requestor Location	McMaster University MDCL 4084 McMaster University 1200 Main Street West Hamilton, ON L8N 3Z5 Canada Attn: McMaster University
Billing Type	Invoice
Billing Address	McMaster University MDCL 4084 McMaster University 1200 Main Street West

Hamilton, ON L8N 3Z5
Canada
Attn: McMaster University

Total 0.00 CAD

Terms and Conditions

Terms and Conditions:

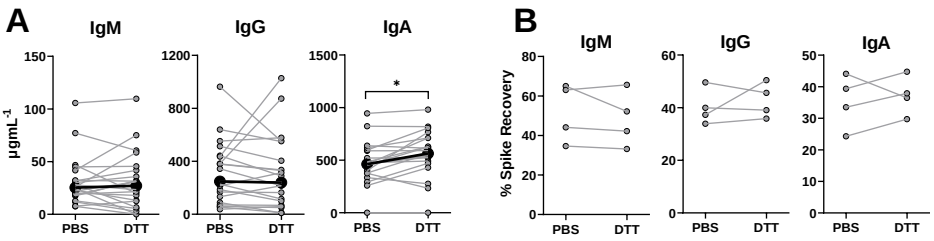

Appendix Figure 1. DTT and PBS processing buffers are comparable in matched sputum samples. (A) Paired analysis of matched subject samples processed in PBS or DTT. Bold line represents median Ig recovery per isotype. (B) Spike recovery of 4.1mg of immunoglobulin in processed samples. Mean ± SD. Paired Wilcoxon T test (A-B). Two-way ANNOVA with repeated measures (C). *p = <0.05.

Ig Standard	IgM		IgA		IgG	
Pre-treatment	**PBS**	**DTT**	**PBS**	**DTT**	**PBS**	**DTT**
ng/mL (±SD)	130.1 ± 17.7	59.0 ± 5.0	8.0 ± 0.3	7.3 ± 0.5	115.2 ± 10.6	133.1 ± 10.2
p value		<0.0001		0.0182		0.0138
% PBS recovery		45.3		92.3		115.5

Table 1. Sandwich ELISA processing buffer interference. Ig standard pre-treated for 15 minutes with 0.1% DTT or PBS. Sample then diluted 4-fold in PBS prior to Ig detection. Welch's T test.

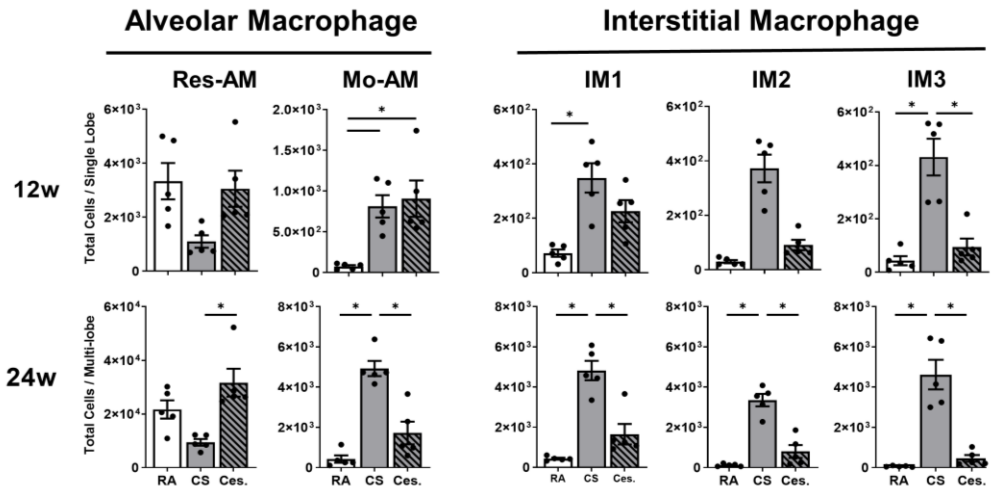

Appendix Figure 2. Macrophage subpopulation composition following cigarette smoke cessation. Mice were cigarette smoke exposed for 8-weeks. Mice then either continued cigarette smoking or were exposed to room air only for an addition 4 or 16-weeks for a total exposure protocol of 12 or 24-weeks. RA – room air (open). CS – cigarette smoke (grey). Ces. – cessation (cross-hatched). *p = <0.05. Ordinary one-way ANNOVA.

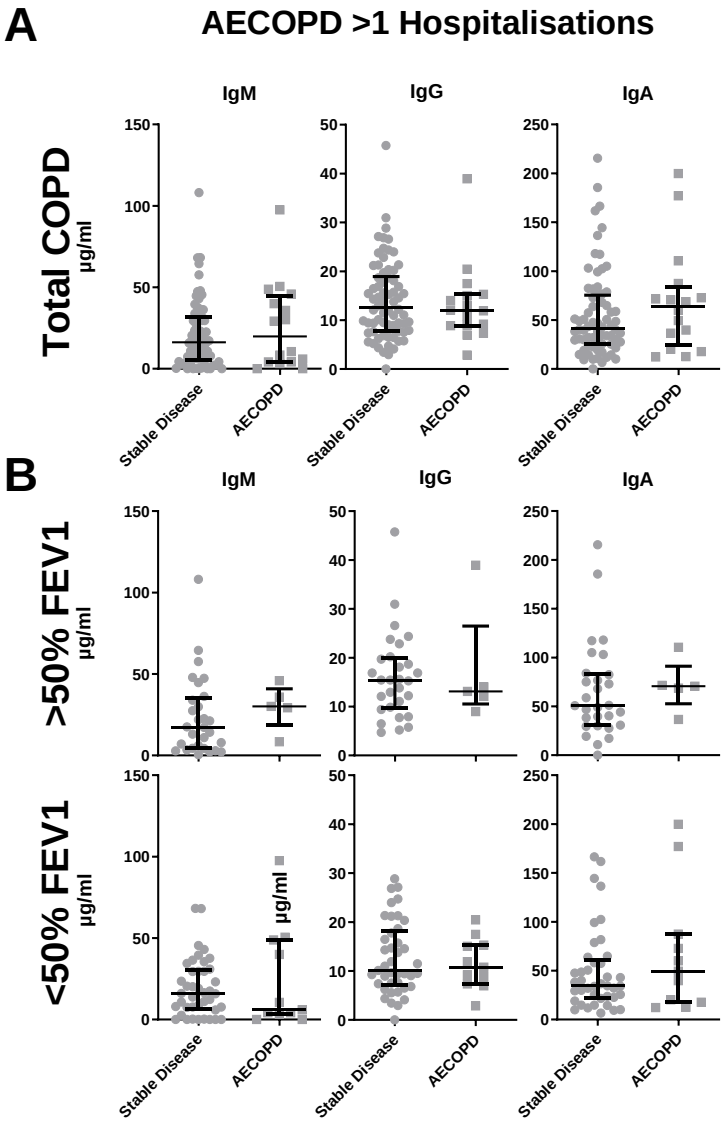

Appendix Figure 3. Total IgM, IgG and IgA antibodies were not associated with increased hospitalisation visits. IgM, IgG and IgA antibodies from patients with COPD stratified into subjects with stable disease in the previous year versus those subjects who experiment greater than one hospitalisation event because of an acute exacerbation of COPD. (A) All COPD subjects. (B) Subjects split into greater than or less than 50% forced expiratory volume in 1 second. Median ± Interquartile range.

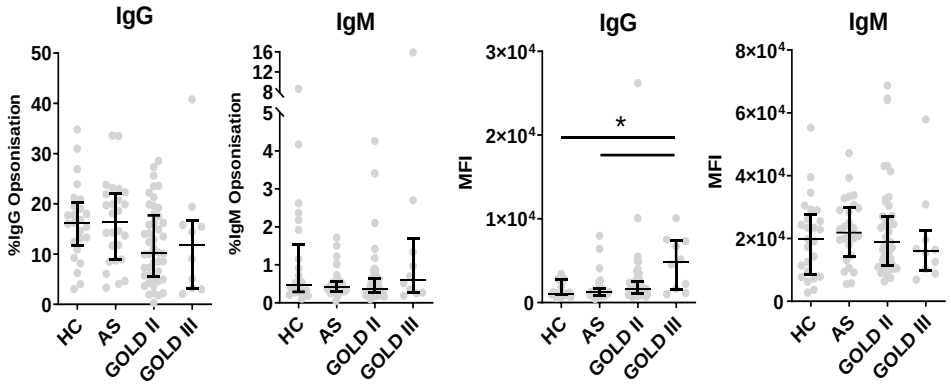

Appendix Figure 4. Autoantibodies opsonise dying A549 epithelial cells. % opsonisation of ADEPT sputum IgG and IgM antibodies versus A549 cells induced to undergo apoptosis by cigarette smoke extract. AU – Arbitrary units. MFI – Median fluorescence intensity. *p = < 0.05. HC – Healthy control, AS – Asymptomatic smokers.

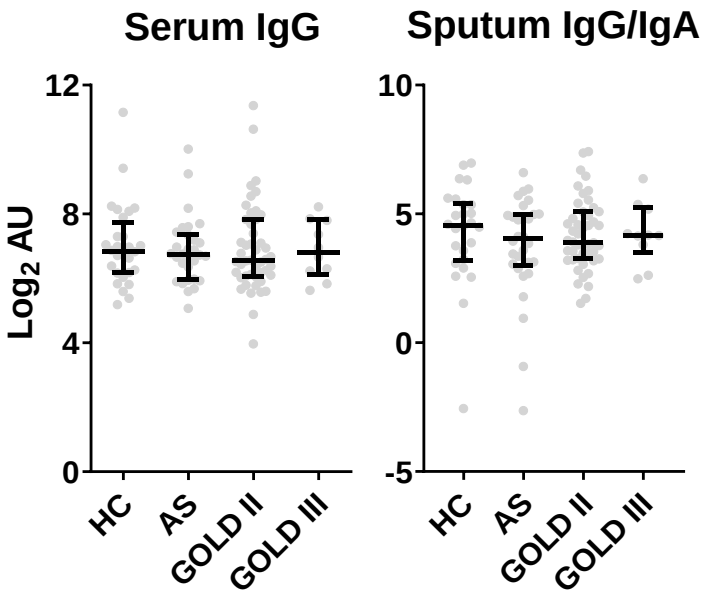

Appendix Figure 5. Anti-cyclic citrullinated peptide (CCP) do no increase in induced sputum and serum. IgG CCP3 serum and IgG/A CCP3.1 sputum autoantibodies were measured by ELISA in the ADEPT cohort. Each point represents one subject. Plots (A-D) show median and inter-quartile range. *p = < 0.05. AU – Arbitrary units. HC – Healthy control, AS – Asymptomatic smokers

REFERENCES

1. World Health Organization (WHO). Tobacco Fact Sheet. https://www.who.int/news-room/fact-sheets/detail/tobacco (2020).
2. U.S. Department of Health and Human Services. *How Tobacco Smoke Causes Disease The Biology and Behavioral Basis for Smoking-Attributable Disease A Report of the Surgeon General*. *Centers for Disease Control and Prevention (US)* (2010).
3. U.S. Department of Health and Human Services. *The Health Consequences of Smoking - 50 Years of Progress: A Report of the Surgeon General Executive Summary*. http://www.surgeongeneral.gov/library/reports/50-years-of-progress/full-report.pdf (2014).
4. Johnson, P. B. & Richter, L. The relationship between smoking, drinking, and adolescents' self-perceived health and frequency of hospitalization: Analyses from the 1997 National Household Survey on Drug Abuse. *J. Adolesc. Heal.* **30**, 175–183 (2002).
5. Wang, M. P., Ho, S. Y., Lo, W. S., Lai, M. K. & Lam, T. H. Smoking is associated with poor self-rated health among adolescents in Hong Kong. *Nicotine Tob. Res.* **14**, 682–7 (2012).
6. Ng, M. *et al.* Smoking prevalence and cigarette consumption in 187 countries, 1980-2012. *JAMA* **311**, 183–92 (2014).
7. Statistics Canada. Table 13-10-0096-10 Smokers, by age group. https://www150.statcan.gc.ca/t1/tbl1/en/tv.action?pid=1310009610 (2020) doi:https://doi.org/10.25318/1310009601-eng.
8. Jha, P. *et al.* 21st-century hazards of smoking and benefits of cessation in the United States. *N. Engl. J. Med.* **368**, 341–50 (2013).
9. Pirie, K., Peto, R., Reeves, G. K., Green, J. & Beral, V. The 21st century hazards of smoking and benefits of stopping: a prospective study of one million women in the UK. *Lancet (London, England)* **381**, 133–41 (2013).
10. Department of Health and Human Services. The Health Consequences of Involuntary Exposure to Tobacco Smoke A Report of the Surgeon General. *Public Health* (2006).
11. Rodgman, A. & Perfetti, T. A. *The Chemical Components of Tobacco and Tobacco Smoke*. (CRC Press, Taylor & Francis Group, 2013). doi:https://doi.org/10.1201/b13973.
12. Smith, C. J. & Hansch, C. The Relative Toxicity of Compounds in Mainstream Cigarette Smoke Condensate. *Food Chem. Toxicol.* **38**, 637–646 (2000).
13. Nouri-Shirazi, M. & Guinet, E. Evidence for the immunosuppressive role of nicotine on human dendritic cell functions. *Immunology* **109**, 365–373 (2003).
14. Santanam, N., Sanchez, R., Hendler, S. & Parthasarathy, S. Aqueous extracts of cigarette smoke promote the oxidation of low density lipoprotein by peroxidases. *FEBS Lett.* **414**, 549–551 (1997).
15. Adler, K. B., Holden-Stauffer, W. J. & Repine, J. E. Oxygen metabolites stimulate release of high-molecular-weight glycoconjugates by cell and

organ cultures of rodent respiratory epithelium via an arachidonic acid-dependent mechanism. *J. Clin. Invest.* **85**, 75–85 (1990).
16. Ma, B., Stepanov, I. & Hecht, S. S. Recent studies on DNA adducts resulting from human exposure to tobacco smoke. *Toxics* **7**, (2019).
17. Geng, Y., Savage, S. M., Razani-Boroujerdi, S. & Sopori, M. L. Effects of nicotine on the immune response: II. Chronic nicotine treatment induces T cell anergy. *J. Immunol.* **156**, 2384–2390 (1996).
18. Davila, D. R., Romero, D. L. & Burchiel, S. W. Human T cells are highly sensitive to suppression of mitogenesis by polycyclic aromatic hydrocarbons and this effect is differentially reversed by α-naphthoflavone. *Toxicol. Appl. Pharmacol.* **139**, 333–341 (1996).
19. Bessede, A. *et al.* Aryl hydrocarbon receptor control of a disease tolerance defense pathway. *Nature* **511**, 184–190 (2014).
20. Sheridan, J. A. *et al.* Decreased expression of the NF-KB family member RelB in lung fibroblasts from Smokers with and without COPD potentiates cigarette smoke-induced COX-2 expression. *Respir. Res.* **16**, 1–16 (2015).
21. Iu, M. *et al.* RelB attenuates cigarette smoke extract-induced apoptosis in association with transcriptional regulation of the aryl hydrocarbon receptor. *Free Radic. Biol. Med.* **108**, 19–31 (2017).
22. Thatcher, T. H. *et al.* Aryl hydrocarbon receptor-deficient mice develop heightened inflammatory responses to cigarette smoke and endotoxin associated with rapid loss of the nuclear factor-κB component RelB. *Am. J. Pathol.* **170**, 855–864 (2007).
23. Vaidyanathan, B. *et al.* The aryl hydrocarbon receptor controls cell-fate decisions in B cells. *J. Exp. Med.* **214**, 197–208 (2017).
24. Mohinta, S. *et al.* Differential regulation of Th17 and T regulatory cell differentiation by aryl hydrocarbon receptor dependent xenobiotic response element dependent and independent pathways. *Toxicol. Sci.* **145**, 233–243 (2015).
25. Heijink, I. H., Brandenburg, S. M., Postma, D. S. & Van Oosterhout, A. J. M. Cigarette smoke impairs airway epithelial barrier function and cell-cell contact recovery. *Eur. Respir. J.* **39**, 419–428 (2012).
26. von Meyerinck, L. *et al.* Exposure of rats and hamsters to sidestream smoke from cigarettes in a subchronic inhalation study. *Exp. Pathol.* **37**, 186–189 (1989).
27. Takahashi, A., Iwasaki, I. & Ide, G. Effects of minute amounts of cigarette smoke with or without nebulized N-nitroso-N-methylurethane on the respiratory tract of mice. *Jpn. J. Cancer Res.* **76**, 324–30 (1985).
28. Laan, M., Bozinovski, S. & Anderson, G. P. Cigarette Smoke Inhibits Lipopolysaccharide-Induced Production of Inflammatory Cytokines by Suppressing the Activation of Activator Protein-1 in Bronchial Epithelial Cells. *J. Immunol.* **173**, 4164–4170 (2004).
29. Bauer, C. M. T. *et al.* Cigarette Smoke Suppresses Type I Interferon-Mediated Antiviral Immunity in Lung Fibroblast and Epithelial Cells. *J. Interf. Cytokine Res.* **28**, 167–179 (2008).
30. Higham, A., Bostock, D., Booth, G., Dungwa, J. V & Singh, D. The effect of electronic cigarette and tobacco smoke exposure on COPD bronchial

epithelial cell inflammatory responses. *Int. J. COPD* **7**, L662–L672 (2018).
31. Shen, P. *et al.* Cigarette Smoke Attenuates the Nasal Host Response to Streptococcus pneumoniae and Predisposes to Invasive Pneumococcal Disease in Mice. *Infect. Immun.* **84**, 1536–47 (2016).
32. Mio, T. *et al.* Cigarette smoke induces interleukin-8 release from human bronchial epithelial cells. *Am. J. Respir. Crit. Care Med.* **155**, 1770–1776 (1997).
33. Nikota, J. K. *et al.* Cigarette smoke primes the pulmonary environment to IL-1α/CXCR-2-dependent nontypeable Haemophilus influenzae-exacerbated neutrophilia in mice. *J. Immunol.* **193**, 3134–45 (2014).
34. Fathi, M. *et al.* Functional and morphological differences between human alveolar and interstitial macrophages. *Exp. Mol. Pathol.* **70**, 77–82 (2001).
35. Nayak, D. K. *et al.* Long-Term Persistence of Donor Alveolar Macrophages in Human Lung Transplant Recipients That Influences Donor-Specific Immune Responses. *Am. J. Transplant.* **16**, 2300–2311 (2016).
36. Guilliams, M. *et al.* Alveolar macrophages develop from fetal monocytes that differentiate into long-lived cells in the first week of life via GM-CSF. *J. Exp. Med.* **210**, 1977–92 (2013).
37. Tan, S. Y. S. & Krasnow, M. A. Developmental origin of lung macrophage diversity. *Development* **143**, 1318–1327 (2016).
38. Hashimoto, D. *et al.* Tissue-resident macrophages self-maintain locally throughout adult life with minimal contribution from circulating monocytes. *Immunity* **38**, 792–804 (2013).
39. Misharin, A. V. *et al.* Monocyte-derived alveolar macrophages drive lung fibrosis and persist in the lung over the life span. *J. Exp. Med.* **214**, 2387–2404 (2017).
40. Gibbings, S. L. *et al.* Transcriptome analysis highlights the conserved difference between embryonic and postnatal-derived alveolar macrophages. *Blood* **126**, 1357–1366 (2015).
41. Joshi, N. *et al.* A spatially restricted fibrotic niche in pulmonary fibrosis is sustained by M-CSF/M-CSFR signalling in monocyte-derived alveolar macrophages. *Eur. Respir. J.* **55**, (2020).
42. Gibbings, S. L. *et al.* Three Unique Interstitial Macrophages in the Murine Lung at Steady State. *Am J Respir Cell Mol Biol* **57**, 66–76 (2017).
43. Chakarov, S. *et al.* Two distinct interstitial macrophage populations coexist across tissues in specific subtissular niches. *Science (80-.).* **363**, (2019).
44. Ural, B. B. *et al.* Identification of a nerve-associated, lung-resident interstitial macrophage subset with distinct localization and immunoregulatory properties. *Sci. Immunol.* **5**, 1–15 (2020).
45. Dewhurst, J. A. *et al.* Characterisation of lung macrophage subpopulations in COPD patients and controls. *Sci. Rep.* **7**, 1–12 (2017).
46. Hussell, T. & Bell, T. J. Alveolar macrophages: Plasticity in a tissue-specific context. *Nat. Rev. Immunol.* **14**, 81–93 (2014).

47. Lavin, Y. *et al.* Tissue-Resident Macrophage Enhancer Landscapes Are Shaped by the Local Microenvironment. *Cell* **159**, 1312–1326 (2014).
48. Murray, P. J. Macrophage Polarization. *Annu. Rev. Physiol.* **79**, 541–566 (2016).
49. Mills, C. D. *et al.* M-1/M-2 Macrophages and the Th1/Th2 Paradigm. *J Immunol* **164**, 6166–6173 (2000).
50. Karimi, K. *et al.* Toll-like receptor-4 mediates cigarette smoke-induced cytokine production by human macrophages. *Respir. Res.* **7**, 1–11 (2006).
51. Shaykhiev, R. *et al.* Smoking-Dependent Reprogramming of Alveolar Macrophage Polarization: Implication for Pathogenesis of Chronic Obstructive Pulmonary Disease. *J Immunol* **183**, 2867–2883 (2009).
52. Eapen, M. S. *et al.* Abnormal M1/M2 macrophage phenotype profiles in the small airway wall and lumen in smokers and chronic obstructive pulmonary disease (COPD). *Sci. Rep.* **7**, 1–12 (2017).
53. Morissette, M. C., Shen, P., Thayaparan, D. & Stämpfli, M. R. Disruption of pulmonary lipid homeostasis drives cigarette smoke-induced lung inflammation in mice. *Eur. Respir. J.* **46**, 1451–60 (2015).
54. Hogg, J. C. *et al.* The Nature of Small-Airway Obstruction in Chronic Obstructive Pulmonary Disease. *N. Engl. J. Med.* **350**, 2645–2653 (2004).
55. Rutgers, S. R. *et al.* Ongoing airway inflammation in patients with COPD who do not currently smoke. *Thorax* **55**, 12–18 (2000).
56. Turato, G. *et al.* Effect of Smoking Cessation on Airway Inflammation in Chronic Bronchitis. *Am J Respir Crit Care Med.* **152**, 1262–1267 (1995).
57. Wilson, A. M. *et al.* Lipid and smoker's inclusions in sputum macrophages in patients with airway diseases. *Respir. Med.* **105**, 1691–1695 (2011).
58. Berenson, C. S. S., Garlipp, M. A. A., Grove, L. J. J., Maloney, J. & Sethi, S. Impaired Phagocytosis of Nontypeable *Haemophilus influenzae* by Human Alveolar Macrophages in Chronic Obstructive Pulmonary Disease. *J. Infect. Dis.* **194**, 1375–1384 (2006).
59. Hodge, S. *et al.* Smoking Alters Alveolar Macrophage Recognition and Phagocytic Ability Implications in Chronic Obstructive Pulmonary Disease. *Am J Respir Cell Mol Biol* **37**, 748–755 (2007).
60. Chen, H., Cowan, M. J., Hasday, J. D., Vogel, S. N. & Medvedev, A. E. Tobacco Smoking Inhibits Expression of Proinflammatory Cytokines and Activation of IL-1R-Associated Kinase, p38, and NF-κB in Alveolar Macrophages Stimulated with TLR2 and TLR4 Agonists. *J. Immunol.* **179**, 6097–6106 (2007).
61. Gaschler, G. J. *et al.* Cigarette smoke exposure attenuates cytokine production by mouse alveolar macrophages. *Am. J. Respir. Cell Mol. Biol.* **38**, 218–226 (2008).
62. Botelho, F. M. *et al.* IL-1α/IL-1R1 expression in chronic obstructive pulmonary disease and mechanistic relevance to smoke-induced neutrophilia in mice. *PLoS One* **6**, e28457 (2011).
63. Russell, R. E. K. *et al.* Alveolar macrophage-mediated elastolysis : roles of matrix metalloproteinases , cysteine , and serine proteases. *Am J*

Physiol Lung Cell Mol Physiol **283**, 867–873 (2002).
64. Pauwels, N. S. *et al.* Role of IL-1 a and the Nlrp3/caspase-1/IL-1 b axis in cigarette smoke-induced pulmonary inflammation and COPD. *Eur. Respir. J.* **38**, 1019–1028 (2011).
65. Xiong, Z., Leme, A. S., Ray, P., Shapiro, S. D. & Lee, J. S. CX3CR1+ Lung Mononuclear Phagocytes Spatially Confined to the Interstitium Produce TNF- and IL-6 and Promote Cigarette Smoke-Induced Emphysema. *J. Immunol.* **186**, 3206–3214 (2011).
66. Finkelstein, R., Fraser, R. S., Ghezzo, H. & Cosio, M. G. Alveolar inflammation and its relation to emphysema in smokers. *Am. J. Respir. Crit. Care Med.* **152**, 1666–1672 (1995).
67. Culpitt, S. V *et al.* Impaired Inhibition by Dexamethasone of Cytokine Release by Alveolar Macrophages from Patients with Chronic Obstructive Pulmonary Disease. *Am J Respir Crit Care Med.* **167**, 24–37 (2003).
68. Vermaelen, B. K. Y., Carro-muino, I., Lambrecht, B. N. & Pauwels, R. A. Specific Migratory Dendritic Cells Rapidly Transport Antigen from the Airways to the Thoracic Lymph Nodes. *J Exp Med* **193**, 51–60 (2001).
69. Vermaelen, K. & Pauwels, R. Accelerated Airway Dendritic Cell Maturation, Trafficking, and Elimination in a Mouse Model of Asthma. *Am. J. Respir. Cell Mol. Biol* **29**, 405–409 (2003).
70. Hildner, K. *et al.* Batf3 deficiency reveals a critical role for CD8alpha+ dendritic cells in cytotoxic T cell immunity. *Science* **322**, 1097–100 (2008).
71. Schlitzer, A. *et al.* Identification of cDC1- and cDC2-committed DC progenitors reveals early lineage priming at the common DC progenitor stage in the bone marrow. *Nat. Immunol.* **16**, 718–728 (2015).
72. Khare, A. *et al.* Cutting Edge: Inhaled Antigen Upregulates Retinaldehyde Dehydrogenase in Lung Cells To Induce Foxp3 De Novo in CD4 + T CD103+ but Not Plasmacytoid Dendritic of Cells and Promote Airway Tolerance. *J Immunol* (2013) doi:10.4049/jimmunol.1300193.
73. Luckheeram, R. V., Zhou, R., Verma, A. D. & Xia, B. CD4 + T Cells : Differentiation and Functions. *Clin. Dev. Immunol.* (2012) doi:10.1155/2012/925135.
74. Lloyd, C. M. & Snelgrove, R. J. Type 2 immunity : Expanding our view. *Sci. Immunol.* **3**, 1–12 (2018).
75. Patel, D. D. & Kuchroo, V. K. Review Th17 Cell Pathway in Human Immunity : Lessons from Genetics and Therapeutic Interventions. *Immunity* **43**, 1040–1051 (2015).
76. Hoffmann, F. M. *et al.* Distribution and interaction of murine pulmonary phagocytes in the naive and allergic lung. *Front. Immunol.* **9**, 1–15 (2018).
77. Leon, B. & Ardavin, C. Monocyte-derived dendritic cells in innate and adaptive immunity. *Immunol. Cell Biol.* **86**, 320–324 (2008).
78. Domingez, P. M. & Ardavin, C. Differentiation and function of mouse monocyte-derived dendritic cells in steady state and inflammation.

Immunol. Rev. **234**, 90–104 (2010).
79. Plantinga, M. *et al.* Article Cells Initiate and Maintain T Helper 2 Cell-Mediated Immunity to House Dust Mite Allergen. *Immunity* **38**, 322–335 (2011).
80. Asselin-paturel, C. *et al.* Mouse type I IFN-producing cells are immature APCs with plasmacytoid morphology. *Nat. Immunol.* **2**, 1144–1160 (2001).
81. Botelho, F. M. *et al.* Innate immune processes are sufficient for driving cigarette smoke-induced inflammation in mice. *Am. J. Respir. Cell Mol. Biol.* **42**, 394–403 (2010).
82. Botelho, F. M. *et al.* Cigarette smoke-induced accumulation of lung dendritic cells is interleukin-1α-dependent in mice. *Respir. Res.* **13**, 81 (2012).
83. Robbins, C. S. *et al.* Cigarette Smoke Decreases Pulmonary Dendritic Cells and Impacts Antiviral Immune Responsiveness. *Am. J. Respir. Cell Mol. Biol.* **30**, 202–211 (2004).
84. Brüggemann, T. R. *et al.* Cigarette smoke increases CD8α+ dendritic cells in an ovalbumin-induced airway inflammation. *Front. Immunol.* **8**, (2017).
85. Dendritic, C. D., Tsoumakidou, M. & Koutsopoulos, A. V. Decreased Small Airway and Alveolar CD83ɦ Dendritic Cells in COPD. *Chest* **136**, 726–733 (2009).
86. Liao, S. X. *et al.* Cigarette smoke affects dendritic cell maturation in the small airways of patients with chronic obstructive pulmonary disease. *Mol. Med. Rep.* **11**, 219–225 (2015).
87. Le Rouzic, O. *et al.* Cigarette smoke alters the ability of human dendritic cells to promote anti-Streptococcus pneumoniae Th17 response. *Respir. Res.* **17**, 1 (2016).
88. Pedersen, K. M. *et al.* Smoking and Increased White and Red Blood Cells: A Mendelian Randomization Approach in the Copenhagen General Population Study. *Arterioscler. Thromb. Vasc. Biol.* **39**, 965–977 (2019).
89. Vermaelen, K. Y., Brusselle, G. G., Joos, G. F. & Pauwels, R. A. Time course of cigarette smoke-induced pulmonary inflammation in mice. *Eur. Respir. J.* **26**, 204–213 (2005).
90. Mortaz, E. *et al.* Cigarette smoke induces CXCL8 production by human neutrophils via activation of TLR9 receptor. *Eur. Respir. J.* **36**, 1143–1154 (2010).
91. Lee, K. H. *et al.* Cigarette smoke extract enhances neutrophil elastase-induced IL-8 production via proteinase-activated receptor-2 upregulation in human bronchial epithelial cells. *Exp. Mol. Med.* **50**, 1–9 (2018).
92. Shapiro, S. D. *et al.* Neutrophil Elastase Contributes to Cigarette Smoke-Induced Emphysema in Mice. *Am. J. Pathol.* **163**, 2329–2335 (2003).
93. McCarthy, C., Reeves, E. P. & McElvaney, N. G. The role of neutrophils in Alpha-1 antitrypsin deficiency. *Ann. Am. Thorac. Soc.* **13**, S297–S304 (2016).
94. Brinkmann, V. *et al.* Neutrophil Extracellular Traps Kill Bacteria.

Science (80-.). **303**, 1532–1535 (2004).
95. Qiu, S.-L. *et al.* Neutrophil extracellular traps induced by cigarette smoke activate plasmacytoid dendritic cells. *Thorax* **0**, 1–10 (2017).
96. Grabcanovic-Musija, F. *et al.* Neutrophil extracellular trap (NET) formation characterises stable and exacerbated COPD and correlates with airflow limitation. *Respir. Res.* **16**, 59 (2015).
97. Zhang, Y., Geng, S., Prasad, G. L. & Li, L. Suppression of neutrophil antimicrobial functions by total particulate matter from cigarette smoke. *Front. Immunol.* **9**, 1–9 (2018).
98. Xu, M. *et al.* The influence of nicotine on granulocytic differentiation - Inhibition of the oxidative burst and bacterial killing and increased matrix metalloproteinase-9 release. *BMC Cell Biol.* **9**, 1–14 (2008).
99. Kumar, B. V., Connors, T. J. & Farber, D. L. Human T Cell Development, Localization, and Function throughout Life. *Immunity* **48**, 202–213 (2018).
100. Cederbom, L., Hall, H. & Ivars, F. Stimulatory Molecules on Antigen-Presenting Cells. *Cell* 1538–1543 (2000).
101. Kaech, S. M. & Cui, W. Transcriptional control of effector and memory CD8+ T cell differentiation. *Nat. Rev. Immunol.* **12**, 749–761 (2012).
102. Nurieva, R. I. & Chung, Y. Understanding the development and function of T follicular helper cells. *Cell. Mol. Immunol.* **7**, 190–197 (2010).
103. Zavitz, C. C. J. *et al.* Impact of cigarette smoke on T and B cell responsiveness. *Cell. Immunol.* **253**, 38–44 (2008).
104. Kalra, R., Singh, S. P., Savage, S. M., Finch, G. L. & Sopori, M. L. Effects of cigarette smoke on immune response: Chronic exposure to cigarette smoke impairs antigen-mediated signaling in T cells and depletes IP3-sensitive Ca2+ stores. *J. Pharmacol. Exp. Ther.* **293**, 166–171 (2000).
105. Tan, D. B. A. *et al.* Impaired function of regulatory T-cells in patients with chronic obstructive pulmonary disease (COPD). *Immunobiology* **219**, 975–979 (2014).
106. Li, X.-N., Pan, X. & Qiu, D. Imbalances of Th17 and Treg cells and their respective cytokines in COPD patients by disease stage. *Int. J. Clin. Exp. Med.* **7**, 5324–9 (2014).
107. Barceló, B. *et al.* Phenotypic characterisation of T-lymphocytes in COPD: Abnormal CD4+CD25+ regulatory T-lymphocyte response to tobacco smoking. *Eur. Respir. J.* **31**, 555–562 (2008).
108. McKendry, R. T. *et al.* Dysregulation of antiviral function of CD8 T cells in the chronic obstructive pulmonary disease lung role of the PD-1-PD-L1 axis. *Am. J. Respir. Crit. Care Med.* **193**, 642–651 (2016).
109. Freeman, C. M. *et al.* Cytotoxic potential of lung CD8(+) T cells increases with chronic obstructive pulmonary disease severity and with in vitro stimulation by IL-18 or IL-15. *J. Immunol.* **184**, 6504–13 (2010).
110. Korn, S. *et al.* Characterization of the interstitial lung and peripheral blood T cell receptor repertoire in cigarette smokers. *Am. J. Respir. Cell Mol. Biol.* **32**, 142–148 (2005).
111. Freeman, C. M. *et al.* Lung CD8+ T cells in COPD have increased expression of bacterial TLRs. *Respir Res* **14**, 13 (2013).

112. Feng, Y. *et al.* Exposure to cigarette smoke inhibits the pulmonary T-cell response to influenza virus and mycobacterium tuberculosis. *Infect. Immun.* **79**, 229–237 (2011).
113. Kerdidani, D. *et al.* Cigarette Smoke-Induced Emphysema Exhausts Early Cytotoxic CD8+ T Cell Responses against Nascent Lung Cancer Cells. *J. Immunol.* ji1700700 (2018) doi:10.4049/jimmunol.1700700.
114. Biton, J. *et al.* Impaired Tumor-infiltrating T Cells in Patients with COPD Impacts Lung Cancer Response to PD-1 Blockade. *Am. J. Respir. Crit. Care Med.* **198**, rccm.201706-1110OC (2018).
115. Pieper, K., Grimbacher, B. & Eibel, H. B-cell biology and development. *J. Allergy Clin. Immunol.* **131**, 959–971 (2013).
116. Kurosaki, T., Kometani, K. & Ise, W. Memory B cells. *Nat. Rev. Immunol.* **15**, 149–159 (2015).
117. Montecino-Rodriguez, E. & Dorshkind, K. B-1 B Cell Development in the Fetus and Adult. *Immunity* **36**, 13–23 (2012).
118. Weber, G. F. *et al.* Pleural innate response activator B cells protect against pneumonia via a GM-CSF-IgM axis. *J. Exp. Med.* **211**, 1243–1256 (2014).
119. Holodick, N. E., Tumang, J. R. & Rothstein, T. L. Continual signaling is responsible for constitutive ERK phosphorylation in B-1a cells. *Mol. Immunol.* **46**, 3029–3036 (2009).
120. Kantor, A. B., Merrill, C. E., Herzenberg, L. A. & Hillson, J. L. An unbiased analysis of V(H)-D-J(H) sequences from B-1a, B-1b, and conventional B cells. *J. Immunol.* **158**, 1175–86 (1997).
121. Grönwalla, C. *et al.* IgM autoantibodies to distinct apoptosis-associated antigens correlate with protection from cardiovascular events and renal disease in patients with SLEblic Access. *Clin Immunol* **142**, 390–398 (2012).
122. Nagele, E. P. *et al.* Natural IgG Autoantibodies Are Abundant and Ubiquitous in Human Sera, and Their Number Is Influenced By Age, Gender, and Disease. *PLoS One* **8**, (2013).
123. Haas, K. M., Poe, J. C., Steeber, D. A. & Tedder, T. F. B-1a and B-1b cells exhibit distinct developmental requirements and have unique functional roles in innate and adaptive immunity to S. pneumoniae. *Immunity* **23**, 7–18 (2005).
124. Ochsenbein, A. F. *et al.* Control of Early Viral and Bacterial Distribution and Disease by Natural Antibodies. *Science (80-.).* **286**, 2156–2159 (1999).
125. Zhou, Z.-H. *et al.* The Broad Antibacterial Activity of the Natural Antibody Repertoire is due to Polyreactive Antibodies. *Cell Host Microbe* **15**, 5161 (2007).
126. Baumgarth, N. *et al.* B-1 and B-2 cell-derived immunoglobulin M antibodies are nonredundant components of the protective response to influenza virus infection. *J Exp Med* **192**, 271–280 (2000).
127. Elkon, K. & Casali, P. Nature and Functions of Autoantibodies. *Nat Clin Pr. Rheumatol* **4**, 491–498 (2008).
128. Grönwall C., Vas J., and S. G. J. Protective roles of natural IgM antibodies. *Front. Immunol.* **3**, 1–10 (2012).

129. Schroeder, H. W. & Cavacini, L. Structure and function of immunoglobulins. *J. Allergy Clin. Immunol.* **125**, S41-52 (2010).
130. Brandtzaeg, P. Role of secretory antibodies in the defence against infections. *Int. J. Med. Microbiol.* **293**, 3–15 (2003).
131. Wang, W., Erbe, A. K., Hank, J. A., Morris, Z. S. & Sondel, P. M. NK Cell-Mediated Antibody-Dependent Cellular Cytotoxicity in Cancer Immunotherapy. *Front. Immunol.* **6**, 368 (2015).
132. Nash, J. T. *et al.* Immune complex processing in C1q-deficient mice. *Clin. Exp. Immunol.* **123**, 196–202 (2001).
133. Chen, K. *et al.* Immunoglobulin D enhances immune surveillance by activating antimicrobial, proinflammatory and B cell-stimulating programs in basophils. *Nat. Immunol.* **10**, 889–98 (2009).
134. Brandsma, C.-A. A. *et al.* Increased levels of (class switched) memory B cells in peripheral blood of current smokers. *Respir. Res.* **10**, 1–11 (2009).
135. Bracke, K. R. *et al.* Role of CXCL13 in cigarette smoke-induced lymphoid follicle formation and chronic obstructive pulmonary disease. *Am. J. Respir. Crit. Care Med.* **188**, 343–355 (2013).
136. Morissette, M. C. *et al.* Role of BAFF in pulmonary autoantibody responses induced by chronic cigarette smoke exposure in mice. *Physiol. Rep.* **4**, 1–11 (2016).
137. Wolfe, W. H., Miner, J. C. & Michalek, J. E. Immunological parameters in current and former US Air Force personnel. *Vaccine* **11**, 545–547 (1993).
138. Mili, F., Flanders, W. D., Boring, J. R., Annest, J. L. & Destefano, F. The associations of race, cigarette smoking, and smoking cessation to measures of the immune system in middle-aged men. *Clin. Immunol. Immunopathol.* **59**, 187–200 (1991).
139. McMillan, S. A., Douglas, J. P., Archbold, G. P., McCrum, E. E. & Evans, A. E. Effect of low to moderate levels of smoking and alcohol consumption on serum immunoglobulin concentrations. *J. Clin. Pathol.* **50**, 819–22 (1997).
140. Qvarfordt, I., Riise, G. C., Andersson, B. A. & Larsson, S. IgG subclasses in smokers with chronic bronchitis and recurrent exacerbations. *Thorax* **56**, 445–449 (2001).
141. Norhagen Engström, G. & Engström, P. E. Effects of tobacco smoking on salivary immunoglobulin levels in immunodeficiency. *Eur. J. Oral Sci.* **106**, 986–91 (1998).
142. Kärkkäinen, M. *et al.* Effect of smoking and comorbidities on survival in idiopathic pulmonary fibrosis. *Respir. Res.* **18**, 1–10 (2017).
143. Hill, K. *et al.* Prevalence and underdiagnosis of chronic obstructive pulmonary disease among patients at risk in primary care. *CMAJ* **182**, 673–8 (2010).
144. World Health Organization. Chronic Obstructive Pulmonary Disease (COPD) Fact Sheet. *WHO* https://www.who.int/news-room/fact-sheets/detail/chronic-obstructive-pulmonary-disease-(copd) (2017).
145. Global Burden of Disease (GBD) 2017 Causes of Death Collaborators. Global, regional, and national age-sex-specific mortality for 282 causes of death in 195 countries and territories, 1980–2017: a systematic

analysis for the Global Burden of Disease Study 2017. *Lancet* **392**, 1736–1788 (2018).
146. Hogg, J. C. Pathophysiology of airflow limitation in chronic obstructive pulmonary disease. *Lancet* **364**, 709–721 (2004).
147. Castaldi, P. J. *et al.* Do COPD subtypes really exist? COPD heterogeneity and clustering in 10 independent cohorts. *Thorax* **0**, 1–9 (2017).
148. Agusti, A. & Faner, R. Lung function trajectories in health and disease. *Lancet Respir. Med.* **7**, 358–364 (2019).
149. Global Initiative for Chronic Obstructive Lung Disease. GOLD Report 2020. *Glob. Initiat. Chronic Obstr. Lung Dis.* 141 (2020).
150. Brode, S. K., Ling, S. C. & Chapman, K. R. Alpha-1 antitrypsin deficiency: A commonly overlooked cause of lung disease. *Cmaj* **184**, 1365–1371 (2012).
151. Silverman, E. K., Ph, D., Sandhaus, R. A. & Ph, D. Alpha 1 -Antitrypsin Deficiency. *N. Engl. J. Med.* **360**, 2749–2757 (2009).
152. Stern, D. A., Morgan, W. J., Wright, A. L., Guerra, S. & Martinez, F. D. Poor airway function in early infancy and lung function by age 22 years: a non-selective longitudinal cohort study. *Lancet* **370**, 758–764 (2007).
153. Barker, D. J. P. *et al.* Relation of birth weight and childhood respiratory infection to adult lung function and death from chronic obstructive airways disease. *Br. Med. J.* **303**, 671–675 (1991).
154. Kohansal, R. *et al.* The natural history of chronic airflow obstruction revisited: An analysis of the Framingham Offspring Cohort. *Am. J. Respir. Crit. Care Med.* **180**, 3–10 (2009).
155. Barnes, P. J. Mediators of chronic obstructive pulmonary disease. *Pharmacol. Rev.* **56**, 515–48 (2004).
156. O'Shaughnessy, T. C., Ansari, T. W., Barnes, N. C. & Jeffery, P. K. Inflammation in bronchial biopsies of subjects with chronic bronchitis: Inverse relationship of CD8+ T lymphocytes with FEV1. *Am. J. Respir. Crit. Care Med.* **155**, 852–857 (1997).
157. Saetta, M. *et al.* CD8 +ve Cells in the Lungs of Smokers with. *Am. J. Crit. Care Med.* **160**, 711–717 (1999).
158. Willemse, B. W. M., Postma, D. S., Timens, W. & Hacken, N. H. T. The impact of smoking cessation on respiratory symptoms , lung function , airway hyperresponsiveness and inflammation. *Eur. Respir. J.* **23**, 464–476 (2004).
159. Godtfredsen, N. S. *et al.* COPD-related morbidity and mortality after smoking cessation: status of the evidence. *Eur. Respir. J.* **32**, 844–853 (2008).
160. Lapperre, T. S. *et al.* Relation between duration of smoking cessation and bronchial inflammation in COPD. *Thorax* **61**, 115–121 (2006).
161. Polverino, F. *et al.* B cell-activating factor an orchestrator of lymphoid follicles in severe chronic obstructive pulmonary disease. *Am. J. Respir. Crit. Care Med.* **192**, 695–705 (2015).
162. van der Strate, B. W. A. *et al.* Cigarette Smoke–induced Emphysema. *Am. J. Respir. Crit. Care Med.* **173**, 751–758 (2006).
163. Faner, R. *et al.* Network analysis of lung transcriptomics reveals a distinct b-cell signature in emphysema. *Am. J. Respir. Crit. Care Med.* **193**,

1242–1253 (2016).
164. Stämpfli, M. R. & Anderson, G. P. How cigarette smoke skews immune responses to promote infection, lung disease and cancer. *Nat. Rev. Immunol.* **9**, 377–384 (2009).
165. Yip, N. H. *et al.* Immunoglobulin G levels before and after lung transplantation. *Am. J. Respir. Crit. Care Med.* **173**, 917–921 (2006).
166. Pilette, C. *et al.* Reduced epithelial expression of secretory component in small airways correlates with airflow obstruction in chronic obstructive pulmonary disease. *Am. J. Respir. Crit. Care Med.* **163**, 185–194 (2001).
167. Polosukhin, V. V. *et al.* Bronchial secretory immunoglobulin a deficiency correlates with airway inflammation and progression of chronic obstructive pulmonary disease. *Am. J. Respir. Crit. Care Med.* **184**, 317–327 (2011).
168. Polosukhin, V. V. *et al.* Secretory IgA Deficiency in Individual Small Airways Is Associated with Persistent Inflammation and Remodeling. *Am. J. Respir. Crit. Care Med.* **195**, 1010–1021 (2017).
169. Richmond, B. W. *et al.* Monocyte-derived dendritic cells link localized secretory IgA deficiency to adaptive immune activation in COPD. *Mucosal Immunol.* **14**, 431–442 (2021).
170. Kaetzel, C. S. The polymeric immunoglobulin receptor: Bridging innate and adaptive immune responses at mucosal surfaces. *Immunol. Rev.* **206**, 83–99 (2005).
171. Richmond, B. W. *et al.* Airway bacteria drive a progressive COPD-like phenotype in mice with polymeric immunoglobulin receptor deficiency. *Nat. Commun.* **7**, 11240 (2016).
172. McCullagh, B. N. *et al.* Antibody deficiency in patients with frequent exacerbations of Chronic Obstructive Pulmonary Disease (COPD). *PLoS One* **12**, 1–13 (2017).
173. Cowan, J. *et al.* A retrospective longitudinal within-subject risk interval analysis of immunoglobulin treatment for recurrent acute exacerbation of chronic obstructive pulmonary disease. *PLoS One* **10**, 1–12 (2015).
174. Burge, S. & Wedzicha, J. A. COPD exacerbations: definitions and classifications. *Eur. Respir. J. Suppl.* **41**, 46s-53s (2003).
175. Donaldson, G. C. *et al.* Longitudinal changes in the nature, severity and frequency of COPD exacerbations. *Eur. Respir. J.* **22**, 931–936 (2003).
176. Donaldson, G. C., Seemungal, T. A. R., Bhowmik, A. & Wedzicha, J. A. Relationship between exacerbation frequency and lung function decline in chronic obstructive pulmonary disease. *Thorax* **57**, 847–52 (2002).
177. Steer, J., Gibson, G. J. & Bourke, S. C. Longitudinal change in quality of life following hospitalisation for acute exacerbations of COPD. *BMJ Open Respir. Res.* **2**, 1–8 (2015).
178. Costenbader, K. H. & Karlson, E. W. Cigarette smoking and autoimmune disease: what can we learn from epidemiology? *Lupus* **15**, 737–45 (2006).
179. Agusti, A., MacNee, W., Donaldson, K. & Cosio, M. Hypothesis: Does COPD have an Autoimmune Component? *Thorax* **58**, 829 (2003).
180. Feghali-Bostwick, C. A. *et al.* Autoantibodies in Patients with Chronic Obstructive Pulmonary Disease. *Am. J. Respir. Crit. Care Med.* **177**,

156–63 (2008).
181. Núñez, B. *et al.* Anti-tissue Antibodies are Related to Lung Function in Chronic Obstructive Pulmonary Disease. *Am. J. Respir. Crit. Care Med.* **183**, 1025–1031 (2011).
182. Bonarius, H. P. J. *et al.* Antinuclear Autoantibodies are more Prevalent in COPD in Association with Low Body Mass Index but not with Smoking History. *Thorax* **66**, 101–7 (2011).
183. Daffa, N. I., Tighe, P. J., Corne, J. M., Fairclough, L. C. & Todd, I. Natural and disease-specific autoantibodies in chronic obstructive pulmonary disease. *Clin. Exp. Immunol.* **180**, 155–163 (2015).
184. Shindi, R. *et al.* Autoantibodies of IgM and IgG classes show differences in recognition of multiple autoantigens in chronic obstructive pulmonary disease. *Clin. Immunol.* **183**, 344–353 (2017).
185. Ma, A. *et al.* Serum levels of autoantibodies against extracellular antigens and neutrophil granule proteins increase in patients with COPD compared to non-COPD smokers. *Int. J. COPD* **15**, 189–200 (2020).
186. Packard, T. A., Li, Q. Z., Cosgrove, G. P., Bowler, R. P. & Cambier, J. C. COPD is associated with production of autoantibodies to a broad spectrum of self-antigens, correlative with disease phenotype. *Immunol. Res.* **55**, 48–57 (2013).
187. Leidinger, P. *et al.* Novel autoantigens immunogenic in COPD patients. *Respir. Res.* **10**, 1–7 (2009).
188. Brandsma, C. A. *et al.* The search for autoantibodies against elastin, collagen and decorin in COPD. *Eur. Respir. J.* **37**, 1288–1289 (2011).
189. Lee, S.-H. *et al.* Antielastin autoimmunity in tobacco smoking-induced emphysema. *Nat. Med.* **13**, 567–569 (2007).
190. Rinaldi, M. *et al.* Antielastin B-cell and T-cell immunity in patients with chronic obstructive pulmonary disease. *Thorax* **67**, 694–700 (2012).
191. Peng, Y., Kowalewski, R., Kim, S. & Elkon, K. B. The role of IgM antibodies in the recognition and clearance of apoptotic cells. *Mol. Immunol.* **42**, 781–787 (2005).
192. Quartier, P., Potter, P. K., Ehrenstein, M. R., Walport, M. J. & Botto, M. Predominant role of IgM-dependent activation of the classical pathway in the clearance of dying cells by murine bone marrow-derived macrophages in vitro. *Eur. J. Immunol.* **35**, 252–260 (2005).
193. Comer, D. M., Kidney, J. C., Ennis, M. & Elborn, J. S. Airway epithelial cell apoptosis and inflammation in COPD, smokers and nonsmokers. *Eur. Respir. J.* **41**, 1058–67 (2013).
194. Murray, L. A. *et al.* Acute cigarette smoke exposure activates apoptotic and inflammatory programs but a second stimulus is required to induce epithelial to mesenchymal transition in COPD epithelium. *Respir. Res.* **18**, 1–12 (2017).
195. Rajan, T. V. The Gell-Coombs classification of hypersensitivity reactions: A re-interpretation. *Trends Immunol.* **24**, 376–379 (2003).
196. Nauta, A. J. *et al.* Opsonization with C1q and mannose-binding lectin targets apoptotic cells to dendritic cells. *J. Immunol.* **173**, 3044–50 (2004).
197. Mevorach, D., Mascarenhas, J. O., Gershov, D. & Elkon, K. B.

Complement-dependent clearance of apoptotic cells by human macrophages. *J. Exp. Med.* **188**, 2313–20 (1998).
198. Semple, J. W. & Freedman, J. Autoimmune pathogenesis and autoimmune hemolytic anemia. *Semin. Hematol.* **42**, 122–130 (2005).
199. Schifferli, J. A., Ng, Y. C. & Peters, and D. K. The Role of Complement and its Receptor in the Elimination of Immune Complexes. *N. Engl. J. Med.* **315**, 488–495 (1986).
200. Kenyon, K. D. *et al.* IgG Autoantibodies against Deposited C3 Inhibit Macrophage-Mediated Apoptotic Cell Engulfment in Systemic Autoimmunity. *J. Immunol.* **187**, 2101–2111 (2011).
201. Chen, Y., Park, Y.-B., Patel, E. & Silverman, G. J. IgM Antibodies to Apoptosis-Associated Determinants Recruit C1q and Enhance Dendritic Cell Phagocytosis of Apoptotic Cells. *J. Immunol.* **182**, 6031–6043 (2009).
202. Wandstrat, A. E. *et al.* Autoantibody profiling to identify individuals at risk for systemic lupus erythematosus. *J. Autoimmun.* **27**, 153–160 (2006).
203. Li, Q.-Z. *et al.* Risk factors for ANA positivity in healthy persons. *Arthritis Res. Ther.* **13**, R38 (2011).
204. Baumgarth, N. The double life of a B-1 cell: self-reactivity selects for protective effector functions. *Nat. Rev. Immunol.* **11**, 34–46 (2011).
205. Poon, I. K. H., Lucas, C. D., Rossi, A. G. & Ravichandran, K. S. Apoptotic cell clearance: basic biology and therapeutic potential. *Nat. Rev. Immunol.* **14**, 166–80 (2014).
206. Ryu, J. H., Colby, T. V., Hartman, T. E. & Vassallo, R. Smoking-related interstitial lung diseases: A concise review. *Eur. Respir. J.* **17**, 122–132 (2001).
207. Lederer, D. J. & Martinez, F. J. Idiopathic pulmonary fibrosis. *New Englanc J. Med.* **29**, 1811–23 (2018).
208. Kalchiem-Dekel, O., Galvin, J., Burke, A., Atamas, S. & Todd, N. Interstitial Lung Disease and Pulmonary Fibrosis: A Practical Approach for General Medicine Physicians with Focus on the Medical History. *J. Clin. Med.* **7**, 476 (2018).
209. Davidson, R. Idopathic Pulonary Fibrosis; Patient Information Guide. *The Canadian Pulmonary Fibrosis Foundation* 19 (2016).
210. Selman, M. & Pardo, A. The leading role of epithelial cells in the pathogenesis of idiopathic pulmonary fibrosis. *Cell. Signal.* **66**, 109482 (2020).
211. Henson, P. M. *et al.* Deletion of c-FLIP from CD11b high Macrophages Prevents Development of Bleomycin-induced Lung Fibrosis. *Am. J. Respir. Cell Mol. Biol.* **58**, 66–78 (2018).
212. Reyfman, P. A. *et al.* Single-cell transcriptomic analysis of human lung provides insights into the pathobiology of pulmonary fibrosis. *Am. J. Respir. Crit. Care Med.* **199**, 1517–1536 (2019).
213. Wang, Y. *et al.* Overexpression of TIM-3 in macrophages aggravates pathogenesis of pulmonary fibrosis in mice. *Am. J. Respir. Cell Mol. Biol.* **61**, 727–736 (2019).
214. Sugimoto, N. *et al.* IL-9 blockade suppresses silica-induced lung

inflammation and fibrosis in mice. *Am. J. Respir. Cell Mol. Biol.* **60**, 232–243 (2019).
215. Fernandez, I. E. & Eickelberg, O. The impact of TGF-β on lung fibrosis: From targeting to biomarkers. *Proc. Am. Thorac. Soc.* **9**, 111–116 (2012).
216. Ard, S. *et al.* Sustained Smad2 Phosphorylation Is Required for Myofibroblast Transformation in Response to TGF-b To. *Am. J. Respir. Cell Mol. Biol.* **60**, 367–369 (2019).
217. Prasse, A. *et al.* A vicious circle of alveolar macrophages and fibroblasts perpetuates pulmonary fibrosis via CCL18. *Am. J. Respir. Crit. Care Med.* **173**, 781–792 (2006).
218. King, T. E., Tooze, J. A., Schwarz, M. I., Brown, K. R. & Cherniack, R. M. Predicting Survival in Idiopathic Pulmonary Fibrosis Scoring System and Survival Model. *Am. J. Respir. Crit. Care Med.* **164**, 1171–1181 (2001).
219. Kishaba, T., Nagano, H., Nei, Y. & Yamashiro, S. Clinical characteristics of idiopathic pulmonary fibrosis patients according to their smoking status. *J. Thorac. Dis.* **8**, 1112–1120 (2016).
220. Antoniou, K. M. *et al.* Idiopathic pulmonary fibrosis: Outcome in relation to smoking status. *Am. J. Respir. Crit. Care Med.* **177**, 190–194 (2008).
221. Baumgartner, K. B., Samet, J. M., Stidley, C. A., Colby, T. V & Waldron, J. A. Cigarette Smoking: A Risk Fador for Idiopathic Pulmonary Fibrosis. *Am. J. Crit. Care Med.* **155**, 242–248 (1997).
222. Allden, S. J. *et al.* The Transferrin Receptor CD71 Delineates Functionally Distinct Airway Macrophage Subsets during Idiopathic Pulmonary Fibrosis. *Am. J. Respir. Crit. Care Med.* **200**, 209–219 (2019).
223. Ayaub, E. A. *et al.* Overexpression of OSM and IL-6 impacts the polarization of pro- fibrotic macrophages and the development of bleomycin-induced lung fibrosis. *Sci. Rep.* **7**, 1–16 (2017).
224. Ji, W. J. *et al.* Temporal and spatial characterization of mononuclear phagocytes in circulating, lung alveolar and interstitial compartments in a mouse model of bleomycin-induced pulmonary injury. *J. Immunol. Methods* **403**, 7–16 (2014).
225. Gibbons, M. A. *et al.* Ly6C hi monocytes direct alternatively activated profibrotic macrophage regulation of lung fibrosis. *Am. J. Respir. Crit. Care Med.* **184**, 569–581 (2011).
226. Renegar, K. B., Small, P. a, Boykins, L. G. & Wright, P. F. Role of IgA versus IgG in the control of influenza viral infection in the murine respiratory tract. *J. Immunol.* **173**, 1978–1986 (2004).
227. Tarbiah, N., Todd, I., Tighe, P. J. & Fairclough, L. C. Cigarette smoking differentially affects immunoglobulin class levels in serum and saliva: an investigation and review. *Basic Clin. Pharmacol. Toxicol.* **125**, 474–483 (2019).
228. Gonzalez-Quintela, A. *et al.* Serum levels of immunoglobulins (IgG, IgA, IgM) in a general adult population and their relationship with alcohol consumption, smoking and common metabolic abnormalities. *Clin. Exp. Immunol.* **151**, 42–50 (2008).
229. Pizzichini, E. *et al.* Indices of airway inflammation in induced sputum: Reproducibility and validity of cell and fluid-phase measurements. *Am.*

J. Respir. Crit. Care Med. **154**, 308–317 (1996).
230. Bafadhel, M. *et al.* Profiling of sputum inflammatory mediators in asthma and chronic obstructive pulmonary disease. *Respiration* **83**, 36–44 (2012).
231. Von Hertzen, L., Leinonen, M., Surcel, H. M., Karjalainen, J. & Saikku, P. Measurement of sputum antibodies in the diagnosis of acute and chronic respiratory infections associated with Chlamydia pneumoniae. *Clin. Diagn. Lab. Immunol.* **2**, 454–457 (1995).
232. Mukherjee, M. *et al.* Sputum autoantibodies in patients with severe eosinophilic asthma. *J. Allergy Clin. Immunol.* **141**, 1269–1279 (2018).
233. Mouthuy, J., Detry, B., Sohy, C., Pirson, F. & Pilette, C. Presence in sputum of functional dust mite-specific IgE antibodies in intrinsic asthma. *Am. J. Respir. Crit. Care Med.* **184**, 206–214 (2011).
234. Baumann, U., Göcke, K., Gewecke, B., Freihorst, J. & von Specht, B. U. Assessment of pulmonary antibodies with induced sputum and bronchoalveolar lavage induced by nasal vaccination against Pseudomonas aeruginosa: A clinical phase I/II study. *Respir. Res.* **8**, 1–10 (2007).
235. Puttur, F., Gregory, L. G. & Lloyd, C. M. Airway macrophages as the guardians of tissue repair in the lung. *Immunol. Cell Biol.* **97**, 246–257 (2019).
236. Hogg, J. C. & Pierce, R. A. Remodelling of peripheral lung tissue in COPD. *Eur. Respir. J.* **31**, (2008).
237. Pain, M. *et al.* Tissue remodelling in chronic bronchial diseases: from the epithelial to mesenchymal phenotype. *Eur. Respir. Rev.* **23**, 118–30 (2014).
238. Degryse, A. L. *et al.* Repetitive intratracheal bleomycin models several features of idiopathic pulmonary fibrosis. *Am. J. Physiol. - Lung Cell. Mol. Physiol.* **299**, 442–452 (2010).
239. Reinert, T., Baldotto, C. S. da R., Nunes, F. A. P. & Scheliga, A. A. de S. Bleomycin-Induced Lung Injury. *J. Cancer Res.* **2013**, 1–9 (2013).
240. Chaudhary, N. I., Schnapp, A. & Park, J. E. Pharmacologic differentiation of inflammation and fibrosis in the rat bleomycin model. *Am. J. Respir. Crit. Care Med.* **173**, 769–776 (2006).
241. Izbicki, G., Segel, M. J., Christensen, T. G., Conner, M. W. & Breuer, R. Time course of bleomycin-induced lung fibrosis. *Int. J. Exp. Pathol.* **83**, 111–119 (2002).
242. Chung, M. P. *et al.* Role of repeated lung injury and genetic background in bleomycin-induced fibrosis. *Am. J. Respir. Cell Mol. Biol.* **29**, 375–380 (2003).
243. Louis, R. *et al.* The effect of processing on inflammatory markers in induced sputum. *Eur. Respir. J.* **13**, 660–667 (1999).
244. Fried, A. J. & Bonilla, F. A. Pathogenesis, diagnosis, and management of primary antibody deficiencies and infections. *Clin. Microbiol. Rev.* **22**, 396–414 (2009).
245. Barnes, P. P. J. Alveolar Macrophages as Orchestrators of COPD. *COPD J. Chronic Obstr. Pulm. Dis.* **1**, 59–70 (2004).
246. A, S. T. Adhesion Receptors of the Immune System. *Nature* **346**, 425

(1990).
247. Lee, C. G. *et al.* Interleukin-13 Induces Tissue Fibrosis by Selectively Stimulating and Activating Transforming Growth Factor Beta 1. *J Exp Med* **194**, 809–821 (2001).
248. Agraval, H. & Yadav, U. C. S. MMP-2 and MMP-9 mediate cigarette smoke extract-induced epithelial-mesenchymal transition in airway epithelial cells via EGFR/Akt/GSK3β/β-catenin pathway: Amelioration by fisetin. *Chem. Biol. Interact.* **314**, (2019).
249. Lin, C. *et al.* Matrix metalloproteinase-9 cooperates with transcription factor Snail to induce epithelial – mesenchymal transition. *Cancer Sci.* **102**, 815–827 (2011).
250. Willis, B. C., Roland, M. & Borok, Z. Epithelial Origin of Myofibroblasts during Fibrosis in the Lung. *Proc Am Thorac Soc* **3**, 377–382 (2006).
251. Hong, R. & Gupta, S. Selective immunoglobulin M deficiency in an adult with Streptococcus pneumoniae sepsis and invasive aspergillosis. *J. Investig. Allergol. Clin. Immunol.* **18**, 214–218 (2008).
252. Gupta, S. & Gupta, A. Selective IgM deficiency-An underestimated primary immunodeficiency. *Front. Immunol.* **8**, 1–7 (2017).
253. Shen, P. *et al.* Streptococcus pneumoniae colonization is required to alter the nasal microbiota in cigarette smokeexposed mice. *Infect. Immun.* **85**, 1–14 (2017).
254. Cruz, T. *et al.* Multi-level immune response network in mild-moderate Chronic Obstructive Pulmonary Disease (COPD). *Respir. Res.* **20**, 1–9 (2019).
255. Arcavi, L. & Benowitz, N. L. Cigarette smoking and infection. *Arch. Intern. Med.* **164**, 2206–2216 (2004).
256. Takizawa, H. *et al.* Increased expression of transforming growth factor-β1 in small airway epithelium from tobacco smokers and patients with chronic obstructive pulmonary disease (COPD). *Am. J. Respir. Crit. Care Med.* **163**, 1476–1483 (2001).
257. Dullaers, M. *et al.* A T Cell-Dependent Mechanism for the Induction of Human Mucosal Homing Immunoglobulin A-Secreting Plasmablasts. *Immunity* **30**, 120–129 (2009).
258. Gohy, S. T. *et al.* Polymeric immunoglobulin receptor down-regulation in chronic obstructive pulmonary disease: Persistence in the cultured epithelium and role of transforming growth factor-β. *Am. J. Respir. Crit. Care Med.* **190**, 509–521 (2014).
259. Ladjemi, M. Z. *et al.* Increased IgA Expression in Lung Lymphoid Follicles in Severe COPD. *Am. J. Respir. Crit. Care Med.* **199**, 592–602 (2019).
260. Filho, F. S. L. *et al.* Serum IgG Levels and Risk of COPD Hospitalization: A Pooled Meta-Analysis. *Chest* **158**, 1420–1430 (2020).
261. Liang, Z. *et al.* Identification of clinically relevant subgroups of COPD based on airway and circulating autoantibody profiles. *Mol. Med. Rep.* **20**, 2882–2892 (2019).
262. Wickman, G., Julian, L. & Olson, M. F. How apoptotic cells aid in the removal of their own cold dead bodies. *Cell Death Differ.* **19**, 735–742 (2012).

263. Bouts, Y. M. *et al.* Apoptosis and NET formation in the pathogenesis of SLE. *Autoimmunity* **45**, 597–601 (2012).
264. Schaefer, L. Complexity of danger: The diverse nature of damage-associated molecular patterns. *J. Biol. Chem.* **289**, 35237–35245 (2014).
265. Darrah, E. & Andrade, F. NETs: the missing link between cell death and systemic autoimmune diseases? *Front. Immunol.* **3**, 428 (2012).
266. Zhang, Y., Zhang, J., Liu, Z., Liu, Y. & Tuo, S. A network-based approach to identify disease-associated gene modules through integrating DNA methylation and gene expression. *Biochem. Biophys. Res. Commun.* **465**, 437–442 (2015).
267. Wynn, T. A. & Vannella, K. M. Macrophages in Tissue Repair, Regeneration, and Fibrosis. *Immunity* **44**, 450–462 (2016).
268. Kisseleva, T. & Brenner, D. A. Mechanisms of fibrogenesis. *Exp. Biol. Med.* **233**, 109–122 (2008).
269. Filderman, A. E., Genovese, L. A. & Lazo, J. S. Alterations in pulmonary protective enzymes following systemic bleomycin treatment in mice. *Biochem. Pharmacol.* **37**, 1111–1116 (1988).
270. Filderman, A. E. & Lazo, J. S. Murine strain differences in pulmonary bleomycin metabolism. *Biochem. Pharmacol.* **42**, 195–198 (1991).
271. Silverstein, P. Smoking and wound healing. *Am. J. Med.* **93**, 22–24 (1992).
272. Murray, L. A. *et al.* Serum amyloid P therapeutically attenuates murine bleomycin-induced pulmonary fibrosis via its effects on macrophages. *PLoS One* **5**, 1–9 (2010).
273. Tomasek, J. J., Gabbiani, G., Hinz, B., Chaponnier, C. & Brown, R. A. Myofibroblasts and mechano: Regulation of connective tissue remodelling. *Nat. Rev. Mol. Cell Biol.* **3**, 349–363 (2002).
274. Lemjabbar, H. *et al.* Overexpression of Alveolar Macrophage Gelatinase B (MMP-9) in Patients with Idiopathic Pulmonary Fibrosis Effects of Steroid and Immunosuppressive Treatment. *Am J Respir Cell Mol Biol* **20**, 903–913 (1999).
275. Kui Tan, T. *et al.* Matrix metalloproteinase-9 of tubular and macrophage origin contributes to the pathogenesis of renal fibrosis via macrophage recruitment through osteopontin cleavage. *Lab. Investig.* **93**, 434–449 (2013).
276. Whitacre, C. C. Sex differences in autoimmune disease. *Nat. Immunol.* **2**, 777–780 (2001).
277. Wang, Z. *et al.* Protein carbamylation links inflammation, smoking, uremia and atherogenesis. *Nat. Med.* **13**, 1176–1184 (2007).
278. Kirkham, P. A. *et al.* Oxidative stress-induced antibodies to carbonyl-modified protein correlate with severity of chronic obstructive pulmonary disease. *Am. J. Respir. Crit. Care Med.* **184**, 796–802 (2011).
279. Lugli, E. B. *et al.* Expression of citrulline and homocitrulline residues in the lungs of non-smokers and smokers: implications for autoimmunity in rheumatoid arthritis. *Arthritis Res. Ther.* **17**, 9 (2015).
280. Shi, J. *et al.* Autoantibodies recognizing carbamylated proteins are present in sera of patients with rheumatoid arthritis and predict joint damage. *Proc. Natl. Acad. Sci.* **108**, 17372–17377 (2011).

281. Riella, L. V. *et al.* Role of the PD-1 Pathway in the Immune Response. *Am J Transpl.* **12**, 2575–2587 (2012).
282. Kalathil, S. G. *et al.* T-regulatory cells and programmed death 1+ T cells contribute to effector T-Cell dysfunction in patients with chronic obstructive pulmonary disease. *Am. J. Respir. Crit. Care Med.* **190**, 40–50 (2014).
283. Stoll, P. *et al.* Imbalance of dendritic cell co-stimulation in COPD. *Respir. Res.* **16**, 19 (2015).